AN ABSTRACT OF THE DISSERTATION OF

Susan C. Tilton for the degree of Doctor of Philosophy in Toxicology presented on December 14, 2005.
Title: Application of Toxicogenomics to Determine Mechanism of Tumor Modulation by Dietary Indole Phytochemicals in Hepatocellular Carcinoma.

Abstract approved: Redacted for Privacy
David E. Williams

Indole-3-carbinol (I3C) and 3,3'-diindolylmethane (DIM), a primary I3C derivative *in vivo*, are known chemopreventive agents available as dietary supplements. I3C was found to suppress or enhance tumors in several animal models. Chemoprotection is attributed to the ability of indoles to alter carcinogen metabolism effectively blocking initiation. However, mechanisms for enhancement are unknown. In rainbow trout, I3C promotes hepatocarcinogenesis at concentrations that differentially activated estrogen receptor (ER) or aryl hydrocarbon receptor (AhR)-mediated responses. The relative importance of these pathways was evaluated using toxicogenomics in juvenile trout exposed to I3C and DIM compared to ER and AhR agonists, 17β-estradiol (E2) and β-naphthoflavone. I3C and DIM acted transcriptionally similar to E2 by correlation analysis indicating I3C promotes hepatocarcinogenesis through estrogenic mechanisms in trout and suggesting DIM may be a more potent tumor promoter.

The ability of DIM to enhance hepatocarcinogenesis was evaluated in trout initiated with aflatoxin B_1 compared to E2. Tumor incidence was significantly elevated in initiated trout fed 400 ppm DIM. To evaluate the mechanism of promotion, hepatic gene expression profiles were examined in animals on promotional diets during the

course of tumorigenesis and in hepatocellular carcinomas (HCCs) using a trout 70-mer oligonucleotide array. DIM altered gene expression profiles similar to E2 at all timepoints measured. Expression profiles in trout HCC were similar to transcriptional changes reported in human and rodent HCC further supporting the validity of the trout tumor model. Further, transcription in HCCs from DIM and E2 treatments indicated decreased invasive potential compared to control HCCs. These findings confirm importance of estrogenic signaling in the mechanism of indoles and indicate a possible dual effect that enhances tumor incidence and decreases potential for metastasis.

The estrogenic response of DIM in trout liver was characterized by measuring its *in vitro* biological activity, its ability to bind to ER and its potential for metabolism to estrogenic metabolites. The results support the role of DIM as a potent estrogen in trout liver that may require metabolism for ligand-dependent activation of ER or activation of extracellular signaling pathways for ligand-independent activation of ER. It is likely that multiple mechanisms are involved for DIM estrogenic activity.

Application of Toxicogenomics to Determine Mechanism of Tumor Modulation by Dietary Indole Phytochemicals in Hepatocellular Carcinoma

by

Susan C. Tilton

A DISSERTATION

submitted to

Oregon State University

in partial fulfillment of
the requirements for the
degree of

Doctor of Philosophy

Presented December 14, 2005
Commencement June 2006

Doctor of Philosophy dissertation of Susan C. Tilton presented on December 14, 2005.

APPROVED:

Redacted for Privacy

Major Professor, representing Toxicology

Redacted for Privacy

Head of the Department of Environmental and Molecular Toxicology

Redacted for Privacy

Dean of the Graduate School

I understand that my dissertation will become part of the permanent collection of Oregon State University libraries. My signature below authorizes release of my dissertation to any reader upon request.

Redacted for Privacy

Susan C. Tilton, Author

ACKNOWLEDGEMENTS

I would like to thank everyone who contributed to this project. In particular, I would like to thank my advisor, Dr. David Williams, for his guidance in these studies and his support of my career outside the lab. I would also like to thank Dr. George Bailey for his advice and kind acknowledgements along with my other committee members, Drs. Rod Dashwood, Larry Curtis and Gary DeLander, for their assistance during my graduate studies. I thank all who were involved with the rainbow trout microarray, including Dr. Chris Bayne, Dr. Lena Gerwick, Dr. Graham Corley-Smith, Dr. Scott Givan, Caprice Rosato and members of the microarray journal club, for their technical advice, collaboration and thoughtful discussions. I thank Dr. Jerry Hendricks, Dr. Gayle Orner, Sheila Cleveland, Eric Johnson and Greg Gonnerman for their advice, historical knowledge and tremendous amount of hard work at the Sinnhuber Aquatic Research Laboratory. I also thank Dr. Cliff Pereira for his advice and statistical support on these projects and all coauthors for their assistance. Finally, I would like to thank my husband and friends and members of the Williams lab, MFBSC, LPI and toxicology department for their enduring support and making my time at Oregon State more enjoyable. This work was supported by the NIEHS toxicology training grant (ES07060), Linus Pauling Institute graduate fellowship and NIH grants ES03850, ES00210, ES11267 and CA90890.

CONTRIBUTION OF AUTHORS

Dr. David E. Williams provided guidance and critical review of experimental design, data analysis and manuscript preparation. Dr. George S. Bailey was involved in the development of the rainbow trout oligonucleotides array, OSUrbt v. 2.0, and provided critical review of data analysis and manuscript preparation. Drs. Christopher J. Bayne, Lena G. Gerwick and Graham Corley-Smith were involved in the development of the rainbow trout oligonucleotide array and provided critical review of manuscripts. Dr. Scott A. Givan provided microarray bioinformatic support, while Caprice S. Rosato provided technical microarray support. Dr. Jerry D. Hendricks provided assistance with gross pathology and histologic analysis of tumor tissue. Dr. Cliff B. Pereira provided guidance in microarray study experimental designs and performed statistical modeling and analysis. Dr. Gayle Orner provided assistance with experimental design of the tumor study. Dr. James White, Dr. Alexandre Yokochi and Christopher Lincoln determined the X-ray crystal structure of DIM and performed computer modeling of DIM.

TABLE OF CONTENTS

TABLE OF CONTENTS (Continued)

LIST OF FIGURES

LIST OF FIGURES (Continued)

LIST OF FIGURES (Continued)

LIST OF TABLES

Application of Toxicogenomics to Determine Mechanism of Tumor Modulation by Dietary Indole Phytochemicals in Hepatocellular Carcinoma

Chapter 1. Introduction

Dietary Indole Phytochemicals

Indole-3-carbinol (I3C) is a naturally occurring plant alkaloid present in cruciferous vegetables, such as broccoli, cauliflower, cabbage and Brussels sprouts, in the form of an indole glucosinolate (glucobracissin). When cruciferous vegetables are cut or chewed, glucobracissin is hydrolyzed by myrosinase to form I3C (McDanell *et al.*, 1988). I3C has been shown to modulate chemically-induced carcinogenesis through mechanisms that are primarily attributed to the actions of its acid condensation products (ACPs) instead of I3C itself. In the acid environment of the

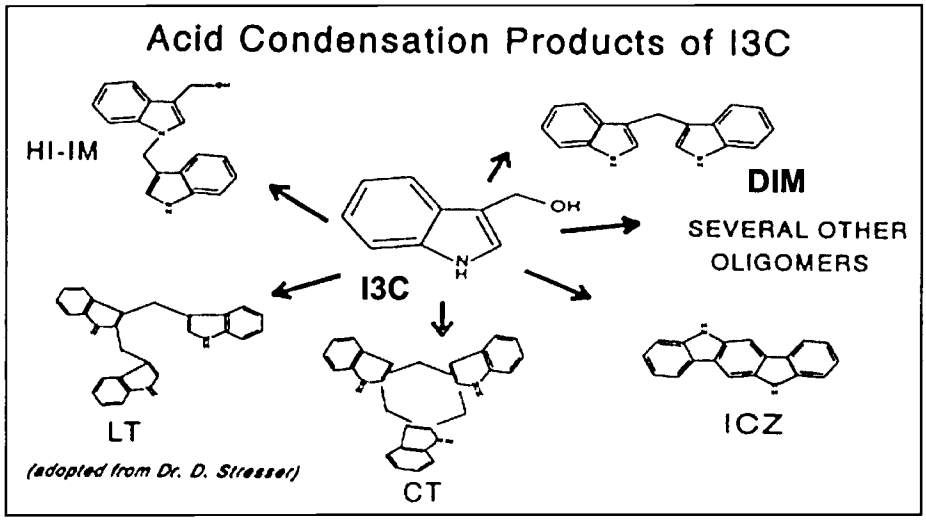

Figure 1-1. Formation of acid condensation products from I3C.

stomach, I3C is unstable and undergoes oligomerization to several different ACPs (Fig. 1-1; Bradfield and Bjeldanes, 1987). The two primary products formed are a dimer, 3,3'-diindolylmethane (DIM), and a linear trimer, 2-(indol-3-ylmethyl)-3.3-diindolylmethane (LTR). Other important oligomerization products produced in minor amounts include a cyclic trimer, 5,6,11,12,17,18-hexahydrocyclonona[1,2-b:4,5-b':7,8-b"]triindole (CTR), and indolo-[3,2-b]-carbazole (ICZ) among others.

Pharmacokinetic studies indicate that DIM is also a primary *in vivo* component of I3C after absorption and disposition in mouse, trout and rat models (Anderton *et al.*, 2004; Dashwood *et al.*, 1989; Stresser *et al.*, 1995a). These studies show that DIM and other ACPs are absorbed systemically and may preferentially target the liver, while relatively little I3C is measured in serum or tissues. A heavy eater of cruciferous vegetables consuming 200 g of Brussels sprouts would receive approximately 12 mg DIM in the diet (Leong *et al.*, 2001). However, both I3C and DIM are available over-the-counter as dietary supplements with recommended dosages ranging 400 – 1200 mg/day, indicating significant concentrations of dietary indoles can be consumed outside of the diet. I3C has been found to suppress or enhance tumors in several animal models. Interestingly, studies in trout and rat models indicate that its promotional potency is at least as great as its potency as an anti-initiating agent (Bailey *et al.*, 1991; Oganesian *et al.*, 1999; Stoner *et al.*, 2002). These findings emphasize the importance of determining the mechanism of action of dietary indoles to establish the relative risks, as well as benefits, before they are used long-term for supplementation and cancer prevention.

Chemoprotection by indole-3-carbinol and 3,3'-diindolylmethane

I3C and DIM are promoted for their well established chemoprotective effects, particularly in estrogen-sensitive neoplasias such as breast cancer. Both I3C and DIM have been found to inhibit 7,12-dimethylbenzanthracene-induced mammary carcinogenesis in Sprague-Dawley rats when fed in the diet post-initiation (Chen *et al.*, 1998; Grubbs *et al.*, 1995). However, chemoprotection by I3C is most consistently observed in various target organs, including mammary and stomach (Wattenberg and Loub, 1978), liver (Bailey *et al*, 1991; Tanaka *et al.*, 1990), lung (Morse *et al.*, 1990) and colon (Xu *et al.*, 1996), of rodent and rainbow trout models when administered prior to and/or concurrent with the carcinogen effectively blocking initiation. The ability of I3C to act as a blocking agent is supported by studies in which decreased tumor incidence was correlated with inhibition of carcinogen-DNA adducts (Dashwood *et al.*, 1994). Dietary indoles are thought to act as anti-initiating agents primarily through modulation of Phase I (cytochrome P450s; CYP450) and Phase II (UDP-glucuronyltransferase, sulfotransferase, glutathione-s-transferase, epoxide hydrolase and NADPH quinine reductase) metabolizing enzymes involved in detoxication of procarcinogens (Bradfield and Bjeldanes, 1984).

Other chemoprotective mechanisms of I3C and DIM measured *in vitro* include their ability to alter cell cycle progression, proliferation, and apoptosis suggesting indoles may also target other stages of carcinogenesis (Kim and Milner, 2005). Of particular interest is the ability of indoles to act as anti-estrogens in certain systems by antagonizing estrogen receptor (ER)-mediated actions of endogenous 17β-estradiol (E2) or by metabolizing E2 to less estrogenic forms through induction of CYP450s

(Meng *et al.*, 2000; Lord *et al.*, 2002). The cytostatic properties of DIM have been attributed to both anti-estrogenic and estrogenic effects that were not dependent on ligand binding to ER, but through cross-talk of ER signaling with aryl hydrocarbon receptor (AhR) or extracellular kinase pathways (Chen *et al.*, 1998; Leong *et al.*, 2004).

Tumor enhancement by indole-3-carbinol

Despite clear evidence for chemoprotective effects, I3C has also been found to promote tumor formation in multiple organs in rat models (Kim *et al.*, 1997; Pence *et al.*, 1986; Stoner *et al.*, 2002; Suzui *et al.*, 2005; Yoshida *et al.*, 2004) and in trout liver (Bailey *et al.*, 1987; Dashwood *et al.*, 1991; Oganesian *et al.*, 1999) after dietary exposure post-initiation. Mechanisms for enhancement are not well understood, but have been attributed to altered estrogen metabolism in endometrial adenocarcinoma, inhibition of apoptosis in colon carcinogenesis and biphasic activation of ER- and AhR-mediated responses in trout liver (Oganesian *et al.*, 1998; Suzui *et al.*, 2005; Yoshida *et al.*, 2004). In trout, I3C promoted hepatocarcinogenesis at concentrations that differentially induced markers of ER and AhR-mediated signaling (Oganesian *et al.*, 1999) suggesting estrogenic mechanisms may play a role. The potential for I3C to cause tumor enhancement by estrogenic mechanisms is supported by the fact that I3C and estrogens are both tumor promoters in rat and trout models, but inhibitors in mouse models post-initiation (Oganesian *et al.*, 1997; Poole and Drinkwater, 1996). Further, i*n vitro* studies with DIM have shown it to have estrogenic activity in cancer cells by ligand-independent activation of ER (Leong *et*

al., 2004; Riby *et al.*, 2000a) and we have also found DIM to induce an estrogenic protein marker, vitellogenin (VTG), in trout (Shilling and Williams, 2001). The ability of DIM to enhance tumor formation in models similar to I3C has not been evaluated until now, but DIM has been increasingly promoted as a chemoprotective agent over I3C due to its chemical stability. Some of the I3C acid-catalyzed oligomerization products are known potent AhR agonists (Bjeldanes *et al.*, 1991). However, as described above, it is not known if the adverse tumor enhancing effects of I3C are due to these AhR-mediated effects, estrogen-mediated effects or to other unknown properties.

Hepatocellular carcinoma

Heptatocellular carcinoma (HCC) is one of the most common malignancies in humans worldwide, particularly in Southeast Asia, Japan and Africa. Even the relatively low incidence of HCC in the United States is rising and exhibits the fastest increase among solid tumors (El-Serag and Mason, 1999). The prevalence of HCC has been correlated with a number of environmental factors including chronic inflammatory liver diseases caused by viral infection and dietary exposure to aflatoxin B_1 (AFB_1), a fungal metabolite that contaminates grain and legume supplies in the same parts of the world. AFB_1 is a potent carcinogen in certain animal models and epidemiological studies support the conclusion that it is also hepatocarcinogenic in humans (Chen *et al.*, 1996; Groopman *et al.*, 1996). Despite the fact that HCC is one of the few human cancers with known etiology, the molecular mechanisms involved in tumorigenesis are poorly understood and have only recently been investigated (Choi *et*

al., 2004; Graveel *et al.*, 2001; Meyer *et al.*, 2003; Okabe *et al.*, 2001). Tumorigenesis is a multistage process that involves a number of genetic alterations during initiation, promotion and progression of the disease. Increased understanding of molecular mechanisms in HCC will provide new therapeutic targets for treatment and chemoprevention, possibly by dietary indole phytochemicals.

Application of toxicogenomics to the rainbow trout model

The carcinogenicity of aflatoxins was first recognized in rainbow trout (Ashley and Halver, 1961), which have subsequently proven to be an excellent research model for the study of human hepatocarcinogenesis induced by AFB_1 and other environmental carcinogens. The strengths of the trout model include its sensitivity to many classes of carcinogens, low spontaneous background tumor incidence and low cost husbandry for large-scale statistically valuable studies. More importantly, certain mechanisms of carcinogenesis have been well characterized in trout including carcinogen metabolism, DNA adduction and repair, oncogene activation and tumor pathology (reviewed by Bailey et al., 1996). Results from the study of tumor promotion and chemoprevention by environmental and dietary factors in AFB_1-initiated trout (Breinholt *et al.*, 1995; Oganesian *et al.*, 1999) have also been confirmed and extended in rodent studies (Manson *et al.*, 1998; Stoner *et al.*, 2002) as well as human clinical intervention trials (Egner *et al.*, 2001).

Currently, however, the molecular mechanisms involved during tumorigenesis have not been described in trout and are not well understood in lower vertebrate models in general. A number of recent studies have been published utilizing

microarray technology in trout and other salmonid models to examine gene expression patterns and functional classes important for stress responses, chemical toxicology and immune function supporting the use of this model in biomedical research (Krasnov *et al.*, 2005a; Krasnov *et al.*, 2005b; Rise *et al.*, 2004a). One of the inherent strengths of microarray platforms is the ability to extrapolate data across multiple species. Such comparative analyses can highlight mechanisms that have a key role in processes such as carcinogenesis. Studies that have examined the relationship of gene profiles across diverse species found that transcriptional responses conserved across evolution were more likely to correspond to true functional interactions (Segal *et al.*, 2005). Existence of an array for rainbow trout targeted to mechanisms of carcinogenesis would provide a powerful tool to evaluate global molecular changes in the trout model.

Hypotheses and objectives

Based on the information presented above, we hypothesize that the dietary indole phytochemical, I3C, is acting through estrogenic mechanisms to promote hepatocarcinogenesis in trout. Further, we hypothesize that DIM will also enhance tumor formation in the trout model similar to I3C by acting through a common estrogenic mechanism. The development of a novel rainbow trout oligonucleotide array targeted to mechanisms of carcinogenesis, toxicology, immunology, endocrinology and stress physiology will allow for the mechanistic evaluation of the effect of dietary indoles in trout during carcinogenesis. We hypothesize that DIM treatment will induce ER-mediated mitogenic signaling and will result in liver and

tumor samples with transcriptional profiles indicating aggressive cell growth and proliferation. The mechanisms identified in trout hepatocellular carcinoma and those modified by dietary indoles will be compared to other models to further validate trout as a cancer model. Species comparisons will also allow us to determine if the mechanisms identified in trout can be extrapolated to other models. Overall, these studies will provide information about the mechanisms for tumor modulation, particularly during enhancement, by dietary indole phytochemicals.

Chapter 2. Toxicogenomic profiling of the hepatic tumor promoters indole-3-carbinol, 17β-estradiol and β-naphthoflavone in rainbow trout

Susan C. Tilton[*], Scott A. Givan[†], Cliff B. Pereira[‡§], George S. Bailey[*‡] and David E. Williams[*‡]

[*]Department of Environmental and Molecular Toxicology, Marine and Freshwater Biomedical Sciences Center and Linus Pauling Institute, [†]Center for Gene Research and Biotechnology, [‡]Environmental Health Sciences Center and [§]Department of Statistics, Oregon State University, Corvallis, Oregon, 97331

Toxicological Sciences

http://toxsci.oxfordjournals.org/

Advanced Access Sept. 28, 2005. 10.1093/toxsci/kfi341

ABSTRACT

Indole-3-carbinol (I3C), from cruciferous vegetables, has been found to suppress or enhance tumors in several animal models. We previously reported that dietary I3C promotes hepatocarcinogenesis in rainbow trout (*Oncorhynchus mykiss*) at concentrations that differentially activated estrogen receptor (ER) or aryl hydrocarbon receptor (AhR)-mediated responses based on individual protein biomarkers. In this study, we evaluated the relative importance of these pathways as potential mechanisms for I3C on a global scale. Hepatic gene expression profiles were examined in trout after dietary exposure to 500 and 1500 ppm I3C and 3,3'-diindolylmethane (DIM), a major *in vivo* component of I3C, and were compared to the transcriptional signatures of two model hepatic tumor promoters; 17β-estradiol (E2), an ER agonist, and β-naphthoflavone, an AhR agonist. We demonstrate that I3C and DIM acted similar to E2 at the transcriptional level based on correlation analysis of expression profiles and clustering of gene responses. Of the genes regulated by E2 (fold change $\geq$2.0 or $\leq$0.50), most genes were regulated similarly by DIM (87-92%) and I3C (71%) suggesting a common mechanism of action. Of interest were upregulated genes associated with signaling pathways for cell growth and proliferation, vitellogenesis, and protein folding, stability and transport. Other genes downregulated by E2, including those involved in acute-phase immune response, were also downregulated by DIM and I3C. Gene regulation was confirmed by qRT-PCR and western blot. These data indicate I3C promotes hepatocarcinogenesis through

estrogenic mechanisms in trout liver and suggest DIM may be an even more potent hepatic tumor promoter in this model.

INTRODUCTION

Indole-3-carbinol (I3C) is a naturally occurring glucosinolate hydrolysis product found in significant concentrations in *Brassica* vegetables such as broccoli, cauliflower and cabbage (Fig. 2-1; McDanell *et al.*, 1988). 3,3'-Diindolylmethane (DIM) is the major I3C acid condensation product formed after oral administration and measured in the liver after absorption and distribution in trout and rodent models (Anderton *et al.*, 2004; Dashwood *et al.*, 1989; Stresser *et al.*, 1995a). Both indole phytochemicals are also available as dietary supplements and are promoted for their well established chemoprotective effects. I3C is chemoprotective in a number of animal models particularly when administered in the diet concurrent with, or prior to, the carcinogen effectively blocking initiation (Grubbs *et al.*, 1995; Kojima *et al.*, 1994). In some studies, decreased tumor incidence was correlated with inhibition of carcinogen-DNA adducts indicating that the ability of indoles to induce cytochrome P450s (CYPs) involved in detoxication of procarcinogens through the aryl hydrocarbon receptor (AhR) or inhibition of CYPs capable of bioactivation are possible mechanisms for chemoprevention (Dashwood *et al.*, 1994; Stresser *et al.*, 1995b). Other mechanisms determined *in vitro*, including the ability of both I3C and DIM to alter cell cycle progression, proliferation, and apoptosis, suggest indoles may

also target other stages of carcinogenesis (Kim and Milner, 2005). Of particular interest is the ability of indoles to act as anti-estrogens in certain systems by antagonizing the estrogen receptor (ER)-mediated actions of endogenous 17β-estradiol (E2) or by metabolizing E2 to less estrogenic forms through induction of CYPs (Meng *et al.*, 2000; Lord *et al.*, 2002).

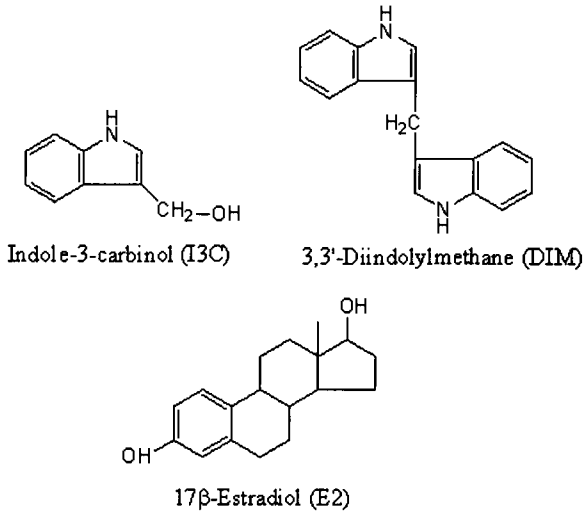

Figure 2-1. Molecular structures of I3C, DIM and E2.

Despite clear evidence for chemoprotective effects, I3C has also been found to promote tumor formation in multiple organs in rodent and trout models after dietary exposure post-initiation (Oganesian *et al.*, 1999; Stoner *et al.*, 2002; Yoshida *et al.*, 2004). Some studies suggest that the promotional potency of I3C is at least as great as its potency as an anti-initiating agent (Bailey *et al.*, 1991; Oganesian *et al.*, 1999; Stoner *et al.*, 2002). Although the mechanisms for promotion are not well understood, it is possible that ER and/or AhR-mediated processes similar to those described for chemoprevention may be important. We have previously reported that I3C promotes

aflatoxin B_1 (AFB_1)-induced hepatocarcinogenesis in trout at concentrations that differentially induced vitellogenin (VTG) and not CYP1A, while higher concentrations induced both proteins (Oganesian *et al.*, 1999). The relative induction of VTG and CYP1A, which are frequently used as markers for activation of ER and AhR-mediated pathways, respectively, suggest that ER-mediated responses may be important for promotion by I3C in trout. Further, *in vitro* studies with DIM have shown it to have estrogenic activity in certain cancer cells by ligand-independent activation of ER (Leong *et al.*, 2004; Riby *et al.*, 2000a) and we have also found DIM to induce VTG in trout (Shilling and Williams, 2001). However, promotion of endometrial adenocarcinoma by I3C in rats was recently correlated with the induction of CYP1A and CYP1B enzymes and sequential formation of toxic E2 catechol metabolites suggesting AhR-mediated pathways may be more important (Yoshida *et al.*, 2004). Therefore, while the mechanisms of action for I3C and DIM have been found to involve both ER and AhR-mediated pathways, the relative importance of either in trout liver has not been evaluated by a comprehensive toxicogenomics approach.

In this study, we determined the relative importance of ER and AhR-mediated pathways in the mechanism of indole phytochemicals by microarray analysis. One of the inherent strengths of microarray technology is the ability to perform correlation analyses on compounds of interest to reveal commonality in global gene networks and provide insight into potential mechanisms of action. Hepatic gene expression profiles were examined in trout after dietary exposure to I3C and DIM at concentrations mimicking those from the tumor promotion study. Indole profiles were compared to

the transcriptional signatures of two model hepatic tumor promoters; E2, an ER-agonist, and β-naphthoflavone (βNF), an AhR-agonist (Bailey *et al.*, 1989; Nunez *et al.*, 1989). We demonstrate that transcriptional profiles of I3C and DIM strongly overlap with E2 based on correlation analyses. These data indicate that I3C acts similar to E2 in trout liver *in vivo* and likely promotes hepatocarcinogenesis through estrogenic mechanisms. Interestingly, these data also suggest DIM may have a greater promotional potency than I3C in the trout tumor model based on this mechanism.

MATERIALS AND METHODS

Materials. Analytical grade I3C, βNF and E2 were purchased from Sigma Chemical (St. Louis, MO). DIM was kindly donated by BioResponse (Boulder, CO) and the purity was confirmed by HPLC. All other compounds were purchased from Sigma unless otherwise stated.

Experimental animals and treatments. Mt. Shasta strain rainbow trout were hatched and reared at the Oregon State University Sinnhuber Aquatic Research Laboratory in 14°C carbon-filtered flowing well water on a 12:12 h light:dark cycle. All animal protocols were performed in accordance with Oregon State University Institutional Animal Care and Use Committee guidelines. Juvenile trout, 12-18 months old, were maintained in separate 375-L tanks (n=2 tanks) for each treatment with 6 fish per tank. Animals were fed a maintenance ration (2.8% w/w) of Oregon

test diet, a semi-purified casein-based diet (Lee *et al.*, 1991). Administration of 500 or 1500 ppm I3C or DIM, 5 ppm E2, 500 ppm βNF or 0.15 % dimethyl sulfoxide vehicle control in the diet was carried out for 12 days. The indole concentrations in the diet for 500 and 1500 ppm are equivalent to 25 and 76 mg/kg/day, respectively, and were chosen to mimic those used in a trout tumor promotion study with I3C in which 1500 ppm I3C maximally induced both VTG and CYP1A protein biomarkers (Oganesian *et al.*, 1999). Concentrations of E2 and βNF were also chosen based on their ability to maximally induce VTG and CYP1A, respectively, and act as hepatic tumor promoters in trout (Bailey *et al.*, 1989; Nunez *et al.*, 1989). On day 13, fish were euthanized by deep anesthesia with 250 ppm tricaine methanesulfonate. Approximately 100 mg liver tissue from individual fish was minced, stored in TRIzol Reagent (Invitrogen, Carlsbad, CA) and quick frozen in liquid nitrogen for gene expression analysis. The rest of the liver was quick frozen in liquid nitrogen for protein analysis. All tissues were taken within 1 h of the scheduled time period.

RNA isolation. Total hepatic RNA was isolated from individual trout liver using TRIzol Reagent followed by cleanup with RNeasy Mini Kits (Qiagen, Valencia, CA) according to manufacturer instructions. Equal amounts of RNA (μg) were pooled from each of the 6 fish per tank for every treatment (n=2), except vehicle control in which RNA was pooled for use as a reference sample from 12 fish in both tanks. RNA quality and quantity were assessed by agarose gel electrophoresis, spectrophotometric absorbency at 260/280 nm and bioanalyzer trace (Bioanalyzer 2100, Agilent, Palo Alto, CA).

Microarray hybridization and analysis. Salmonid cDNA microarrays (GRASP3.7k v.1) were purchased from B. F. Koop and W. Davidson (Genome Research on Atlantic Salmon Project, University of Victoria, BC, Canada; http://web.uvic.ca/cbr/grasp). Microarray fabrication and quality control have been described previously (Rise *et al.*, 2004b). The array contains 3,119 unique Atlantic salmon cDNAs and 438 unique rainbow trout cDNAs (printed in duplicate) which have been found to have high cross-reactivity with rainbow trout targets, >73% and >61%, respectively, similar to that for Atlantic salmon targets. Hybridizations were performed with the Genisphere Array350 kit and instructions (Hatfield, PA) using standard reference design with dye-swapping. Briefly, 10 μg total RNA was reverse-transcribed with Superscript II (Invitrogen) using the Genisphere oligo d(T) primer containing a capture sequence for the Cy3 or Cy5 labelling reagents. Each reaction was spiked with increasing concentrations of three of the *Arabidopsis thaliana* cDNA controls included on the array; PSII oxygen-evolving complex protein 2 (clone ID 175B23T7), ferrodoxin (clone ID 249A17T7) and protochlorophyllide reductase precursor (clone ID 166N16T7) provided as a gift from Dr. Ed Allen, Oregon State University. Test arrays were hybridized using cDNAs without spiking controls and resulted in no cross-reactivity of trout samples to Arabidopsis control spots on the array (data not shown). Each cDNA sample containing the capture sequence for the Cy3 or Cy5 label was combined with equal amounts reference cDNA (pooled from vehicle control) containing the sequence for the opposite label. Every cDNA sample was dye-swapped and hybridized to two slides as technical replicates. Prior to hybridization, microarrays were processed post-printing by washing twice in 0.1% SDS for 5 min,

twice in Milli-Q water for 5 min, immersion in boiling water for 3 min and then dried by centrifugation. Arrays were then washed in 2X SSC, 0.1% SDS at 49°C for 20 min, 0.1X SSC for 5 min and Milli-Q water for 3 min prior to drying by centrifugation. The cDNAs (35 μl) were hybridized to arrays in formamide buffer [50% formamide, 8X SSC, 1% SDS, 4X Denhardt's solution] for 16 h at 49°C with 22x60 mm Lifterslips (Erie Scientific, Portsmouth, NH). Arrays were then washed once in 2X SSC, 0.1% SDS at 49°C for 10 min, twice in 2X SSC, 0.1% SDS for 5 min, twice in 1X SSC for 5 min, twice in 0.1X SSC for 5 min and dried by centrifugation. Shaded from light, the Cy3 and Cy5 fluorescent molecules (3DNA capture reagent, Genisphere) were hybridized in formamide buffer for 3 h at 49°C to corresponding capture sequences on cDNAs bound to the arrays. Arrays were washed in the dark with SSC containing 0.1 M DTT and dried as described earlier.

Scanned images (5 μm) were acquired with ScanArray Express (PerkinElmer, Boston, MA) at an excitation of 543 nm for Cy3 and 633 for Cy5 and at 90% power. The photomultiplier tube (PMT) settings for each fluor were set based on intensity of spiked internal Arabidopsis controls to normalize among all slides in the experiment. Image files were quantified in QuantArray (PerkinElmer) and raw mean signal and background values were exported to BioArray Software Environment (BASE) for analysis. Data were background subtracted and normalized by LOWESS, which is recommended for two-color experiments to eliminate dye-related artifacts and produce ratios that are not affected by signal intensity values (Supplementary Table 1). Stringent criteria were used to filter for genes that were regulated at least 2-fold compared to

vehicle controls consistently in all features (n=8 per treatment) from biological replicates, dye-swapped technical replicates and duplicate spots printed on arrays. The genes that met these criteria were minimally categorized based on function using Gene Ontology and OMIM databases for putative homolog descriptions. Hierarchical clustering of gene expression profiles was performed with the agglomerative hierarchical clustering method provided in BASE using weighted (center of mass) averaging. Pearson correlation coefficients were calculated in GraphPad Prism (GraphPad Software, San Diego, CA) and venn diagrams were created with Array File Maker 4.0.

Real time qRT-PCR. To confirm results from microarray analysis, the expression of some genes was also analyzed by real time qRT-PCR. Total RNA was isolated as described previously and was treated with DNase (Invitrogen) according to manufacturer's protocol. cDNA was synthesized from 2 μg RNA with an oligo $(dT)_{18}$ primer using SuperScript II (Invitrogen) following manufacturer's instructions with a final volume of 100 μl. Synthesized cDNAs (1 μl) were used as templates for amplification of specific gene products in total volumes of 20 μl containing 1X SYBR Green master mix (DyNAmo qPCR kit, Finnzymes, Finland) and 0.3 μM of each primer. Primer sequences are listed in Table 2-1. Primer sequences were chosen so that the product was contained in the array cDNA sequence to ensure validation of the microarray experiment. PCR was performed using a DNA Engine Cycler and Opticon 2 Detector (MJ Research, Waltham, MA). PCR was carried out for 40 cycles with denaturation at 94°C for 10 s, annealing at optimum temperature for primers (56-

TABLE 2-1

Sequences of Primer Sets Used for Real Time RT-PCR Analysis of Gene Expression

Gene	Forward primer	Reverse primer	Size (bp)
β-Actin	5′-TCCCTGGAGAAGAGCTATGAGC-3′	5′-GCTTGCTGATCCACATCTGCTG-3′	376
Apolipoprotein B	5′-CGTGAGCCGTATGTATGCAG -3′	5′-AACAATGGCAGAGGTAGCAG-3′	323
Cathepsin D	5′-TAAAAGTTGCACAAGTTTCC-3′	5′-AAAGGTCGCTTCTGATCGTC-3′	182
C-type Lectin 2-2	5′-GTACCAGTTCATGCAAGCAC-3′	5′-TTCCACTCACAGGGCACGTC-3′	211
CYP1A[a]	5′-TCAACTTACCTCTGCTGGAAGC-3′	5′-GGTGAACGGCAGGAAGGA-3′	68
Serine-threonine kinase	5′-AACACCACAACCCAGTCAGG-3′	5′-AAACCATGTCGAAGAGAAGC-3′	327
Thioredoxin	5′-ACAAGCTGGTGGTAGTGGAC-3′	5′-AGCATTAGCCTCATGACCTC-3′	259
Vitellogenin	5′-GCTGCCCTTGATGAGAACGAC-3′	5′-TCCCAAGACAACCTCAGACGA-3′	158

[a]Rees and Li (2004)

58°C) for 20 s and extension at 72°C for 12 s. DNA amplification was quantified (pg) from the C(T) value based on standard curves to ensure quantification was within a linear range. Standards were created from gel-purified PCR products (QIAX II, Qiagen, Valencia, CA) for each primer set after quantification with PicoGreen dsDNA Quantification Kit (Molecular Probes, Eugene, OR) and serial dilutions ranging from 0.25 to 100 ng DNA. All signals were normalized against β-actin and ratios were calculated for treated samples compared to vehicle control as for the microarray analysis. Expression of β-actin was not altered by treatment based on either microarray analysis or RT-PCR and so was found to be an appropriate housekeeping gene for normalization in this study.

Subcellular fractionation and immunoblot analysis. Microsomal and cytosolic fractions were prepared from individual livers as described previously (Shilling and Williams, 2001). Protein concentrations were determined by the BioRad protein assay (Hercules, CA). CYP1A and zona radiata (ZR) were detected in liver microsomes and cytosol, respectively. Each sample (10 μg protein) was separated on NuPAGE 3-8% Tris-acetate polyacrylamide gels (Invitrogen) by electrophoresis and transferred to PVDF membranes. Membranes were incubated in BSA block buffer [2% BSA in PBS, pH 7.4] for 1 h at room temperature. Blots were probed with CYP1A mouse anti-trout monoclonal clone C10-7 (1:500 dilution) and ZR rabbit anti-salmon polyclonal clone O-146 (1:1000 dilution; Biosense, Bergen, Norway) for 1 h at room temperature. Membranes were washed four times for 5 min in Tween buffer

[0.05% Tween-20 in PBS, pH 7.4]. Membranes were incubated in the appropriate antimouse or antirabbit secondary horseradish peroxidase-conjugated antibodies (1:500; BioRad) for 1 h at room temperature and washed again in Tween buffer. Peroxidase activity was detected using Western Lighting Chemiluminescence Reagent (PerkinElmer) according to the manufacturer's instructions. Bands were visualized using an Alpha Image 1220 Documentation and Analysis System (Alpha Innotech, San Leandro, CA) and quantified as percent above control with Scion Image software (Frederick, MD).

Quantification of VTG by ELISA. Trout liver cytosol was prepared as described above and quantification of VTG was based on an ELISA previously described (Donohoe and Curtis, 1996; Shilling and Williams, 2001). Briefly, cytosol samples were incubated in 96-well plates at 4°C for 24 h with rabbit anti-chum salmon VTG (1:1500), which was graciously provided by A. Hara at Hokkaido University. Samples were transferred to plates coated with 25 ng/well purified rainbow trout VTG (pre-blocked with 1% BSA) and incubated for 24 h at 4°C. Plates were then incubated with biotin-linked donkey anti-rabbit IgG and streptavidin horseradish peroxidase conjugate (Amersham, Buckinghamshire, England) for 2 h at 37°C and developed with 0.01% 3,3'5,5'-tetramethylbenzidine and 0.01% hydrogen peroxide in 0.5 M sodium acetate, pH 6.0. Colorimetric reactions were stopped after 10 min with 2 M sulfuric acid and optical density was measured on a SpectraMax 190 plate reader with SoftMax Pro 4.0 software (Molecular Devices, Sunnyvale, CA). VTG concentrations were determined based on comparison to a trout VTG standard curve with a detection

limit for this assay of 6.25 ng/ml. VTG was normalized to protein concentration for each sample and ratios were calculated for treated samples compared to vehicle control similar to microarray analysis.

RESULTS

Gene expression profiles by I3C, DIM, E2 and BNF

In this study, we determined the relative importance of ER- and AhR-mediated pathways in the mechanism of action of indole phytochemicals in trout by examining hepatic gene expression profiles after dietary exposure to I3C and DIM. Changes in gene expression were analyzed using salmonid cDNA microarrays (GRASP3.7kv.1) to characterize the effects of I3C and DIM in comparison to E2 and βNF. As described in Material and Methods, two replicates of pooled RNA from six treated animals were hybridized to arrays with dye-swapping. The relationship of gene expression profiles among the different treatments were examined in scatter-plot graphs in which a correlation coefficient (R value) was calculated for each graph based on the linear regression between two profiles (Fig. 2-2). Pairwise analysis of all 8,736 features on the array indicated high correlations between E2 and 500 ppm DIM, 1500 ppm DIM and 1500 ppm I3C, R = 0.77, 0.73 and 0.73, respectively (Fig. 2-2, panels A-C). Comparison of the DIM and I3C treatments resulted in the highest correlation coefficient of R = 0.84 (Fig. 2-2E), which would be expected since DIM is the primary

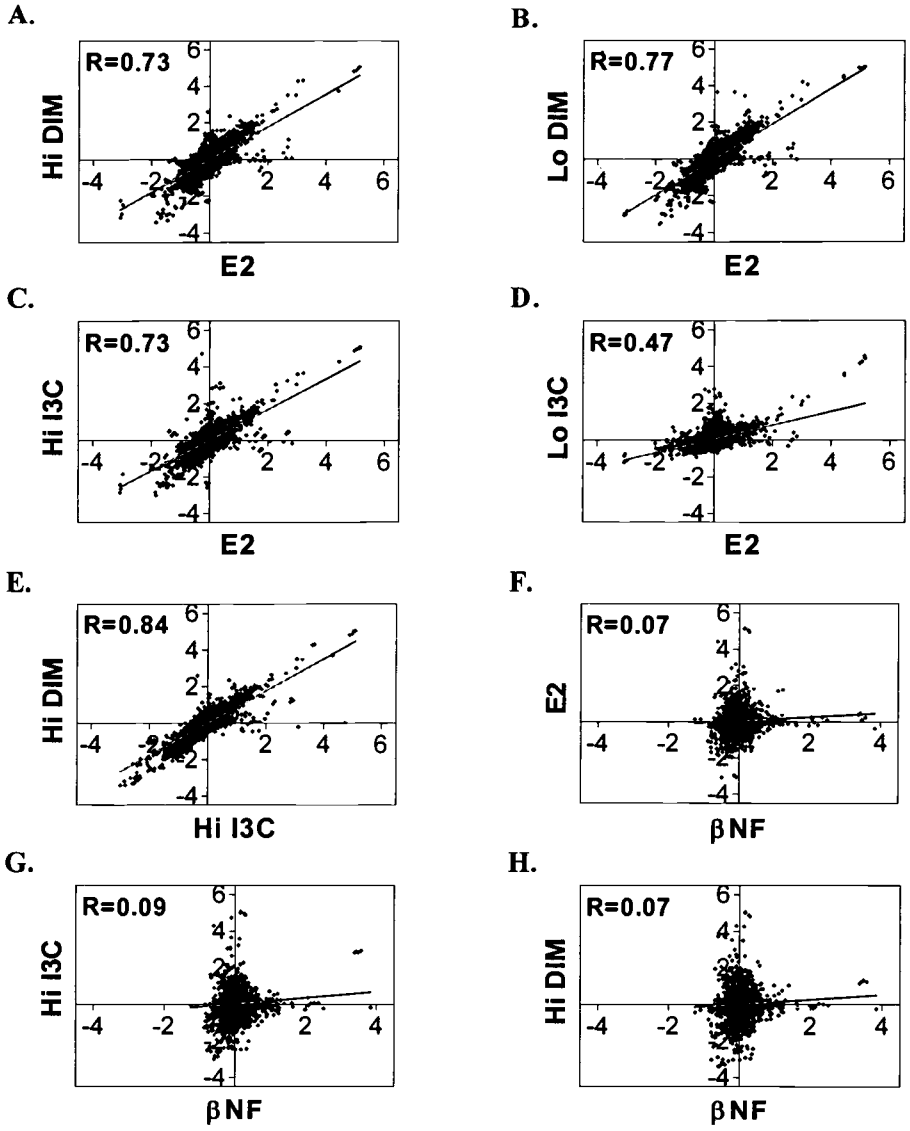

Figure 2-2. Pairwise correlations of microarray data from liver samples after treatment with 500 ppm βNF, 1500 ppm DIM or I3C and 5 ppm E2. Values are fold change (log2) compared to vehicle-treated control samples and were plotted to generate correlation coefficients (R) among the treatments.

gastric oligomerization product of I3C after dietary consumption (Dashwood *et al.*, 1989). In contrast, pairwise analysis suggested a low degree of similarity in gene expression patterns between βNF and the dietary indoles, R = 0.07-0.09 (Fig. 2-2, panels G and H), which were similar to that for comparison of βNF to E2, R = 0.07 (Fig. 2-2F).

Genes were considered differentially expressed if they were ≥ 2.0 or ≤ 0.5 fold changed compared to vehicle control in all intra- and inter-array technical replicates and in both biological replicates for a treatment. Genes that passed the stringency filter are listed in Table 2-2. Gene descriptions are provided based on sequence homology using the most significant ($E<10^{-6}$) BLASTX hit against the current GenBank databases. Supplementary Table 2 lists the E-values and degree of similarity (length and percent identity over aligned region) between salmonid cDNA expressed sequence tags (EST) and the top BLASTX hit. If a salmonid EST had no significant BLASTX hit, then the top BLASTN is listed. Many of the genes listed in Table 2-2 are known trout genes, however others are only putative homologs based on sequence identity.

Hierarchical clustering was used as a visualization tool to identify similarities among biological replicates within a treatment and differences in gene expression between treatments (Fig. 2-3). Bidirectional hierarchical clustering of genes differentially regulated in at least one treatment group also indicated that there was a high degree of similarity in gene expression patterns among I3C, DIM and E2 treatments (Fig. 2-3B). Treatments that clustered together on node II included 500 ppm DIM, 1500 ppm DIM and I3C and 5 ppm E2. This supports the similarities

TABLE 2-2

Select Genes Differentially Regulated by Treatment with Dietary βNF, I3C, DIM or E2

EST Acc.[1]	Gene name (accession number, species)[2]	Average Fold Change[3]					
		E2 5 ppm	DIM 1500 ppm	DIM 500 ppm	I3C 1500 ppm	I3C 500 ppm	βNF 500 ppm
Estrogen-responsive liver proteins (vitellogenesis)							
n/a	Vitelline envelope protein gamma (AAF71260; *Oncorhynchus mykiss*)	35.56	33.56	32.86	33.88	22.03	(1.12)
CB488242	Egg envelope glycoprotein ZP3 (AF180465; *Carassius auratus*)	9.21	20.01	16.78	12.66	5.20	(0.93)
CA054450	Vitellogenin 1 (AY600083; *Salvelinus alpinus*)	21.60	13.30	23.27	19.38	12.43	(0.75)
CB486697	Zona pellucida glycoprotein 2, ZP2 (Z72494; *Cyprinus carpio*)	4.81	8.13	8.50	8.20	3.27	(0.91)
Cell proliferation							
CB486765	Serine/threonine protein kinase (U79240; *Homo sapiens*)	7.84	11.54	9.32	8.30	3.75	(0.86)
CA038486	Nucleoside diphosphate kinase isoform B (D13374; *Rattus norvegicus*)	(1.73)	3.06	2.62	(2.44)	(1.45)	(0.91)
CA043390	Nucleoside diphosphate kinase NM23 (NM_138548; *R. norvegicus*)	(1.75)	2.69	2.58	(2.85)	(1.84)	(0.81)
Protein folding, stability and transport							
CB487725	DnaJ (HSP40), subfamily C, member 3 (AAH65443; *Danio rerio*)	4.57	6.30	5.03	4.55	(2.49)	(0.82)
n/a	Heat shock protein 108 (AF387865; *Gallus gallus*)	3.48	5.37	4.73	4.60	(1.88)	(0.86)
n/a	Cyclophilin B (DQ086177; *Ictalurus punctatus*)	2.70	4.22	3.79	3.06	(1.77)	(0.70)
CA061577	Peptidylprolyl isomerase B (BC071458; *Danio rerio*)	2.70	3.15	3.29	2.45	(1.27)	(0.77)
CA047174	Peptidyl propyl isomerase B (BC059560; *Danio rerio*)	3.03	4.05	4.10	3.22	(1.42)	(0.83)
CB498073	Cathepsin D (U90321; *Oncorhynchus mykiss*)	2.72	3.99	3.65	3.43	(2.36)	(1.02)
CA039299	Protein disulfide isomerase precursor (AF364317; *Cricetulus griseus*)	3.57	4.29	3.89	3.98	(2.28)	(0.94)
CA042407	Protein disulfide isomerase-related protein (AF387900; *Danio rerio*)	(2.16)	3.64	3.33	3.61	(1.56)	(0.82)
CA064165	Protein disulfide isomerase-associated 4 (BC063979; *Danio rerio*)	(3.16)	2.76	3.57	3.48	(1.86)	(0.85)
CA044731	Ribosome associated membrane protein 4 (AJ238236; *Rattus norvegicus*)	2.43	2.82	2.74	(2.33)	(1.57)	(1.01)
CA044589	Protein translocation complex Sec61 beta (AY826154; *Aedes albopictus*)	2.50	2.84	2.49	(2.28)	(1.24)	(0.99)
CA047574	TRAP-complex gamma subunit (BC047859; *Danio rerio*)	(2.22)	3.50	3.78	(2.48)	(1.80)	(0.94)
CA044039	Calcium binding protein calumenin (BX465210; *Danio rerio*)	(2.25)	3.86	3.45	(2.97)	(1.53)	(1.00)
Extracellular matrix and vascularization factors							
CA057815	Tissue factor pathway inhibitor 2 (XM_683974; *Danio rerio*)	(2.29)	3.94	4.16	(1.90)	(0.93)	(1.03)

TABLE 2-2 (Continued)

EST Acc.[1]	Gene name (accession number, species)[2]	Average Fold Change[3]					
		E2 5 ppm	DIM 1500 ppm	DIM 500 ppm	I3C 1500 ppm	I3C 500 ppm	βNF 500 ppm
n/a	Angiogenin related protein (NM_007449; *Mus musculus*)	0.37	0.10	0.12	0.17	(0.70)	(0.71)
CA038551	Angiogenin precursor (AF441670; *Saimiri sciureus*)	0.31	0.11	0.13	0.18	(0.67)	(0.73)
CA038317	Putative collagen alpha 1 (AAG30018; *Oncorhynchus mykiss*)	(0.38)	0.13	0.34	0.19	(0.96)	(1.24)
Drug metabolism							
CA048564	20Beta-hydroxysteroid dehydrogenase B (AF100932; *O. mykiss*)	3.18	3.61	3.46	2.90	(1.82)	(1.22)
CA044359	Cytochrome P450 1A3 (AAD45967; *Oncorhynchus mykiss*)	(1.38)	(2.35)	(2.37)	7.44	(2.31)	10.71
CA044631	Cytochrome P450 2K5 (AF151524; *Oncorhynchus mykiss*)	(0.50)	(0.35)	0.29	(0.60)	(0.80)	(1.22)
Redox regulation							
CA770853	Omega class glutathione-S-transferase (AF325922; *Takifugu rubripes*)	0.36	(0.47)	0.38	(0.58)	(0.76)	(0.94)
CA043161	Thioredoxin (BC049031; *Danio rerio*)	0.38	(0.93)	(0.88)	(1.40)	(0.97)	(1.05)
Lipid, glucose and retinol metabolism							
CA039244	Fatty acid binding protein H-FABP (AAB53643; *Oncorhynchus mykiss*)	2.41	(2.00)	(2.26)	(1.93)	(1.79)	(0.76)
CA038346	Liver-basic fatty acid binding protein (JC7571; *Lateolabrax japonicus*)	(0.45)	0.16	0.18	0.24	(0.70)	(0.97)
CA039371	Liver-basic fatty acid binding protein (AF254642; *Danio rerio*)	(0.52)	0.16	0.16	0.28	(0.69)	(0.92)
CA039342	Apolipoprotein B (X81856; *Salmo salar*)	0.36	0.13	0.15	0.19	(0.57)	(0.89)
CA037318	Adipophilin adipose differentiation-related protein (Q9TUM6; *B. taurus*)	0.36	(0.42)	0.33	0.38	(0.58)	(0.65)
CA038240	Biotinidase fragment 1 (AAG30007; *Oncorhynchus mykiss*)	0.28	0.10	0.09	0.13	(0.74)	(0.67)
CA039519	Acyl-CoA-binding protein (Q9PRL8; *Gallus gallus*)	(0.41)	0.29	0.28	0.35	(0.78)	(0.92)
CA051408	Acyl -coenzyme A-binding protein (S63594; *Anas platyrhynchos*)	(0.52)	0.39	0.32	(0.48)	(0.88)	(0.77)
CB505010	Phosphoglucoonate dehydrogenase (AAQ91261; *Danio rerio*)	0.12	0.11	0.12	0.14	(0.55)	(0.72)
CA064428	Phosphoglucoonate dehydrogenase (AAQ91261; *Danio rerio*)	0.27	0.26	0.24	(0.35)	(0.72)	(0.84)
CA042536	Transaldolase (AF544969; *Ctenopharyngodon idella*)	0.26	0.26	0.22	(0.37)	(0.73)	(0.88)
CA037817	Retinol binding protein 7 XM_692687; *Danio rerio*)	0.12	0.22	0.13	0.19	(0.44)	(0.95)
Potential immunoregulators and acute phase response							
CA037891	Chemotaxin (AAG28030; *Oncorhynchus mykiss*)	0.29	0.14	0.13	0.20	(0.74)	(0.65)
CA037495	Trout C-polysaccharide binding protein 1 (AAG30020; *O. mykiss*)	0.33	0.15	0.32	0.19	(1.03)	(1.28)

TABLE 2-2 (Continued)

EST Acc.[1]	Gene name (accession number, species)[2]	Average Fold Change[3]					
		E2 5 ppm	DIM 1500 ppm	DIM 500 ppm	I3C 1500 ppm	I3C 500 ppm	βNF 500 ppm
CA038178	T-cell antigen receptor (BG936652; Salmo salar)	0.38	0.34	0.36	0.37	(0.79)	(0.72)
CA038603	Differentially regulated trout protein 1 (AAG30030; O. mykiss)	(0.50)	(0.48)	0.29	0.26	(0.76)	(0.70)
CA038422	C-type lectin 2-2 (AAG30026; Oncorhynchus mykiss)	(0.96)	0.20	0.20	0.19	(0.98)	(0.61)
CA056544	Serotransferrin I precursor (P80426; *Salmo salar*)	(0.82)	0.27	0.29	0.37	(0.90)	(1.04)
CA037852	Inter-alpha-trypsin inhibitor heavy chain (XM_688091; *Danio rerio*)	(0.70)	0.36	0.36	0.41	(0.84)	(1.06)
CA037882	Transferrin (L20313; *Salmo salar*)	(0.77)	0.26	0.32	(0.48)	(0.97)	(0.92)
CA039500	Precerebellin-like protein (AAF04305; *Oncorhynchus mykiss*)	(0.75)	0.39	0.40	(0.68)	(0.88)	(0.76)
Miscellaneous							
CB498453	Na/K ATPase alpha subunit 2 (AY319387; *O. mykiss*)	(2.82)	3.51	3.19	(2.70)	(1.65)	(1.15)
CA039857	ERCC4 (AB017635; *Cricetulus griseus*)	(2.55)	3.19	3.17	(2.75)	(1.86)	(0.99)
CB491090	Metallothionein A (M18103; *Oncorhynchus mykiss*)	(0.58)	0.31	0.31	0.42	(0.74)	(1.21)

[1]GenBank accession number of EST corresponding to GRASP microarray feature. n/a = not available (EST not yet submitted).

[2]The most significant (lowest E-value) BLASTX is shown. If an EST has no significant (E-value < 10^{-6}) BLASTX hit, then the most significant BLASTN hit is shown. E-values and degree similarity (length and % identity over aligned region) are listed in Supplementary Table 2. Genes have been categorized by function based on putative trout homolog using Gene Ontology and OMIM databases.

[3]Average fold change values represent background corrected, Lowess normalized signal ratios for biological replicates (n=2). Stringent criteria were used to filter for genes that were regulated ≥ 2-fold compared to vehicle controls consistently in all features (n=8 per treatment) from both biological replicates, both dye-swapped slides (technical replicates) and duplicate spots printed on arrays. Fold change values for genes that did not pass stringency criteria are shown in parentheses. Individual slide data are available in Supplementary Table 1.

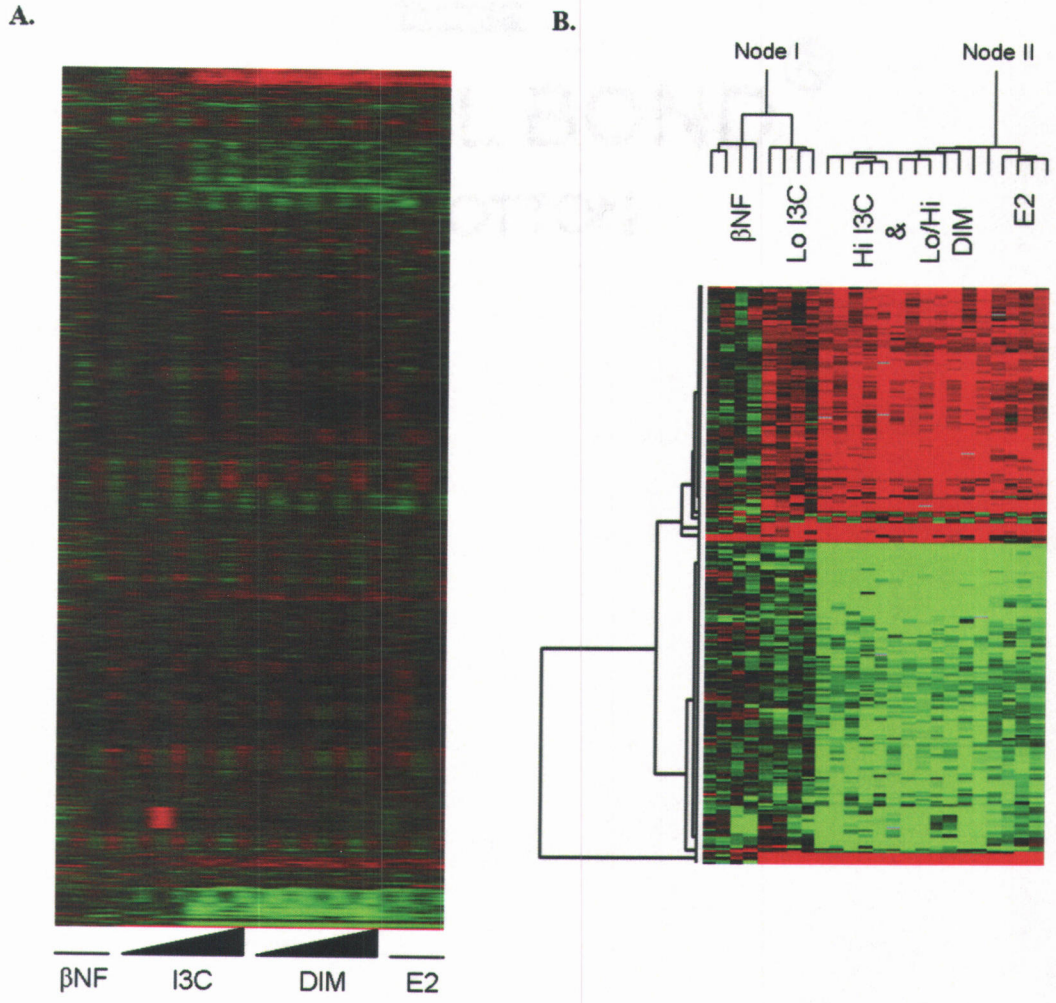

Figure 2-3. Clustering of gene expression in trout liver by Pearson correlation after dietary treatment with 500 ppm βNF, 500 and 1500 ppm DIM and I3C and 5 ppm E2. Results are shown as fold change compared to vehicle-treated control of dye-swapped slides for biological replicates (n=2 per treatment). *Red color*, upregulation; *green color*, downregulation; *black*, unchanged expression; *grey*, missing values. (A) Gene expression profiles for all genes on the array. (B) Subgroup reflects gene expression profiles for genes differentially regulated 2-fold up or down in at least one treatment group.

observed between indoles and E2 by pairwise correlation analysis. Interestingly, βNF clustered with 500 ppm I3C in node I separately from most other indole treatments, however this is more likely due to the low number of genes differentially regulated overall by these two treatments than to similarity between βNF and 500 ppm I3C. The 500 ppm I3C treatment did not have a strong correlation with E2 by pairwise analysis (R = 0.49; Fig. 2-2D), however all genes differentially regulated by 500 ppm I3C were also regulated by E2 whereas none were regulated similarly to βNF (Table 2-2 and Fig. 2-4). The only two array features differentially regulated by βNF were for different cDNAs of CYP1A, which were also similarly regulated by the high dose of I3C.

Of the 38 cDNAs differentially regulated at least 2-fold by E2, 87% or 92% were similarly regulated by DIM, depending on dose, and 71% were regulated by I3C (Fig. 2-4). Further, all cDNAs regulated 2-fold by E2, except for thioredoxin, were also regulated at least 1.5-fold by either DIM or I3C suggesting a common mechanism of action in trout liver. Transcripts encoding vitellogenic liver proteins were the most sensitive markers for the estrogenic response in trout with expression profiles for VTG 13 to 23-fold above controls by microarray analysis and 250 to 1000-fold by qRT-PCR (Table 2-2). Other upregulated genes include those involved in cell proliferation, protein stability and transport. Genes commonly downregulated by these treatments include those important for lipid, glucose and retinol metabolism, immune regulation and angiogenesis. While most cDNAs altered by E2 were also altered by treatment with DIM and I3C, there were some treatment-specific effects by the dietary indoles in trout liver (Fig. 2-4). The majority of these include genes involved in immune

A.

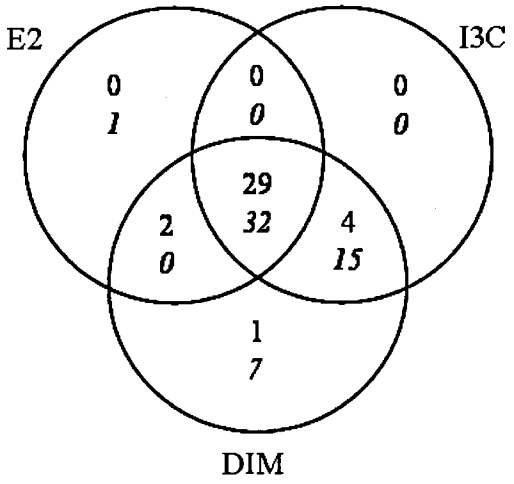

B.

Treatment	Up 2-fold	Down 2-fold	Total
E2	21	17	38
βNF	2	0	2
Lo I3C	5	0	5
Hi I3C	22	30	52
Lo DIM	37	51	88
Hi DIM	36	54	90
E2 & Lo I3C	5 (*24%*)	0	5 (*13%*)
E2 & Hi I3C	16 (*76%*)	11 (*65%*)	27 (*71%*)
E2 & Lo DIM	19 (*91%*)	16 (*94%*)	35 (*92%*)
E2 & Hi DIM	19 (*91%*)	14 (*82%*)	33 (*87%*)

Figure 2-4. Differential gene expression in trout liver after dietary treatment with 5 ppm E2, and 500 and 1500 ppm DIM and I3C. (A) Genes regulated ≥ 2-fold in one treatment and at least 1.5-fold in the other treatments. In each section, top number indicates genes upregulated and bottom number (italics) indicates genes down regulated. (B) List of genes regulated up or down 2-fold only among the treatments. In parentheses are the percent of genes regulated 2-fold by E2 that are also regulated 2-fold by either I3C or DIM.

function and acute phase response that were downregulated by DIM and I3C and were not differentially regulated by E2, many of which were represented by multiple cDNAs on the array. In cases where there were multiple entries for the same gene, the gene was only entered once in Table 2-2 unless there were differences in treatment-related responses. It is interesting that most non-vitellogenic genes were almost always more strongly regulated by DIM than E2 based on fold-change values by microarray and qRT-PCR (Table 2-2, Fig. 2-5). For purposes of comparison, the concentrations of E2 and βNF were chosen based on their ability to promote tumors and maximally induce VTG and CYP1A, respectively, which was confirmed in this study. It is apparent, however, that not all estrogen-responsive genes were equally regulated by concentrations that maximally expressed VTG because it was such a sensitive marker supporting the conservative nature of the comparison.

Microarray confirmation by qRT-PCR and immunoassay

The expression profiles of select genes that were found to be differentially regulated by some treatments, including CYP1A, VTG, C-type lectin 2-2 (CTL2-2), serine/threonine kinase (STK), cathepsin D (CTSD), thioredoxin (TRX) and apolipoprotein B (APOB), were confirmed for all treatments by qRT-PCR using SYBR Green (Fig. 2-5). Overall, gene expression profiles measured by qRT-PCR confirmed those measured by cDNA array analysis. However, qRT-PCR was more sensitive in several cases than microarray analysis and detected greater changes. In some instances, genes that were not differentially regulated by certain treatments as measured by microarray analysis were found to be differentially regulated at least 2-

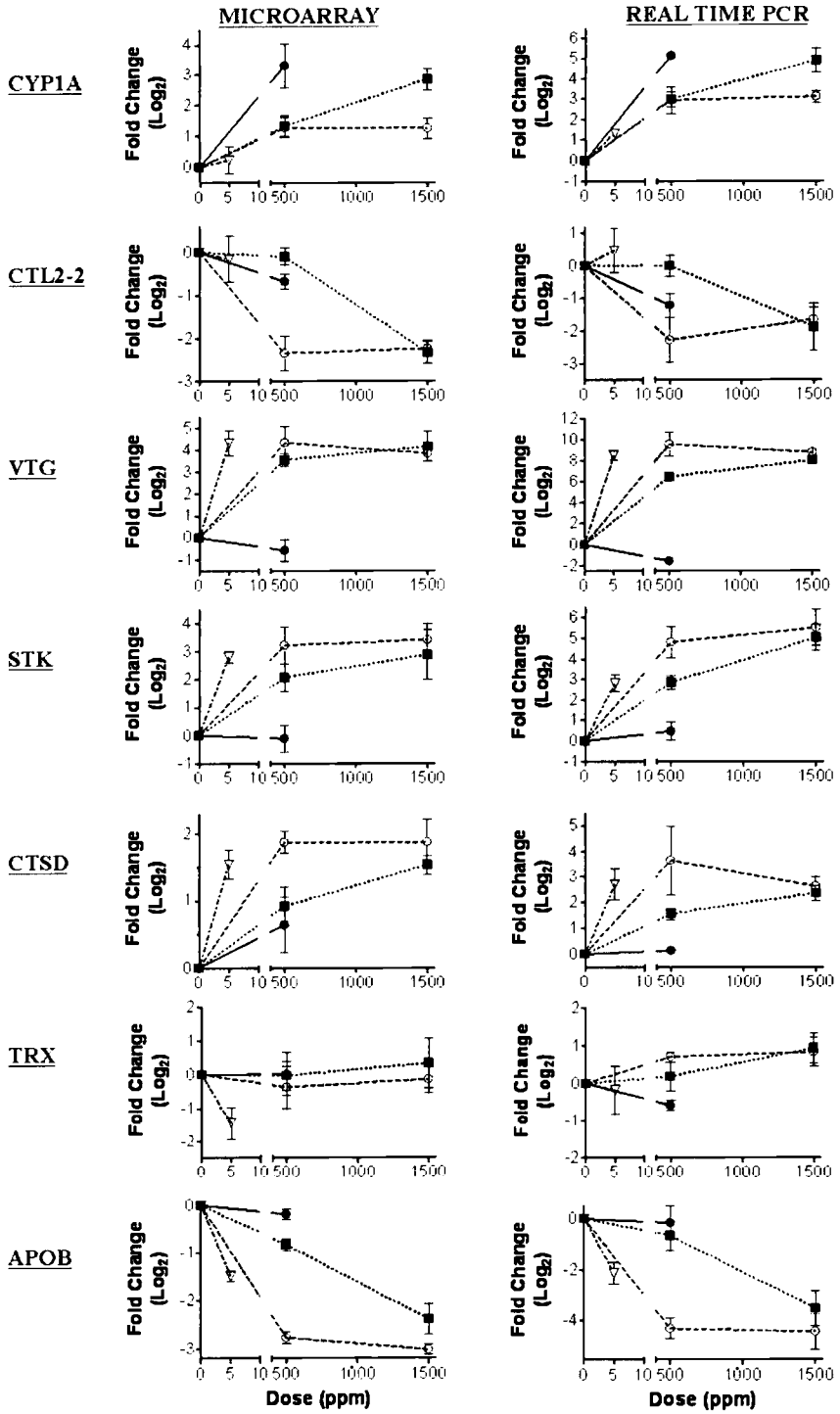

Figure 2-5. Hepatic gene expression in trout after dietary exposure to E2 (▽), βNF (●), DIM (○) and I3C (■) measured by microarray and real time RT-PCR. Values are expressed as fold change (log2) compared to vehicle-treated control for select genes including cytochrome P4501A (CYP1A), C-type lectin 2-2 (CTL2-2), vitellogenin (VTG), serine-threonine kinase (STK), cathepsin D (CTSD), thioredoxin (TRX) and apolipoprotein B (APOB).

fold by qRT-PCR. For example, CYP1A was only upregulated by 1500 ppm I3C and βNF by microarray analysis. However, qRT-PCR analysis of cDNAs did result in greater than 2-fold detection of CYP1A for both concentrations of I3C and DIM (Fig. 2-5). Similarly, E2 treatment even caused an unexpected 2-fold upregulation of CYP1A as determined by qRT-PCR. This indicates there were some sensitivity differences between the two methods and microarray analysis is likely much more conservative at detecting changes than qRT-PCR. Some genes were also confirmed by examining corresponding protein induction for CYP1A, VTG and zona radiata (ZR), also known as vitelline envelope, by immunoassay (Fig. 2-6). These proteins were found to correlate well with transcript profiles measured by microarray analysis.

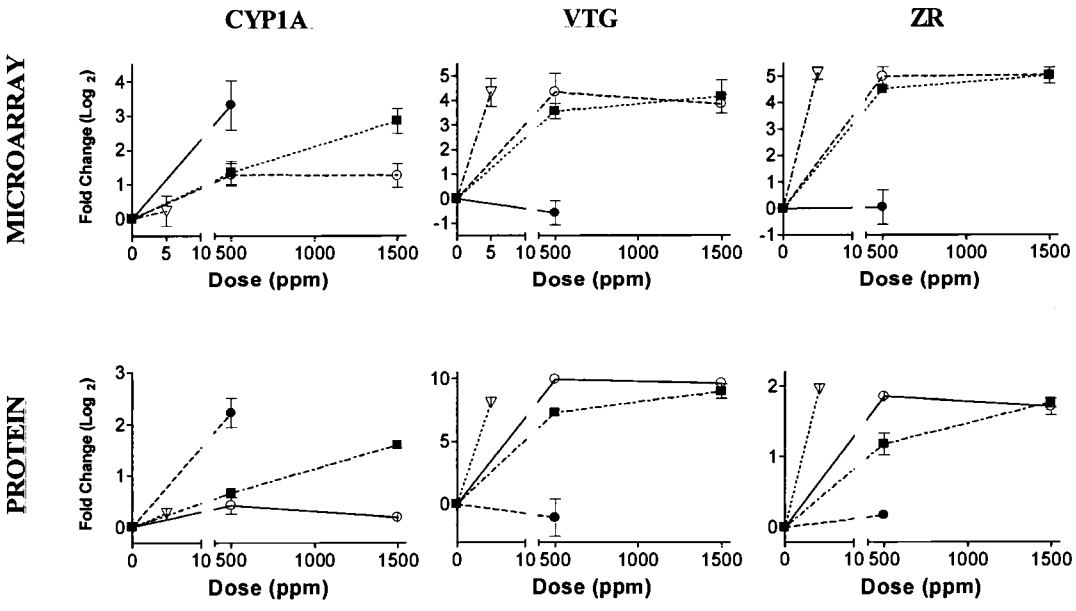

Figure 2-6. Hepatic cytochrome P4501A (CYP1A), vitellogenin (VTG) and zona radiata (ZR) protein and microarray gene expression in trout after dietary exposure to E2 (▽), βNF (●), DIM (○) and I3C (■). Values are expressed as fold change (log2) compared to vehicle-treated control.

DISCUSSION

We have previously reported that I3C promotes AFB_1-induced hepatocarcinogenesis post-initiation at concentrations in the diet that were able to induce VTG, but not CYP1A (Oganesian *et al.*, 1999). These data suggest that estrogenic mechanisms may be important for promotion by indoles particularly at lower dietary levels. VTG and CYP1A are frequently used as markers for activation of ER and AhR-mediated pathways, respectively, in fish and other models. The mechanisms of action for I3C and DIM have been found to involve both pathways, however the relative importance of either in trout liver has not been evaluated on a global scale. The purpose of this study was to examine hepatic gene expression profiles after dietary exposure to two indole supplements, I3C and DIM, compared to E2, an ER agonist, and βNF, an AhR agonist. We demonstrate that I3C and DIM acted similar to E2 at the transcriptional level based on correlation analysis of expression profiles and on clustering of gene responses. Of all the genes 2-fold differentially regulated by E2, approximately 87 – 92% were also similarly regulated by DIM and 71% by I3C. The correlations are likely conservative based on the stringent criteria used to determine differential regulation by array analysis and the lower sensitivity of microarray results observed in comparison to qRT-PCR. These data highlight the strong overlap in transcriptional signatures of dietary indoles with endogenous E2 and suggests that the promotional ability of I3C in trout is through estrogenic mechanisms.

Overall, transcripts encoding vitellogenic liver proteins were the most sensitive markers for the estrogenic response in trout. This is similar to other teleost microarray studies in which VTG and egg envelope proteins were the most responsive hepatic genes regulated after *in vivo* exposure to estrogenic compounds (Larkin *et al.*, 2002; 2003). The VTG response in trout is also confirmed by prior studies that found DIM induced VTG protein with similar efficacy as E2, although with approximately 200-fold less potency than E2 and 5-fold greater potency than I3C (Shilling and Williams, 2001). Our data show that DIM and I3C were able to induce an estrogenic response at the transcriptional level with similar efficacy to E2 and that DIM was more potent than I3C *in vivo*, also supporting its role as the active *in vivo* component of I3C (Anderton *et al.*, 2004; Dashwood *et al.*, 1989; Stresser *et al.*, 1995a).

It was interesting that treatment with βNF resulted in upregulation of only CYP1A and that this transcript was also upregulated above control levels by all treatments in this study, including E2, as determined by qRT-PCR. Therefore, it is possible that AhR-mediated pathways may also be relevant at lower concentrations of dietary indoles and that cross-talk between AhR and ER-mediated mechanisms are involved. Cross-talk between these pathways have been observed previously and suggest AhR agonists inhibit ER-mediated signaling (Safe *et al.*, 1998). Antagonism was observed with βNF, which upregulated CYP1A and downregulated VTG as measured by qRT-PCR. The significance of cross-talk in this study is in need of further research. However, the fact that dietary indoles so strongly mimicked E2 and did not result in antagonism of ER-mediated transcripts with upregulation of CYP1A further support their similarities to E2 compared to βNF.

We observed consistent downregulation of genes involved in redox regulation and lipid, glucose and retinol homeostasis and metabolism by estrogenic treatments. Similar downregulation of these genes and gene classes in liver have been reported for rats treated with the potent estrogen and tumor promoter 17α-ethinylestradiol (Stahlberg *et al.*, 2005). Also, an unexpected and consistent downregulation of genes important for angiogenesis, formation of the extracellular matrix, and immune response were measured after estrogenic treatment. Estrogens have been found to activate pro-angiogenic and matrix-membrane factors in certain cell types, however the inhibitory effect of estrogens on inflammation in vascular endothelia and subsequent inhibition of chemoattractant and acute phase proteins is well documented (Koh, 2002). These signals directly regulate cell adhesion molecules, such as tissue factor, and other vascularization components and may be important for regulation in trout liver endothelial cells. Downregulation of other angiogenic and matrix-related factors in liver after *in vivo* exposure to estrogens has been documented previously (Larkin et al., 2003; Stahlberg et al., 2005). These data indicate evolutionary conservation of a dual role for estrogens in which they can simultaneously stimulate tumor growth, but may also inhibit tumor invasion and motility (Platet *et al.*, 2004).

The liver is a major metabolic organ responsive to estrogens, which are known hepatic tumor promoters in a number of animal models (Nunez *et al.*, 1989; Yager and Liehr, 1996). The transcriptional profiles in this study for E2, DIM and I3C provide insight into the estrogenic mechanisms that may be important for promotion in trout liver including cell proliferation, signaling pathways and protein stability. Many genes involved in protein folding, stability and transport were upregulated by

estrogens in this study including protein disulfide isomerase (PDI), heat shock proteins, peptidylpropyl cis-trans isomerase (PPI), cathepsin D and translocation proteins. Some genes, such as cathepsin D, are known estrogen-responsive targets. Cathepsin D is a lysosomal protease important for yolk formation in oviparous animals, but the human form also contains an estrogen responsive element in its promoter and is upregulated by E2 (Cavailles *et al.*, 1991; Kwon *et al.*, 2001). Other genes regulated in this study may be involved in the stability or formation of the ER complex for interaction with the DNA binding domains of target genes. PDI encodes a protein that is involved in enhancement of ER transcriptional activity by stabilizing DNA binding and has also been observed to be transcriptionally upregulated by E2 exposure in human, rat and fish models (Bowman *et al.*, 2002; Yoshikawa *et al.*, 2000). Hsp108 was previously found in oviparous animals and has a high homology with chaperone hsp90, which is part of a large molecular complex that stabilizes unliganded ER in the cytoplasm and protects it from proteosomal degradation (Kulomaa *et al.*, 1986). Other members of this ER multi-complex include PPI immunophilins and accessory chaperone hsp40 (Carrello *et al.*, 2004). Transcriptional upregulation of both ER chaperone proteins and downstream targets indicate the responses to E2 and dietary indoles are ER-mediated.

DIM has previously been found to be estrogenic *in vitro* through strong ligand-independent activation of ER that is mediated by PKA and MAPK signaling pathways (Riby *et al.*, 2000a; Leong *et al.*, 2004). Recent evidence suggests that MAPK and other serine/threonine kinases also mediate estrogenic signaling in trout liver, which may result in ligand-independent activation of ER and subsequent gene transcription

(Kullman *et al.*, 2003). We observed upregulation of several kinases by E2, I3C and DIM treatments in this study, including serine/threonine protein kinase (similar to PAS kinase) and NM23-H2/nucleoside diphosphate kinase B (NDPK-B), indicating that it is possible other intracellular signaling cascades may be activated by estrogens in trout liver. PAS kinase is a novel PAS domain-containing serine/threonine kinase in eukaryotes, however it is highly conserved throughout evolution (Rutter *et al.*, 2001). The signaling mechanisms of this recently identified kinase are not well understood, but PAS domains regulate the function of many intracellular signaling pathways in response to intrinsic and extrinsic stimuli including redox and nutrient status (Lindsley and Rutter, 2004). Also, NDPK-B, which is part of a class of NDPKs originally identified as housekeeping enzymes for synthesis of nucleoside triphosphates, has more recently been found to function in signal transduction and gene expression, including mediating G-protein activation of cell surface receptors and transcriptionally activating c-myc proto-oncogenes (Otero, 2000). NDPK expression is inversely correlated with tumor metastatic potential in a number of cancers including hepatocellular carcinoma (Bei *et al.*, 1998), but can be upregulated by estrogen via ER-alpha activation *in vitro* and by other tumor promoters during neoplastic transformation of epidermal cells (Shah *et al.*, 2004; Wei *et al.*, 2004). Taken together, these data suggest that kinase signaling pathways more typically associated with growth factors may be relevant for estrogenic responses, including dietary indoles, in trout liver. We are currently working to determine the relative importance of these mechanisms in trout by examining post-translational effects of E2 and indoles on kinase signaling pathways in liver.

In summary, we demonstrate that indole phytochemicals, I3C and DIM, acted similar to E2 at the transcriptional level based on correlation analysis of expression profiles and on clustering of gene responses. The transcriptional profiles in this study for E2, DIM and I3C provide insight into the mechanisms that may be important for promotion by estrogens in trout liver including genes involved in cell proliferation, signaling pathways and protein stability. Downregulation of transcripts for immune regulation, angiogenesis and cell adhesion indicate the possibility of estrogens and indoles having some protective effects against tumor invasion and metastasis. This data suggests that DIM may also promote hepatocarcinogenesis in trout by estrogenic mechanisms.

SUPPLEMENTAL DATA

Supplemental data are available at www.toxsci.oupjournals.org and Gene Expression Omnibus accession #GSE3324.

ACKNOWLEDGEMENTS

The authors wish to thank Eric Johnson and Greg Gonnerman for care and maintenance of fish and Caprice Rosato for array technical assistance. This work was supported by NIH grants ES07060, ES03850, ES00210, ES11267 and CA90890.

Chapter 3. Use of a rainbow trout oligonucleotide microarray to determine transcriptional patterns in aflatoxin B_1-induced hepatocellular carcinoma compared to adjacent liver

Susan C. Tilton[*†‡], Lena G. Gerwick[†§], Jerry D. Hendricks[*†], Caprice S. Rosato[¶], Graham Corley-Smith[†§], Scott A. Givan[¶], George S. Bailey[*†‡], Christopher J. Bayne[†§], and David E. Williams[*†‡]

[*]Department of Environmental & Molecular Toxicology, [†]Marine & Freshwater Biomedical Sciences Center, [‡]The Linus Pauling Institute, [§]Department of Zoology, [¶]Center for Gene Research and Biotechnology, Oregon State University, Corvallis, OR, 97331

Toxicological Sciences

http://toxsci.oxfordjournals.org/

88(2): 319-330, 2005.

ABSTRACT

Hepatocellular carcinoma (HCC) is one of the most common malignant tumors worldwide and its occurrence is associated with a number of environmental factors including ingestion of the dietary contaminant aflatoxin B_1 (AFB_1). Research over the last 40 years has revealed rainbow trout (*Oncorhynchus mykiss*) to be an excellent research model for study of AFB_1-induced hepatocarcinogenesis, however little is currently known about changes at the molecular level in trout tumors. We have developed a rainbow trout oligonucleotide array containing 1,672 elements representing over 1,400 genes of known or probable relevance to toxicology, comparative immunology, carcinogenesis, endocrinology and stress physiology. In this study, we applied microarray technology to examine gene expression of AFB_1-induced HCC in the rainbow trout tumor model. Carcinogenesis was initiated in trout embryos with 50 ppb AFB_1 and after 13 months control livers, tumors and tumor-adjacent liver tissues were isolated from juvenile fish. Global gene expression was determined in histologically confirmed HCCs compared to non-cancerous adjacent tissue and sham-initiated control liver. We observed distinct gene regulation patterns in HCC compared to non-cancerous tissue including upregulation of genes important for cell cycle control, transcription, cytoskeletal formation and the acute phase response and down regulation of genes involved in drug metabolism, lipid metabolism and retinol metabolism. Interestingly, the expression profiles observed in trout HCC are similar to the transcriptional signatures found in human and rodent HCC further supporting the validity of the model. Overall, these findings contribute to a better

understanding of the mechanism of AFB_1-induced hepatocarcinogenesis in trout and identify conserved genes important for carcinogenesis in species separated evolutionarily by more than 400 million years.

INTRODUCTION

HCC is one of the most common malignancies in humans worldwide, particularly in Southeast Asia, Japan and Africa. Even the relatively low incidence of HCC in the United States is rising and exhibits the fastest increase among solid tumors (El-Serag and Mason, 1999). The prevalence of HCC has been correlated with a number of environmental factors including chronic inflammatory liver diseases caused by viral infection and dietary exposure to AFB_1, a fungal metabolite that contaminates grain and legume supplies in the same parts of the world. AFB_1 is a potent carcinogen in certain animal models and epidemiological studies support the conclusion that it is also hepatocarcinogenic in humans (Chen *et al.*, 1996; Groopman *et al.*, 1996). Despite the fact that HCC is one of the few human cancers with known etiology, the molecular mechanisms involved in tumorigenesis are poorly understood and have only recently been investigated (Choi *et al.*, 2004; Graveel *et al.*, 2001; Meyer *et al.*, 2003; Okabe *et al.*, 2001).

The carcinogenicity of aflatoxins was first recognized in rainbow trout (Sinnhuber *et al.*, 1968), which have subsequently proven to be an excellent research model for the study of human hepatocarcinogenesis induced by AFB_1 and other

environmental carcinogens. The strengths of the trout model include its sensitivity to many classes of carcinogens, low spontaneous background tumor incidence and low cost husbandry for large-scale statistically valuable studies. More importantly, certain mechanisms of carcinogenesis have been well characterized in trout including carcinogen metabolism, DNA adduction and repair, oncogene activation and tumor pathology (reviewed by Bailey et al., 1996). Results from the study of tumor promotion and chemoprevention by environmental and dietary factors in AFB_1-initiated trout (Breinholt *et al.*, 1995; Oganesian *et al.*, 1999) have also been confirmed and extended in rodent studies (Manson *et al.,* 1998; Stoner *et al.*, 2002) as well as human clinical intervention trials (Egner *et al.*, 2001). Currently, however, the molecular mechanisms involved during tumorigenesis have not been described in trout and are not well understood in lower vertebrate models in general.

In this study, we describe construction of a custom rainbow trout 70-mer oligonucleotide array containing genes important for carcinogenesis, immunology, environmental toxicology, stress physiology and endocrinology. Trout are a well established and sensitive model for the evaluation of these different processes and existence of an array targeted to these mechanisms will provide a powerful tool to evaluate global molecular changes in the trout model. We applied the arrays to assess molecular changes in trout tumorigenesis by examining transcriptional patterns in AFB_1-induced HCC compared to non-cancerous adjacent liver and sham-initiated control liver. Transcriptional changes observed in this study were interpreted within the context of previously compiled data for pathological, physiological and biochemical changes during carcinogenesis. Recent studies have suggested that

comparative analyses of gene profiles across diverse species are more likely to highlight functional gene interactions important in key mechanisms of carcinogenesis (Segal *et al.*, 2005). Global analysis of molecular signatures in trout tumors not only provided information about these processes in an important model for environmental carcinogenesis, but the analyses were extended to identify mechanisms of tumorigenesis conserved throughout vertebrate evolution by comparing gene profiles in trout HCC with rodent and human HCC. Overall, we observed regulation of genes in a number of distinct functional classes important for carcinogenesis in trout, some of which indicate trout as a relevant model for invasive cancers and chronic inflammatory liver disease.

MATERIALS AND METHODS

Experimental animals and treatments. Mt. Shasta strain rainbow trout (*Oncorhynchus mykiss*) were hatched and reared at the Oregon State University Sinnhuber Aquatic Research Laboratory in 14°C carbon-filtered flowing well water on a 12:12 h light:dark cycle. All animal protocols were performed in accordance with Oregon State University Institutional Animal Care and Use Committee guidelines. Approximately 400 embryos were initiated at 21 days post-fertilization with an aqueous exposure of 50 ppb AFB_1 (Sigma, St. Louis, MO) for 30 min. Sham-exposed embryos were exposed to vehicle alone (0.01% ethanol) and served as non-initiated controls. After hatching, fry were fed Oregon Test Diet, a semi-purified casein-based

diet, *ad libitum* (2.8—5.6% body wt) five days per week for 50 weeks (Lee *et al.*, 1991). Initiated and sham-exposed fish were maintained separately at a density of 100 fish per 400 L tank under the same conditions as described for rearing. At 13 months of age trout were sampled for liver tumors over a 2-day period.

Necropsy and histopathology. At termination, fish were euthanized by deep anesthesia with 250 ppm tricaine methanesulfonate. Fish body weights were recorded and livers were removed, weighed and inspected for neoplasms under a dissecting microscope. After marking the size and location of all surface tumors, a portion of each tumor and 100-200 mg of adjacent liver tissue were collected, placed separately in TRIzol Reagent (Invitrogen, Carlsbad, CA) and quick frozen in liquid nitrogen for gene expression analysis. Precautions were taken to avoid contamination of adjacent liver samples with tumor tissue and samples were frozen within minutes of removal. The remaining liver was fixed in Bouin's solution for 2-7 days for histological analysis. Fixed livers were then cut into 1 mm slices with a razor blade to retrieve previously marked tumors. At least one piece of liver from each tumor-bearing fish was then processed by routine histological evaluation and stained with hematoxylin and eosin (H&E). Neoplasms were classified by the criteria of Hendricks *et al.* (1984) as either HCC or mixed carcinoma and only HCC tumors were used for microarray analysis.

Microarray construction and quality control. A rainbow trout 70-mer oligonucleotide array (OSUrbt ver. 2.0) containing 1,672 elements representing

approximately 1,400 genes was created at Oregon State University (Supplementary Table 1; also see http://www.science.oregonstate.edu/mfbsc/facility/micro.htm). Human sequences known to be involved in the physiological processes of carcinogenesis, immunology, endocrinology, toxicology, and other stress responses were chosen for the array based on several methods including interrogation of literature, use of commercially available targeted microarray gene lists and consultation of experts in respective fields for additional genes relevant for each process. The human full length amino acid sequences for each gene were then blasted (tBLASTn) into GenBank and The Institute for Genome Research (TIGR) rainbow trout database (http://www.tigr.org/tdb/tgi/rtgi). Trout sequences with an E-value < 10^{-10} were chosen as putative homologs. Oligonucleotides of 70 bases were designed for unique regions of each gene using ProbeSelect (Li and Stormo, 2001). Other oligonucleotide design considerations to minimize cross-hybridizations included proximity to the 3' end of the gene, avoidance of internal self annealing structures and a narrow T_m range across the entire oligonucleotide set. For each gene at least one 70-mer oligonucleotide was selected; however, for several genes, more than one distinct 70-mer was included in the array. Oligonucleotides were synthesized by Operon Technologies (Alameda, CA) and Sigma Genosys (The Woodlands, TX).

Oligonucleotides were resuspended in spotting buffer (3X SSC and 1.5 M betaine) at 25 μM final concentration and were printed onto Corning UltraGap slides (Acton, MA) using a Biorobotics Microgrid II arrayer (Genomic Solutions, Ann Arbor, MI) with 16 pins. The trout 70-mers were each printed in duplicate and a set of ten SpotReport Alien Oligos (Stratagene, La Jolla, CA) were printed 16 times (once

per block) on the array. Buffer only spots were included as negative controls. Test hybridizations of samples without alien spiking controls indicated that experimental cDNA does not cross-hybridize to alien spots on the array. After printing, slides were desiccated for 24-48 hrs and cross-linked with UV Stratalinker (Stratagene) at 600 mJ. Desiccation was chosen over baking as a post-processing method for drying slides based on resulting spot quality as determined by morphology and spot criteria in test hybridizations (data not shown). To assess printing quality and oligonucleotide retention, all slides were scanned for red reflectance using a ScanArray 4000 scanner (PerkinElmer, Boston, MA) and at least one slide from each printing was stained with Syto 61 (Molecular Probes, Eugene, OR) and scanned at 633 nm. Slides were stored under desiccation for no longer than 6 months prior to use.

RNA isolation. Total RNA was isolated from three individual trout HCC tumors and from corresponding adjacent liver tissue using TRIzol Reagent followed by cleanup with RNeasy Mini Kits (Qiagen, Valencia, CA) according to the manufacturer's instructions. RNA was isolated from only those tumors histologically identified as HCC and that were of an adequate size to yield at least 20 ug total RNA. RNA was also isolated from individual livers of ten sham-initiated trout and aliquots were pooled in equal amounts (μg) for use as a reference sample. RNA quality and quantity were assessed by agarose gel electrophoresis and spectrophotometric absorbance at 260/280 nm.

Microarray hybridization and analysis. Hybridizations were performed with the Genisphere Array 350 kit and instructions (Hatfield, PA) using standard reference design with dye-swapping. Briefly, 7 μg total RNA were reverse-transcribed with Superscript II (Invitrogen) using the Genisphere oligo d(T) primer containing a capture sequence for the Cy3 or Cy5 labelling reagents. Each reaction was spiked with a range of concentrations (0.0049 – 2.5 ng/μl) of the ten SpotReport Alien Oligo controls (Stratagene). Each cDNA sample containing the capture sequence for the Cy3 or Cy5 label was combined with equal amounts of reference cDNA (pooled from sham-initiated controls) containing the capture sequence for the opposite label. cDNA from two of the three biological replicates were dye-swapped and hybridized to two slides as technical replicates. cDNA from the reference sample was also hybridized to dye-swapped slides (against itself) following the same protocol as experimental samples for use as a negative control. Prior to hybridization, microarrays were processed post-printing by washing twice in 0.1% SDS for 5 min, 2X SSC, 0.1% SDS at 47°C for 20 min, 0.1X SSC for 5 min, water for 3 min, then dried by centrifugation. The cDNAs (25 μl) were hybridized to arrays in formamide buffer [50% formamide, 8X SSC, 1% SDS, 4X Denhardt's solution] for 16 h at 47°C with 22x25 mm Lifterslips (Erie Scientific, Portsmouth, NH). Arrays were then washed once in 2X SSC, 0.1% SDS at 47°C for 10 min, twice in 2X SSC, 0.1% SDS for 5 min, twice in 1X SSC for 5 min, twice in 0.1X SSC for 5 min and dried by centrifugation. Shaded from light, the Cy3 and Cy5 fluorescent molecules (3DNA capture reagent, Genisphere) were hybridized in formamide buffer for 3 h at

49°C to the corresponding capture sequences on cDNAs bound to the arrays. Arrays were washed in the dark with SSC containing 0.1 M DTT and dried as described earlier.

Scanned images (5 μm) were acquired with ScanArray Express (PerkinElmer, Boston, MA) at an excitation of 543 nm for Cy3 and 633 nm for Cy5 and at 90% power. The photomultiplier tube (PMT) settings for each fluor were set based on intensity of spiked internal alien controls to normalize among all slides in the experiment. Image files were quantified in QuantArray (PerkinElmer; Supplementary Table 2) and raw median signal and background values were exported to BioArray Software Environment (BASE; Saal *et al.*, 2002) for analysis. Data were background subtracted and normalized by LOWESS, which is recommended for two-color experiments to eliminate dye-related artifacts and produce ratios that are not affected by signal intensity values (Supplementary Table 3). Stringent criteria were used to filter for genes that were regulated at least 2-fold consistently in all features from biological replicates (n=3 per treatment) and had a p-value <0.05 by Welch's t-test (GeneSpring v.6, Silicon Genetics, Redwood City, CA). The genes that met these criteria were minimally categorized based on function using Gene Ontology and OMIM databases for putative homolog descriptions. Hierarchical clustering of gene expression profiles was performed in BASE, further filtering to identify similarities was performed with Array File Maker 4.0 (AFM; Breitkreutz *et al.*, 2001), and comparisons of microarray and real time PCR gene regulation were performed with GraphPad Prism (GraphPad Software, San Diego, CA).

Real time RT-PCR. To assess the authenticity of results from the microarray analyses, mRNAs for select genes were also analyzed by real time RT-PCR. Genes

for confirmation were chosen from each functional category, as determined by Gene Ontology, and were differentially up or down regulated or resulted in no change. Total RNA was isolated as described previously and was treated with DNase (Invitrogen) according to manufacturer's protocol. cDNA was synthesized from 2 μg RNA with an oligo $(dT)_{18}$ primer using SuperScript II (Invitrogen) following the manufacturer's instructions with a final volume of 100 μl. Synthesized cDNAs (1 μl) were used as templates for amplification of specific gene products in total volumes of 20 μl containing 1X SYBR Green master mix (DyNAmo qPCR kit, Finnzymes, Finland) and 0.3 μM of each primer. Primer sequences were as follows: 5'-GCTGCCTCCTCTTCCTCTCT-3' and 5'-GTGTTGGCGTACAGGTCTT-3' for β-actin; 5'-GGATCACTTCTCACGTCCAC-3' and 5'-TTAAACACAGTAAGCCC-ATC-3' for chemotaxin; 5'-CTTTGTTTGACTCCGACACG-3' and 5'-GAGAAA-TTTGCTTTTTGTGC-3' for CD63; 5'-CAGCCACCTGTGGAATGCAC-3' and 5'-AAAAATGGGATTCAATAGCC-3' for urokinase plasminogen activator receptor (UPAR); 5'-CAAATACAGACGCGTTGGAC-3' and 5'-GGCTGGTTCGTGACGG-ATGG-3' for retinol binding protein; 5'-TTGCCTTTGCCAACATCGAC-3' and 5'-CGGACATTGACGTATGCTTT-3' for vitellogenin; 5'- GATGTCTTTCTCACTGC-AACCT -3' and 5'-GCTGTCTTTTTCCTGGTCACT-3' for hepcidin; 5'-CCTGCGG-CACGGTCTT-3' and 5'-CTGACATCTTCATGCATCTCTTG-3' for differentially regulated trout protein (DRTP). Primer sequences were chosen so that the product contained the 70-mer array oligonucleotide sequence to ensure validation of the microarray experiment, except for β-actin which was used only for normalization

purposes. PCR was performed using a DNA Engine Cycler and Opticon 2 Detector (MJ Research, Waltham, MA). PCR was carried out for 35 cycles with denaturation at 94°C for 10 s, annealing at optimum temperature for primers (54-60°C) for 20 s and extension at 72°C for 12 s. DNA amplification was quantified (pg) from the C(T) value based on standard curves to ensure quantification was within a linear range. Standards were created from gel-purified PCR products (QIAX II, Qiagen, Valencia, CA) for each primer set after quantification with PicoGreen dsDNA Quantification Kit (Molecular Probes, Eugene, OR) and serial dilutions ranging from 0.25 to100 ng DNA. All signals were normalized against β-actin and ratios were calculated for treated samples compared to sham-initiated control as for the microarray analysis. Expression of β-actin was not altered by treatment based on either microarray analysis or RT-PCR and so was found to be an appropriate housekeeping gene for normalization in this study.

RESULTS

Liver Histopathology

Exposure of trout embryos to 50 ppb AFB_1 resulted in 5% liver tumor incidence with only one tumor per animal at 13 months of age whereas no tumors were observed in sham-initiated fish. This frequency is similar to what would be expected from historical AFB_1 exposure data (Oganesian *et al.*, 1999). Tumors were

determined to be approximately 30% HCC and 70% mixed carcinoma by histopathological examination and only HCC tumors were further evaluated for gene expression profiles. Histological examination showed distinct structural differences between HCC and non-tumor tissues (Fig. 3-1). The trout liver from both non-initiated controls and non-cancerous adjacent liver showed hepatocytes oriented in tubules with only two hepatocytes between adjacent sinusoids. However, HCC samples showed both increased basophilia and cellularity between adjacent sinusoids. These structural differences provided distinct borders between the HCC tissue and the surrounding liver.

Gene Expression Analysis

The rainbow trout 70-mer spotted oligonucleotide array, OSUrbt v2.0, has been developed as a collaboration between the Marine and Freshwater Biomedical Sciences Center and the Center for Gene Research and Biotechnology at Oregon State University. The OSUrbt v2.0 array contains 1,672 elements representing over 1,400 genes important for processes of carcinogenesis, environmental toxicology, comparative immunology, endocrinology and stress physiology. Existence of an array targeted to these mechanisms provides a powerful tool to evaluate global molecular changes in the trout model. The 70-mer oligonucleotides were designed for trout using multiple BLAST searches against annotated databases in GenBank and TIGR and the resulting oligos are annotated by sequence homology based on the top BLAST hit (E-value $<10^{-10}$; Table 3-1 and Supplementary Table 4). We report methods for spotting, post-processing and hybridization of trout arrays for strong sensitivity and

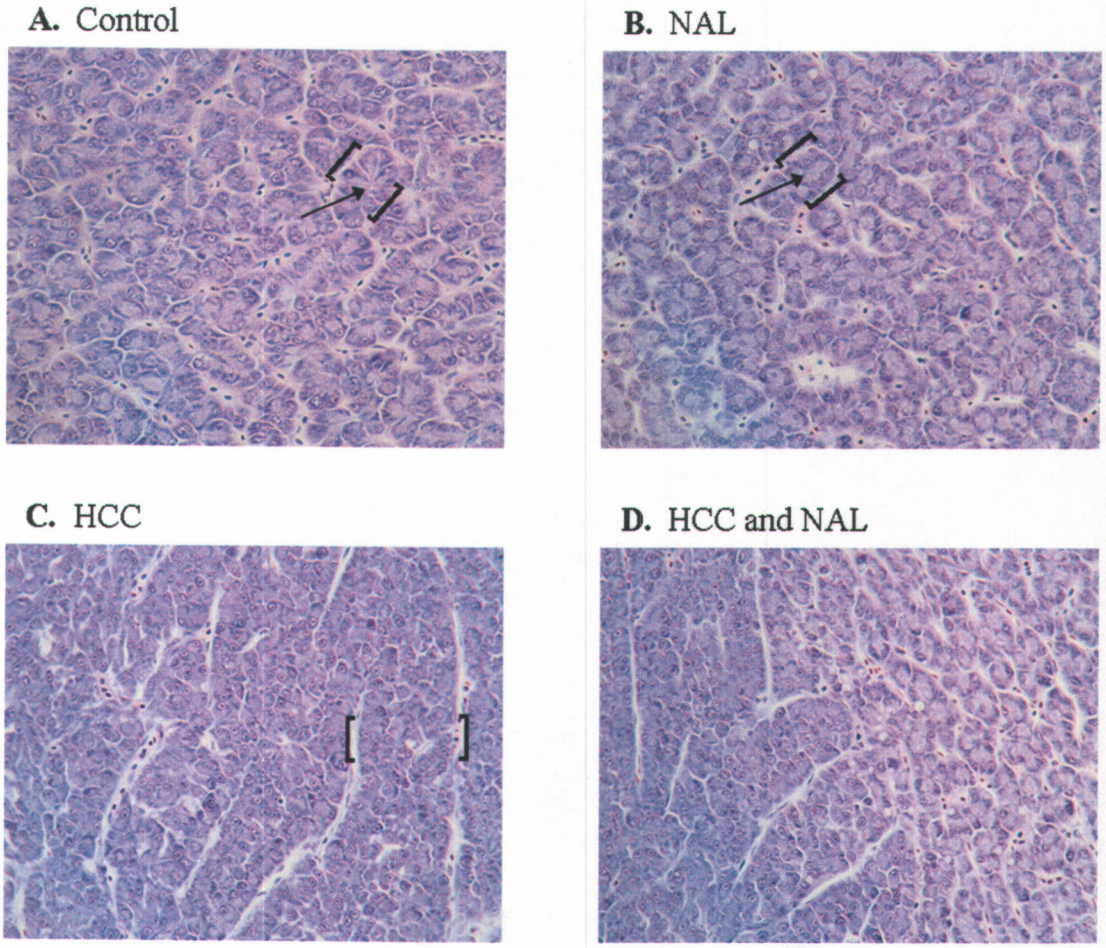

Figure 3-1. Representative H&E-stained histological sections of (A) sham-initiated control liver, (B) non-cancerous adjacent liver (NAL), (C) hepatocellular carcinoma (HCC) and (D) both HCC and NAL. (A, B) Hepatocytes oriented in tubules (shown in brackets) around a central bile canaliculus (arrow) with only two hepatocytes, end-to-end, between adjacent sinusoids. (C) Increased basophilia and cellularity between adjacent sinusoids (shown in brackets). (D) Border between HCC on left and NAL on right with characteristics similar to those described for panels (A, B, C). Magnification 32×.

TABLE 3-1

Select Genes Differentially Regulated in AFB_1-Initiated HCC Compared to Adjacent Liver Tissue

Array ID	TIGR ID[a]	Gene name (accession number, species)[b]	Average Fold Change (p-value)[c,d]			Reported in HCC or other cancers (OC)
			HCC/C	NAL/C	HCC/NAL	
Liver specific proteins (vitellogenesis)						
OmyOSU1540	TC65780	Vitelline envelope protein alpha (AF231706; *O. mykiss*)	**0.22** (0.007)	*1.15*	**0.19** (0.002)	
OmyOSU1552	TC55460	Vitelline envelope protein gamma (AF231708; *O. mykiss*)	**0.27** (0.001)	*1.12*	**0.26** (0.004)	
OmyOSU222	TC47576	Vitellogenin precursor (X92804; *Oncorhynchus mykiss*)	**0.21** (0.015)	*0.44*	*0.64*	
OmyOSU248	TC47577	Vitellogenin (X92804; *Oncorhynchus mykiss*)	**0.34** (0.02)	*0.63*	*0.57*	
OmyOSU203	TC47576	Vitellogenin precursor (X92804; *Oncorhynchus mykiss*)	**0.33** (0.004)	*1.31*	*0.32*	
Cell proliferation (signal transduction, transcription factors and cytokines)						
OmyOSU1615	TC50701	Transmembrane 4 superfamily member (AF281357; *O. mykiss*)	**3.84** (0.003)	*0.81*	**5.44** (0.008)	HCC[e]
OmyOSU39	TC61920	CD63 tetraspan protein (AY593998; *O. mykiss*)	**3.60** (0.028)	*0.95*	**3.79** (0.036)	HCC[e,f]
OmyOSU165	TC57084	Interferon inducible transmembrane protein 2 (AJ291989; *O. mykiss*)	**3.48** (0.029)	*0.77*	**5.34** (0.017)	OC[g]
OmyOSU983	TC86968	Interferon inducible transmembrane protein 1 (AJ291989; *O. mykiss*)	**2.50** (0.012)	*0.88*	**2.99** (0.006)	OC[g]
OmyOSU565	TC85655	Interluekin 8-like chemokine CK2 (AF418561; *O. mykiss*)	*1.30*	*0.52*	**2.50** (0.009)	HCC[h]
OmyOSU804	TC65531	Transcription factor JunB (Q800B3; *Fugu rubripes*)	*2.49*	*0.76*	**3.52** (0.005)	HCC[i]
OmyOSU435	TC54298	Calmodulin (J04046; *Homo sapiens*)	*2.09*	*0.66*	**3.11** (0.035)	HCC[j]
OmyOSU227	NP543968	Estrogen receptor beta (AJ289883; *Oncorhynchus mykiss*)	*2.11*	*0.72*	**2.94** (0.0009)	HCC[k]
OmyOSU347	TC54777	B-cell translocation gene 2 (AB036784; *Danio rerio*)	*2.02*	*0.66*	**3.05** (0.013)	OC[l]
Protein/Ion stability and transport						
OmyOSU471	TC71770	Procathepsin B (Q90WC3; *Oncorhynchus mykiss*)	**2.39** (0.031)	*1.02*	*2.41*	HCC[f,m]
OmyOSU497	TC78415	Cathepsin L-like cysteine peptidase (AY332270; *T. molitor*)	*2.35*	*0.61*	**3.82** (0.027)	HCC[e,f,m]

TABLE 3-1 (Continued)

Array ID	TIGR ID[a]	Gene name (accession number, species)[b]	Average Fold Change (p-value)[c,d]			Reported in HCC or other cancers (OC)
			HCC/C	NAL/C	HCC/NAL	
OmyOSU228	TC55313	Hepcidin (AF281354; *Oncorhynchus mykiss*)	**3.26** (0.015)	*0.40*	**8.33** (0.0006)	HCC[n,o]
OmyOSU685	TC54275	Ferritin middle subunit (S77386; *Salmo salar*)	**0.36** (0.025)	*0.49*	*0.77*	OC[p]
OmyOSU707	TC86600	Ferritin H-3 subunit (D86627; *Oncorhynchus mykiss*)	**0.32** (0.004)	*0.57*	*0.60*	OC[p]
Extracellular matrix and vascularization factors						
OmyOSU1263	TC62562	Plasminogen activator, urokinase receptor (AF007789; *R. norvegicus*)	**13.64**[d]	*0.95*	**13.26** (0.041)	HCC[q]
OmyOSU380	TC62562	Plasminogen activator, urokinase receptor (AF007789; *R. norvegicus*)	**3.57** (0.028)	*0.92*	**4.02** (0.027)	HCC[q]
OmyOSU562	TC62077	Collagen alpha 2(VIII) C1q (AF394686; *Salvelinus fontinalis*)	**3.53** (0.03)	*0.56*	**6.90** (0.006)	HCC[e]
OmyOSU744	TC51973	Putative interlectin, fibrinogen (AF281350; *O. mykiss*)	*3.58*	*0.50*	**7.22** (0.017)	HCC[e]
OmyOSU1502	TC50691	Tissue factor, blood coagulation (AJ295167; *Oncorhynchus mykiss*)	**0.10** (0.011)	*0.34*	*0.87*	HCC[r]
OmyOSU1551	TC54343	CD9 antigen, platelet aggregation (NM_212619; *Danio rerio*)	**0.42** (0.012)	*1.31*	**0.32** (0.0006)	HCC[s]
OmyOSU864	TC72628	Hemagglutinin aggregation factor (M96983; *L. polyphemus*)	**0.33** (0.036)	*2.16*	**0.24**[d]	
Redox regulation						
OmyOSU37	TC58221	Catalase (AAF89686; *Danio rerio*)	*0.63*	*2.11*	**0.30** (0.003)	HCC[t]
OmyOSU1422	TC47183	Thioredoxin (AAH49031; *Danio rerio*)	*2.54*	*0.54*	**4.83** (0.002)	HCC[u]
OmyOSU134	TC62472	Glutathione peroxidase 3 (AAH61950; *Mus musculus*)	*2.24*	*0.94*	**2.46** (0.027)	OC[v]
OmyOSU238	TC56389	Glutathione peroxidase 4 (AAO86704; *Danio rerio*)	*2.06*	*0.81*	**2.59** (0.0009)	HCC[e]
Drug, lipid, glucose and retinol metabolism/homeostasis						
OmyOSU1393	TC69788	Prostaglandin D synthase (AF281353; *Oncorhynchus mykiss*)	**0.05** (0.001)	**0.05** (0.0001)	*1.06*	OC[w]
OmyOSU1395	TC62304	Prostaglandin D synthase (AF281353; *Oncorhynchus mykiss*)	**0.13** (0.019)	**0.08** (0.0008)	*0.62*	OC[w]
OmyOSU1140	TC62082	Retinol binding protein (AF257326; *Oncorhynchus mykiss*)	**0.36** (0.007)	*1.19*	**0.30** (0.007)	HCC[x]

TABLE 3-1 (Continued)

Array ID	TIGR ID[a]	Gene name (accession number, species)[b]	Average Fold Change (p-value)[c,d]			Reported in HCC or other cancers (OC)
			HCC/C	NAL/C	HCC/NAL	
OmyOSU1142	TC62082	Retinol binding protein (AF257326; *Oncorhynchus mykiss*)	**0.37** (0.016)	*1.18*	**0.32** (0.014)	HCC[x]
OmyOSU352	TC72158	Cytochrome P450 2K1v2 (L11528; *Oncorhynchus mykiss*)	**0.26**[d]	*0.84*	**0.30** (0.046)	
OmyOSU354	TC72158	Cytochrome P450 2K3 (AF043551; *Oncorhynchus mykiss*)	**0.23**[d]	*0.79*	**0.27**[d]	
OmyOSU356	TC63105	Cytochrome P450 2P2 (AF117342; *Fundulus heteroclitus*)	**0.25**[d]	*0.90*	**0.26** (0.041)	
OmyOSU1380	TC94217	Cytochrome P450 2K1v3 (AF045053; *Oncorhynchus mykiss*)	**0.19** (0.005)	*0.74*	**0.26** (0.005)	
OmyOSU146	TC63282	Cytochrome P450 1A (AF059711; Oncorhynchus mykiss)	**0.25 (0.044)**	*0.84*	*0.33 (0.049)*	HCCe
OmyOSU460	TC62817	Aldo-keto reductase 1D1 (Z28339; Homo sapiens)	**0.17 (0.002)**	*0.89*	*0.19 (0.0002)*	HCCe
OmyOSU829	TC46928	20β-hydroxysteroid dehydrogenase (AF100931; O. mykiss)	**0.26 (0.022)**	*0.40*	*0.62*	HCCe
OmyOSU164	TC58328	Insulin-like growth factor II (M95184; Oncorhynchus mykiss)	**0.28 (0.018)**	*0.85*	*0.34 (0.002)*	HCCy
OmyOSU1194	TC50776	Tyrosine aminotransferase (Q8QZR1; Mus musculus)	**0.56**	*1.71*	*0.35 (0.013)*	HCCz
OmyOSU1451	TC69925	Cytosolic malate dehydrogenase (Q801E7; Oryzias latipes)	**0.44**	*1.31*	*0.34 (0.006)*	HCCaa
OmyOSU86	TC63296	Glucose-6-phosphatase (XM_702785; Danio rerio)	**0.55**	*2.01*	*0.28 (0.0.04)*	HCCe
Potential immunoregulators and acute phase response proteins						
OmyOSU268	TC71098	Chemotaxin (AF271114; *Oncorhynchus mykiss*)	*3.73*	**0.24** (0.049)	**16.90** (0.041)	HCC[bb]
OmyOSU232	TC91273	Differentially regulated trout protein (AF281355; *O. mykiss*)	**4.49** (0.007)	*0.30*	**23.94** (0.017)	
OmyOSU148	TC91273	Differentially regulated trout protein (AF281355; *O. mykiss*)	**3.91** (0.022)	*0.30*	**19.82** (0.014)	
OmyOSU1512	TC87050	Apolipoprotein A1 (AB183290; *Fugu rubripes*)	**6.69** (0.044)	*1.11*	**6.93** (0.039)	HCC[f]
OmyOSU766	TC78877	MHC class I heavy chain (AF296366; *Oncorhynchus mykiss*)	*3.02*	*0.54*	**6.16** (0.025)	HCC[cc]
OmyOSU756	TC80478	MHC class IA heavy chain precursor (AF115518; *O. mykiss*)	**3.22** (0.037)	*0.87*	**3.86** (0.012)	HCC[cc]
OmyOSU527	TC87038	Precerebellin-like protein (AF192969; *Oncorhynchus mykiss*)	*2.29*	*0.69*	**3.24** (0.022)	
OmyOSU29	TC87038	Precerebellin-like protein (AF192969; *Oncorhynchus mykiss*)	*1.78*	*0.74*	**2.41** (0.015)	
OmyOSU533	TC71048	Novel protein similar to gliacolin, C1Q (AL627248; *D. rerio*)	**2.69** (0.032)	*0.98*	**2.83** (0.016)	OC[dd]

TABLE 3-1 (Continued)

Array ID	TIGR ID[a]	Gene name (accession number, species)[b]	Average Fold Change (p-value)[c,d]			Reported in HCC or other cancers (OC)
			HCC/C	NAL/C	HCC/NAL	
OmyOSU375	TC73041	Complement component C1q (XM_417653; *Gallus gallus*)	*2.11*	*0.70*	**2.95** (0.041)	OC[dd]
OmyOSU407	TC87086	Complement component C7 (AJ566190; *O. mykiss*)	*2.00*	*0.76*	**2.61** (0.018)	OC[ee]
OmyOSU405	TC87533	Complement component 6 (BAD02321; *Homo sapiens*)	*1.93*	*0.72*	**2.62** (0.03)	OC[ee]
OmyOSU219	TC55520	Complement factor Bf-1 (Q9YGE7; *Oncorhynchus mykiss*)	**0.44** (0.003)	*1.85*	**0.28** (0.029)	
OmyOSU1477	TC55253	Trout C-polysaccharide binding protein 1 (AF281345; *O. mykiss*)	**0.14** (0.033)	*0.44*	*0.58*	
OmyOSU1478	TC55253	Trout C-polysaccharide binding protein 1 (AF281345; *O. mykiss*)	**0.10** (0.031)	*0.39*	*0.59*	

[a]TIGR ID number of the tentative consensus or singleton EST sequence corresponding to OSUrbt ver. 2 microarray feature.
[b]The most significant BLASTX is shown. If an EST has no significant (E-value < 10^{-6}) BLASTX hit, then the most significant BLASTN hit is shown (Supplementary Table 4). Genes have been categorized by function based on putative trout homolog using Gene Ontology and OMIM databases.
[c]Average fold change values represent background corrected, Lowess normalized signal ratios. Stringent criteria were used to filter for genes that were regulated at least 2-fold consistently in all features from biological replicates and had a p-value <0.05 by Welch's t-test. HCC = hepatocellular carcinoma; NAL = non-cancerous adjacent liver; C = sham-initiated control liver. Fold change values for genes that passed stringency criteria are in bold and those that did not pass are shown in italics.
[d]A few genes were consistently dysregulated >2.0 or <0.5-fold in all biological replicates, but had a p-value >0.50 by Welch's t-test due to individual variability.
[e]Meyer *et al.*, 2003; [f]Graveel *et al.*, 2001; [g]Jazaeri *et al.*, 2002; [h]Akiba *et al.*, 2001; [i]Borlak *et al.*, 2005; [j]Neo *et al.*, 2004; [k]Carruba *et al.*, 2004; [l]Ficazzola *et al.*, 2001; [m]Tumminello *et al.*, 1996; [n]Leong and Lonnerdal, 2004; [o]Weinstein *et al.*, 2002; [p]Kakhlon *et al.*, 2001; [q]Zheng *et al.*, 2000; [r]Poon *et al.*, 2003; [s]Kanetake *et al.*, 2001; [t]Ding *et al.*, 2004; [u]Choi *et al.*, 2004; [v]Lodygin *et al.*, 2005; [w]Su *et al.*, 2003; [x]Okabe et al., 2001; [y]Lu et al., 2005; [z]Ouyang *et al.*, 2002 ; [aa]Thirunavukkarasu *et al.*, 2001; [bb]Ovejero *et al.*, 2004; [cc]Chen *et al*, 2005; [dd]Bjorge *et al.*, 2005; [ee]Oka *et al.*, 2001.

technical reproducibility (Fig. 3-2). Analysis of technical controls indicate that dye-swapped replicates have a high level of reproducibility as do the duplicate spots printed on each slide. The correlation coefficients, r-values, were 0.93 ($r^2 = 0.86$) and 0.96 ($r^2 = 0.93$) for the duplicate slides and duplicate spots within an array, respectively, $p < 0.001$.

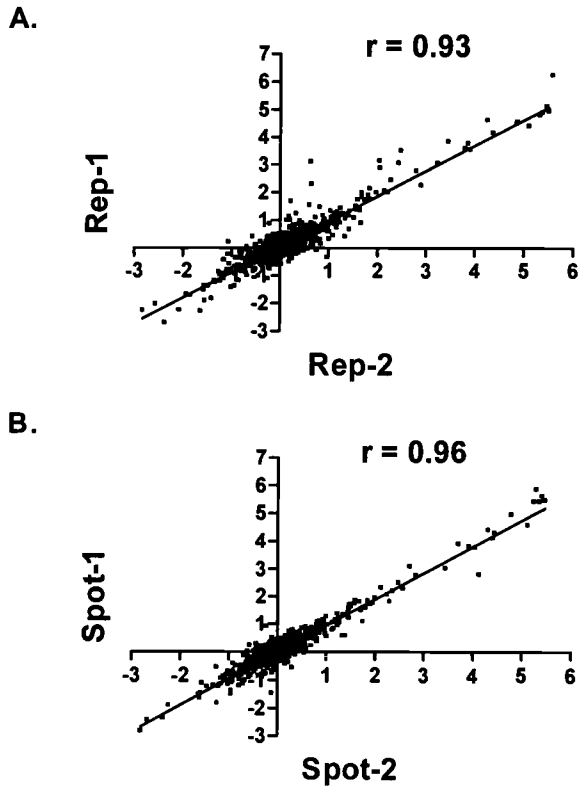

Figure 3-2. Pairwise analysis of gene profiles from (A) dye-swapped replicate slides and (B) replicate spots printed on each array. Values are fold change (log2) compared to reference sample and were plotted to generate correlation coefficients (r) among the replicates.

Hepatic gene expression was analyzed using the OSUrbt v2.0 array to characterize the mRNA profiles for AFB_1-initiated HCC compared to non-cancerous adjacent liver and sham-initiated control liver. As described in Materials and

Methods, RNA from individual HCC and adjacent liver tissue were hybridized to arrays with dye-swapping. Gene expression was examined in tumors and liver samples and genes were considered differentially expressed if their mRNA levels were consistently changed ≥ 2.0 or ≤ 0.5 fold and with a p-value <0.05 (Welch's t-test) among biological replicates (n=3). Hierarchical clustering was used as a visualization tool to identify similarities among biological replicates within a treatment and differences in gene expression between treatments. Bidirectional hierarchical clustering of all genes on the array (Fig. 3-3A) and a filtered subset of genes that were differentially regulated within a treatment (Fig. 3-3B) revealed distinct separations among the treatments by Pearson correlation. The HCC samples and non-cancerous adjacent liver samples were clustered to separate nodes in both instances indicating that there were distinct gene expression patterns between the treatment groups.

Overall, 55 elements were differentially regulated between HCC and the non-cancerous adjacent liver tissue (Table 3-1). Similarly, 40 elements were found to be regulated in HCC compared to sham-initiated control liver, whereas only 6 elements were expressed differentially in the non-cancerous adjacent liver samples compared to sham-initiated controls. Most elements on the array represent different genes; however, a few elements represent distinct oligonucleotide sequences for the same gene. For example, vitellogenin, prostaglandin D synthase, UPAR, retinol binding protein and DRTP are represented by multiple elements on the array and can serve to provide internal validation of our microarray results. In our negative control arrays, where the reference sample was hybridized against itself and dye-swapped, no genes

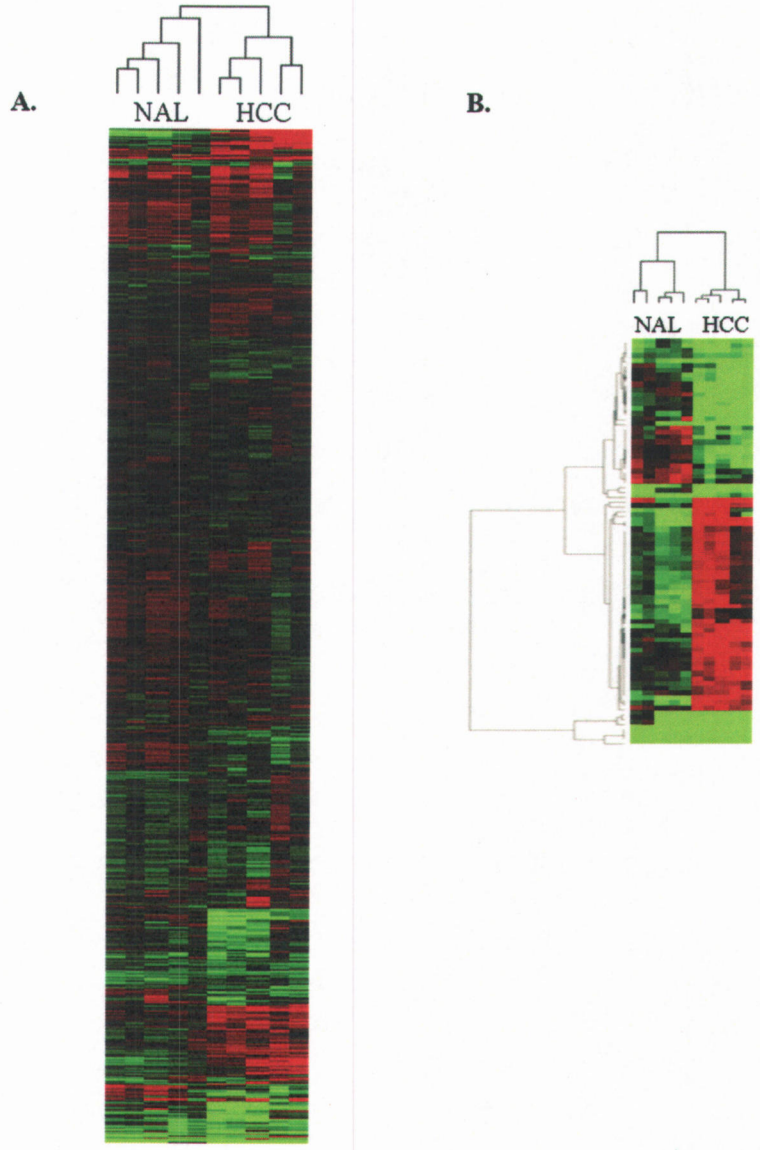

Figure 3-3. Clustering of gene expression in trout liver by Pearson correlation in AFB1-initiated HCC and non-cancerous adjacent liver (NAL). Results are shown as fold change compared to sham-initiated control liver for biological replicates (n=3 per treatment). Two of the three biological replicates were dye-swapped and these data are also included. *Red*, upregulation; *green*, down-regulation; *black*, unchanged expression; *grey*, missing values. (A) Gene expression profiles for all genes on the array. (B) Subgroup reflects gene expression profiles for genes differentially regulated 2-fold up or down in at least one treatment group.

were found to be differentially regulated. These arrays served to provide a technical validation of our microarray results.

The genes most highly upregulated in HCC included those known to be involved in regulation of cell growth, formation and maintenance of the extracellular matrix, immunoregulation and the acute phase response. Some immune- relevant genes, such as chemotaxin, were upregulated in HCC, but down-regulated in the non-cancerous adjacent liver resulting in strong expression of these genes in HCC, 5- to 30-fold above the adjacent tissue. Genes commonly down-regulated in HCC included those involved in drug, lipid, glucose and retinol metabolism, immunoregulation and vitellogenesis (estrogen-responsive liver proteins). The few genes differentially expressed in the non-cancerous adjacent tissue compared to sham controls included prostaglandin D synthase and chemotaxin. Thus, expression of genes from distinct functional classes are altered during AFB_1-initiated HCC in rainbow trout compared to non-cancerous adjacent or non-initiated liver and may be characteristic of molecular pathways important for tumorigenesis.

Real Time PCR Confirmation

The expression profiles of select genes that were found to be differentially increased or decreased in the microarray analysis, including chemotaxin, CD63, retinol binding protein, vitellogenin, UPAR, hepcidin and DRTP, were confirmed by real time RT-PCR using SYBR Green (Fig. 3-4). The same RNA preparations were used for each technique and the mean expression ratios for all samples in each treatment (n=3 biological replicates) were compared. Values for duplicate spots and

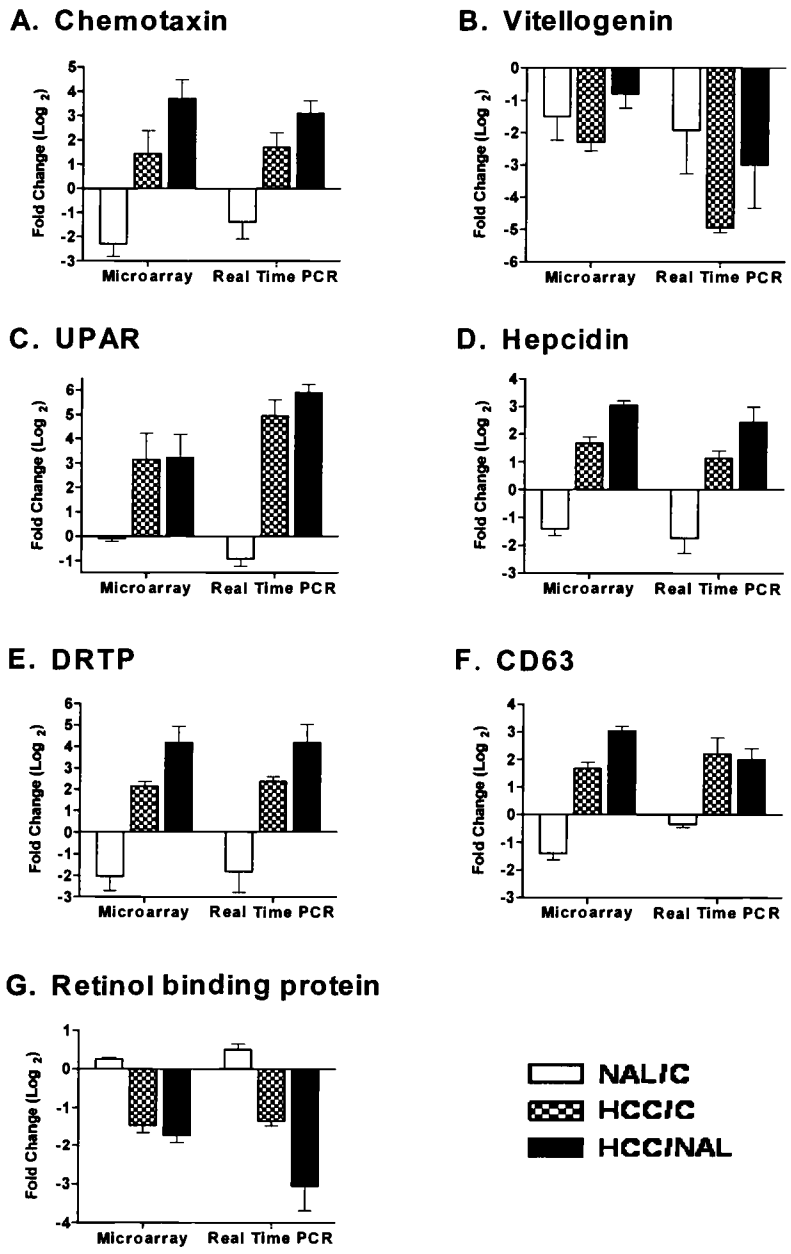

Figure 3-4. Hepatic gene expression in trout AFB1-initiated HCC and non-cancerous adjacent liver (NAL) measured by microarray and real time RT-PCR. HCC = hepatocellular carcinoma; NAL = non-cancerous adjacent liver; C = sham-initiated control liver. Values are expressed as average fold change (log2) with standard deviation (n=3 biological replicates) compared to non-initiated control liver or non-cancerous adjacent liver as indicated for select genes including (A) chemotaxin, (B) vitellogenin, (C) UPAR, (D) hepcidin, (E) DRTP, (F) CD63 and (G) retinol binding protein.

dye-swapped slides were averaged prior to analysis of biological replicates for microarray data. RT-PCR was more sensitive in several cases than microarray analysis and detected greater changes, but also resulted in higher variability among biological replicates in some of our assays. Overall, we were able to confirm gene expression profiles measured by oligonucleotide microarray analysis by RT- PCR. These data indicate that our strict criteria for determining differential gene regulation by array, including 2-fold change in all biological replicates with $p<0.05$, resulted in detection of meaningful changes that could be validated by other methods.

DISCUSSION

Evaluation of Gene Expression Profiles in Trout HCC

Rainbow trout have been used as a research model for environmental carcinogenesis for over 40 years. The strengths of this model have been described previously and include sensitivity to a number of carcinogens, low cost husbandry and well described tumor pathology, carcinogen metabolism, DNA adduction and mutational oncogene activation (Bailey *et al.*, 1996). Recently, a number of studies have been published utilizing microarray technology in trout and other salmonid models to examine gene expression patterns and functional classes important for stress responses, chemical toxicology and immune function supporting the strength of this model in biomedical research (Krasnov *et al.*, 2005a; Krasnov *et al.*, 2005b; Rise *et al.*, 2004a). In this study, we applied the OSUrbt v2.0 array to further evaluate trout as

a model for carcinogenesis based on molecular changes in AFB_1-induced HCC compared to non-cancerous adjacent liver and sham-initiated control liver. Tumorigenesis is a multistage process that involves a number of genetic alterations during initiation, promotion and progression of the disease. We detected distinct gene expression patterns in HCC compared to non-cancerous tissue in rainbow trout which are summarized in Table 3-1 and Fig. 3-3. In our study, the non-cancerous tissue surrounding HCC showed few transcriptional differences compared to non-initiated control liver indicating that it still maintained a relatively "normal" phenotype. This observation is further supported by the structural similarities observed between the two non-cancerous tissue types by histopathology (Fig. 3-1). Consequently, the genes regulated in HCC compared to both types of non-cancerous tissue were very similar and included genes relevant for cell proliferation, synthesis of the extracellular matrix, vascularization, oxidative stress, immune response and drug, lipid and retinol metabolism and homeostasis.

Genes encoding some proteins important for cell signaling and proliferation were upregulated in trout HCC. JunB, a proto-oncogene involved in cell cycle regulation, was the only oncogene transcriptionally upregulated in our study. Previous studies have found that hepatic tumors in trout initiated by AFB_1 and other carcinogens have a high incidence (71 – 100%) of mutationally activated Ki-ras oncogenic alleles (Bailey *et al.*, 1996). However, in this study, we did not observe transcriptional upregulation of the Ki-ras oncogene in HCC tumors. Also of interest was upregulation of the B-cell translocation gene 2 (BTG2), which is an effector protein of tumor suppressor genes important for regulation of the cell cycle. BTG2 is

an antiproliferative factor whose expression is upregulated in response to growth signals during tumorigenesis to promote cell cycle arrest and, thereby, helping to provide a 'growth brake' (Ficazzola *et al.*, 2001).

A number of genes associated with metabolism and homeostasis of drugs, lipids, glucose and retinol were down-regulated in trout HCC. Also down regulated were the liver-specific proteins involved in vitellogenesis. These transcriptional profiles suggest changes in normal liver function and differentiation in trout HCCs. Dedifferentiation in neoplastic development is supported by the step-wise progression from foci to benign to malignant tumors and has been well documented in rodents (Pitot *et al.*, 1996). Histopathological evidence exists for a similar type of progression in fish models; for example, HCC has been observed to develop within benign adenomas in trout liver (Bailey *et al.*, 1996; Okihiro and Hinton, 1999). The current data suggest that transcriptional profiles also support the process of dedifferentiation in trout neoplasia. Of particular interest is the decrease in expression of retinol-binding protein, which provides cellular storage for vitamin A in the liver. Low serum retinol, retinol binding protein or vitamin A has been correlated with neoplastic HCC (Okabe *et al.*, 2001; Schmitt-Graff *et al.*, 2003). Retinol and vitamin A therapy have been applied to patients with HCC or chronic liver disease (Moriwaki *et al.*, 2000) suggesting that reduced expression of these genes may play a crucial role in hepatocarcinogenesis.

Molecular Indicators of Metastatic Potential

A number of genes altered in trout HCC are involved in matrix-membrane associations, cell migration and metastasis and may be indicative of tumor invasive potential. UPAR, which was strongly upregulated, is a serine protease and part of the plasminogen activation system responsible for cell migration and matrix-membrane interactions important for cancer progression. UPAR is on the cell membrane and promotes degradation of the extracellular matrix, which is considered to be an early step in the invasion and metastasis of cancer (Zheng *et al.*, 2000). Two cysteine proteases, cathepsin L and pro-cathepsin B, were also upregulated in trout HCC. Similar to UPAR, these proteases function in protein stability and their activity is attributed to the ability of tumor cells to invade the extracellular matrix (Graveel *et al.*, 2001; Tumminello *et al.*, 1996). A member of the transmembrane 4 superfamily, CD63, which regulates cell growth and motility, was strongly upregulated and appears to also influence tumor progression and metastasis in other models serving as a good prognostic marker for disease (Graveel et al., 2001; Meyer et al., 2003). Other factors involved in coagulation and leukocyte aggregation were down-regulated in trout HCC and have been indicated in tumor metastasis. For example, CD9, which is also a member of the transmembrane superfamily 4, is important for platelet aggregation. Down-regulation of CD9 has been associated with tumor invasiveness and metastatic potential in a number of cancers (Kanetaka et al., 2001; Sauer *et al.*, 2003). Also, the pro-inflammatory cytokine, IL-8, which was upregulated in trout HCC has been found to promote angiogenesis in human HCC and may be important for vascularization required in both invasion and metastasis (Akiba *et al.*, 2001).

These transcriptional profiles indicate that AFB_1-induced HCC in trout is of an invasive and potentially aggressive nature, which further enhances the merits of the trout as a model for human HCC. Trout HCCs are composed of broad tubules with many basophilic hepatocytes between adjacent sinusoids (Fig. 3-1) that are capable of invasion and direct growth into surrounding tissues (Bailey *et al.*, 1996). However, metastasis is more common in trout over 2 years of age and histopathological analysis of HCC tumors in this study does not indicate invasive growth. Therefore, the genes expressed in malignant trout tumors at this stage may be early predictors of metastasis and could provide molecular targets for treatment.

Trout as a Model for Chronic Liver Disease and Inflammation

Also of interest was the regulation of genes found to be important in chronic liver disease and inflammation, including cytokines, chemokines and acute phase response proteins. Teleosts have a robust acute phase response and several of their acute phase proteins are known to exist in mammals where they function in innate immunity and inflammatory responses. Acute phase proteins are generally synthesized as an initial stress response to tissue injury, including such processes as malignant growth, and were upregulated in trout HCC. Hepcidin, for example, is a liver hormone induced during inflammation that controls iron homeostasis by negatively regulating intestinal iron absorption and was recently observed to be important in anemia of chronic liver disease (Leong and Lönnerdal, 2004). Iron-refractory anemia has been observed in liver adenomas of patients with glycogen storage disease caused by a deficiency in glucose-6-phosphatase, which results in the

inability to maintain glucose homeostasis (Weinstein *et al.*, 2002). We have previously observed disruption of iron homeostasis in trout neoplasms in studies where hepatocytes from carcinogen altered-foci and tumors were resistant to iron-loading and were deficient in glucose-6-phosphatase (Hendricks *et al.*, 1984; Lee *et al.*, 1989). In this study, hepcidin upregulation was also correlated with transcriptional down regulation of glucose-6-phosphatase along with down regulation of ferritin subunits in HCC tumors. While the molecular basis of anemia in chronic liver disease is not well understood, production of cytokines and interferons during inflammation has been correlated with anemia in patients and animal models. In our study a number of chemokines and cytokines were upregulated in trout HCC, which can regulate cell growth, differentiation and inflammation during carcinogenesis. These data indicate that rainbow trout may also provide a novel and relevant model for the study of anemia and inflammation in chronic liver disease.

Trout as a Model for Human HCC

One of the inherent strengths of microarray platforms is the ability to extrapolate data across multiple species. Such comparative analyses can highlight mechanisms that have a key role in processes such as carcinogenesis. Studies that have examined the relationship of gene profiles across diverse species found that transcriptional responses conserved across evolution were more likely to correspond to true functional interactions (Segal *et al.*, 2005). In this study, we found that most genes or gene classes differentially expressed in the trout tumor samples are conserved in human and rodent HCC or in other cancers (Table 1; Choi *et al.*, 2004; Graveel *et*

al., 2001; Meyer *et al.*, 2003; Okabe *et al.*, 2001). The fact that these studies utilized HCC of different etiologies (many viral) supports the likelihood that some processes of HCC pathogenesis have been conserved during long periods of evolutionary time.

In summary, we applied a novel rainbow trout oligonucleotide array to examine gene expression profiles in trout HCC compared to adjacent non-cancerous tissue and identified distinct gene classes important in hepatocarcinogenesis in trout. Genes whose altered expression were identified through our microarray studies were typical of those observed in HCC in humans and other mammalian models. This finding is consistent with the notion that HCC pathogenesis has been conserved during vertebrate evolution. The genes that were regulated seem to indicate that AFB_1-induced HCC in trout is of an invasive and aggressive nature and may also be indicative of changes observed during chronic inflammatory liver diseases, which further enhances the merits of the trout as a model for human HCC. Future work will evaluate gene expression during progression over time of HCC in trout and examine how gene expression profiles are altered in the presence of dietary tumor modulators.

SUPPLEMENTAL DATA

Supplemental data are available at www.toxsci.oupjournals.org and Geo Expression Omnibus at www.ncbi.nlm.nih.gov/geo/ accession #GSE2868.

ACKNOWLEDGEMENTS

The authors wish to thank Eric Johnson and Greg Gonnerman for care and maintenance of fish and Sheila Cleveland for histological preparation. This work was supported by NIH grants ES07060, ES03850, ES00210, ES11267 and CA90890.

Chapter 4. Gene expression analysis during tumor enhancement by the dietary phytochemical, 3,3'-diindolylmethane, in rainbow trout

Susan C. Tilton[1,2], Jerry D. Hendricks[1], Cliff B. Pereira[3,4], Gayle A. Orner[2], George S. Bailey[1,2,3] and David E. Williams[1,2,3*]

[1]Department of Environmental and Molecular Toxicology and Marine and Freshwater Biomedical Sciences Center, [2]Linus Pauling Institute, [3]Environmental Health Sciences Center and [4]Department of Statistics, Oregon State University, Corvallis, Oregon, 97331

Formatted for submission to Carcinogenesis

ABSTRACT

Indole-3-carbinol (I3C) and 3,3'-diindolylmethane (DIM), a primary I3C derivative *in vivo*, are known chemopreventive agents available as dietary supplements. However, I3C has also been found to act as a tumor promoter in rat (multi-organ) and trout (liver) models. I3C and DIM were previously found to be estrogenic in trout liver based on toxicogenomic profiles. In this study, we demonstrate that DIM promotes aflatoxin B_1 (AFB_1)-induced hepatocarcinogenesis in trout similar to 17β-estradiol (E2). Trout embryos were initiated with 50 ppb AFB_1 and then juvenile fish were fed diets containing 120 and 400 ppm DIM or 5 ppm E2 for 18 weeks. Tumor incidence was elevated in AFB_1-initiated trout fed 400 ppm DIM and 5 ppm E2. To evaluate the mechanism of tumor promotion, hepatic gene expression profiles were examined in animals on promotional diets during the course of tumorigenesis and in hepatocellular carcinomas (HCCs) of initiated animals using a rainbow trout 70-mer oligonucleotide array. We demonstrate that DIM alters gene expression profiles similar to E2 in liver samples during tumorigenesis and in HCC tumors. Further, HCCs from animals on DIM and E2 promotional diets had a transcriptional signature indicating decreased invasive or metastatic potential compared to HCCs from control animals. Overall, these findings confirm the importance of estrogenic signaling in the mechanism of dietary indoles in trout liver and indicate a possible dual effect that enhances tumor incidence and decreases potential for metastasis.

INTRODUCTION

3,3'-Diindolylmethane (DIM) is a major *in vivo* component of the glucobracissin, indole-3-carbinol (I3C), from cruciferous vegetables (Anderton *et al.*, 2004; Dashwood *et al.*, 1989; Stresser *et al.*, 1995a). DIM and I3C are also available as dietary supplements and promoted for their well established chemoprotective effects, particularly in estrogen-sensitive neoplasias such as breast cancer. Both I3C and DIM have been found to inhibit 7,12-dimethylbenzanthracene (DMBA)-induced mammary carcinogenesis in Sprague-Dawley rats when fed in the diet post-initiation (Chen *et al.*, 1998; Grubbs *et al.*, 1995). However, chemoprotection by I3C is most consistently observed in various target organs, including mammary and stomach (Wattenberg and Loub, 1978), liver (Bailey *et al*, 1991; Tanaka *et al.*, 1990), lung (Morse *et al.*, 1990) and colon (Xu *et al.*, 1996), of rodent and rainbow trout models when administered prior to or concurrent with the carcinogen and is thought to block initiation and subsequent adduct formation by modulation of phase I and phase II drug metabolizing enzymes (Bradfield and Bjeldanes, 1984; Dashwood et al., 1994). Other chemoprotective properties of I3C and DIM determined *in vivo* and *in vitro* include the ability to alter cell cycle progression, proliferation, apoptosis and DNA repair suggesting indoles may target other stages of carcinogenesis post-initiation (Kim and Milner, 2005). Interestingly, the ability of DIM to act as a cytostatic agent *in vitro* has been attributed to both anti-estrogenic and estrogenic effects that were not dependent on ligand binding to estrogen receptor (ER), but through cross-talk of ER signaling

with aryl hydrocarbon receptor (AhR) or kinase pathways (Chen *et al.*, 1998; Leong *et al.*, 2004).

Despite clear evidence for chemoprotection, I3C has been found to enhance tumor formation in multiple organs in rodent models (Kim *et al.*, 1997; Pence *et al.*, 1986; Stoner, *et al.*, 2002; Suzui *et al.*, 2005; Yoshida *et al.*, 2004) and in trout liver (Bailey *et al.*, 1987; Dashwood *et al.*, 1991) when fed in the diet long-term post-initiation. Large-scale studies in trout with multiple concentrations of carcinogen and I3C suggest that the promotional potency of I3C is at least as great as its potency as an anti-initiating agent in this model (Bailey *et al.*, 1991; Oganesian *et al.*, 1998). Mechanisms for enhancement are not well understood, but have been attributed to altered estrogen metabolism in endometrial adenocarcinoma, inhibition of apoptosis in colon carcinogenesis and biphasic activation of ER- and AhR-mediated responses in trout liver (Oganesian *et al.*, 1998; Suzui *et al.*, 2005; Yoshida *et al.*, 2004). The ability of DIM to enhance tumor formation in models similar to I3C has not been evaluated until now, but DIM has been increasingly promoted as a chemoprotective agent over I3C due to its chemical stability. Unlike I3C, it does not undergo acid-catalyzed oligomerization to products known to be potent AhR agonists (Bjeldanes *et al.*, 1991), although it is not known if the adverse tumor enhancing effects of I3C are due to these properties. In fact, we recently compared the transcriptional profiles of I3C in trout liver to those of two known hepatic tumor promoters, 17β-estradiol (E2) and β-naphthoflavone, ER and AhR agonists respectively, and found I3C to act similarly to E2 (Tilton *et al.*, 2005b). Further, DIM had a more potent estrogenic

effect than I3C based on transcriptional profiles suggesting it may also enhance hepatic tumors post-initiation in the trout model.

In this study, we determined the potential for DIM to promote aflatoxin B_1 (AFB_1)-induced hepatocarcinogenesis in trout similar to that previously reported for I3C. We further compared the mechanism of enhancement to E2 using a toxicogenomic approach. Hepatic gene expression profiles were examined in liver during the course of tumorigenesis and in hepatocellular carcinoma (HCC) of animals treated with DIM and E2 experimental diets during promotion. We demonstrate that DIM promotes AFB_1-initiated tumors in trout liver when fed in the diet for only 18 weeks. Transcriptional profiles in liver samples collected during promotion and in HCCs collected at termination showed strong correlation between DIM and E2 treatments. Interestingly, gene expression in HCC from trout on promotinoal diets indicated these tumors had a lower metastatic potential compared to control HCC. Overall, these data indicate that estrogenic mechanisms not only account for the promotional ability of DIM in trout liver, but also for the lower metastatic potential of resulting tumors.

MATERIALS AND METHODS

Materials

Analytical grade AFB_1 and E2 were purchased from Sigma Chemical (St. Louis, MO). DIM was kindly donated by BioResponse (Boulder, CO) and the purity was confirmed by HPLC. All other compounds were purchased from Sigma unless otherwise stated.

Experimental animals and treatments

Mt. Shasta strain rainbow trout (*Oncorhynchus mykiss*) were hatched and reared at the Oregon State University Sinnhuber Aquatic Research Laboratory in 14°C carbon-filtered flowing well water on a 12:12 h light:dark cycle. All animal protocols were performed in accordance with Oregon State University Institutional Animal Care and Use Committee guidelines. Approximately 4000 embryos were initiated at 21 days post-fertilization with an aqueous exposure of 50 ppb AFB_1 (Sigma, St. Louis, MO) for 30 min. Sham-exposed embryos were exposed to vehicle alone (0.01% ethanol) and served as non-initiated controls for each treatment. After hatching, fry were fed Oregon Test Diet, a semi-purified casein-based diet, for 3 months (Lee *et al.*, 1991). Trout were then randomly (within initiator group) divided into experimental treatment groups and fed OTD diets containing 0, 120, 400, 800 or 1200 ppm DIM or 5 ppm E2 in 0.1% DMSO vehicle *ad libitum* (2.8—5.6% body wt) five days per week for 18 weeks. However, due to dramatically low survival in the 800 and 1200 ppm groups (18.9% and 8.8%, respectively) compared to OTD or vehicle control groups ($P <$ 0.0001 Chi square test) for both sham and AFB_1-initiated animals, these treatments

were removed from analysis in the study. Diets were prepared monthly and stored frozen at -20°C until 2-4 days prior to feeding, when diets were allowed to thaw at 4°C. Duplicate 400 L tanks of 120 trout were maintained for each treatment group uder the same conditions described for rearing.

Necropsy and histopathology

Fish were sampled at 3-weeks, 15-weeks and 10 months after start of experimental diets and were euthanized at termination by deep anesthesia with 250 ppm tricaine methanesulfonate. At 3- and 15-week timepoints, livers were removed (n=3 fish per tank) and quick frozen in TRIzol reagent (Invitrogen, Carlsbad, CA) for RNA isolation. At 10 months, trout were sampled for liver tumors over a 5-day period. Fish body weights were recorded and livers were removed, weighed and inspected for neoplasms under a dissecting microscope. After marking the size and location of all surface tumors, a portion of each tumor was collected, placed separately in TRIzol Reagent (Invitrogen, Carlsbad, CA) and quick frozen in liquid nitrogen for gene expression analysis. The remaining liver was fixed in Bouin's solution for 2-7 days for histological analysis. Fixed livers were then cut into 1 mm slices with a razor blade to retrieve previously marked tumors. At least one piece of liver from each tumor-bearing fish was then processed by routine histological evaluation and stained with hematoxylin and eosin (H&E). Neoplasms were classified by the criteria of Hendricks *et al.* (1984).

RNA isolation

Total RNA was isolated from three individual trout HCC tumors and from corresponding adjacent liver tissue using TRIzol Reagent followed by cleanup with RNeasy Mini Kits (Qiagen, Valencia, CA) according to the manufacturer's instructions. RNA was isolated from only those tumors histologically identified as HCC and that were of an adequate size to yield at least 20 ug total RNA. RNA was also isolated from individual livers of ten sham-initiated trout and aliquots were pooled in equal amounts (μg) for use as a reference sample. RNA quality and quantity were assessed by agarose gel electrophoresis, bioanalyzer trace and spectrophotometric absorbance at 260/280 nm.

Microarray hybridization and analysis

Rainbow trout 70-mer oligonucleotide arrays (OSUrbt ver. 2.0) containing 1,672 elements representing approximately 1,400 genes were created at Oregon State University (http://www.science.oregonstate.edu/mfbsc/facility/micro.htm). Microarray construction and quality control have been described previously (Tilton *et al.*, 2005a). Hybridizations were performed with the Genisphere Array 350 kit and instructions (Hatfield, PA) using standard reference design with dye-swapping. Briefly, 7 μg total RNA were reverse-transcribed with Superscript II (Invitrogen) using the Genisphere oligo d(T) primer containing a capture sequence for the Cy3 or Cy5 labelling reagents. Each reaction was spiked with a range of concentrations (0.0049 – 2.5 ng/μl) of the ten SpotReport Alien Oligo controls (Stratagene). Each cDNA sample containing the capture sequence for the Cy3 or Cy5 label was combined with equal amounts of

reference cDNA (pooled from sham-initiated controls) containing the capture sequence for the opposite label. cDNA from two of the three biological replicates were dye-swapped and hybridized to two slides as technical replicates. cDNA from the reference sample was also hybridized to dye-swapped slides (against itself) following the same protocol as experimental samples for use as a negative control. Prior to hybridization, microarrays were processed post-printing by washing twice in 0.1% SDS for 5 min, 2X SSC, 0.1% SDS at 47°C for 20 min, 0.1X SSC for 5 min, water for 3 min, then dried by centrifugation. The cDNAs (25 μl) were hybridized to arrays in formamide buffer [50% formamide, 8X SSC, 1% SDS, 4X Denhardt's solution] for 16 h at 47°C with 22x25 mm Lifterslips (Erie Scientific, Portsmouth, NH). Arrays were then washed once in 2X SSC, 0.1% SDS at 47°C for 10 min, twice in 2X SSC, 0.1% SDS for 5 min, twice in 1X SSC for 5 min, twice in 0.1X SSC for 5 min and dried by centrifugation. Shaded from light, the Cy3 and Cy5 fluorescent molecules (3DNA capture reagent, Genisphere) were hybridized in formamide buffer for 3 h at 49°C to the corresponding capture sequences on cDNAs bound to the arrays. Arrays were washed in the dark with SSC containing 0.1 M DTT and dried as described earlier.

Scanned images (5 μm) were acquired with ScanArray Express (PerkinElmer, Boston, MA) at an excitation of 543 nm for Cy3 and 633 nm for Cy5 and at 90% power. The photomultiplier tube (PMT) settings for each fluor were set based on intensity of spiked internal alien controls to normalize among all slides in the experiment. Image files were quantified in QuantArray (PerkinElmer) and raw median signal and background values were exported to BioArray Software Environment (BASE; Saal *et al.*,

2002) for analysis. Data were background subtracted and normalized by LOWESS, which is recommended for two-color experiments to eliminate dye-related artifacts and produce ratios that are not affected by signal intensity values. Stringent criteria were used to filter for genes that were regulated at least 1.8-fold consistently in all features from biological replicates and had a P value <0.05 by Welch's t-test (GeneSpring v.6, Silicon Genetics, Redwood City, CA). The genes that met these criteria were minimally categorized based on function using Gene Ontology and OMIM databases for putative homolog descriptions. Hierarchical clustering of gene expression profiles was performed in GeneSpring and comparisons of microarray and real time PCR gene regulation were performed with GraphPad Prism (GraphPad Software, San Diego, CA).

Real time RT-PCR

To assess the authenticity of results from the microarray analyses, mRNAs for select genes were also analyzed by real time RT-PCR. Genes for confirmation were chosen from each functional category, as determined by Gene Ontology, and were differentially up or down regulated or resulted in no change. Total RNA was isolated as described previously and was treated with DNase (Invitrogen) according to manufacturer's protocol. cDNA was synthesized from 2 μg RNA with an oligo $(dT)_{18}$ primer using SuperScript II (Invitrogen) following the manufacturer's instructions with a final volume of 100 μl. Synthesized cDNAs (1 μl) were used as templates for amplification of specific gene products in total volumes of 20 μl containing 1X SYBR Green master mix (DyNAmo qPCR kit, Finnzymes, Finland) and 0.3 μM of each

primer. Primer sequences were as follows: 5'-GCTGCCTCCTCTTCCTCTCT-3' and 5'-GTGTTGGCGTACAGGTCTT-3' for β-actin; 5'-GGATCACTTCTCACGTCCA-C-3' and 5'-TTAAACACAGTAAGCCCATC-3' for chemotaxin (CTX); 5'-CAGCCACCTGTGGAATGCAC-3' and 5'-AAAAATGGGATTCAATAGCC-3' for urokinase plasminogen activator receptor (UPAR); 5'-TTGCCTTTGCCAACATCG-AC-3' and 5'-CGGACATTGACGTATGCTTT-3' for vitellogenin (VTG); 5'- GATG-TCTTTCTCACTGCAACCT -3' and 5'-GCTGTCTTTTTCCTGGTCACT-3' for hepcidin (HAMP); 5'-TTAGACCGAACTCCCCCTTG-3' and 5'-AAATCCCAACA-GCATTGCTC-3' for thioredoxin (THX); 5'-GTTGTAGCCCGATTGCCTTT-3' and 5'-GTTTGTGCTTGTGGTGGAAC-3' for collagen alpha 2 (COL2A); 5'- GGCCAA-AGGAGACATCGTTT-3' and 5'-TCCCAACCTACACCCTGACC-3' for trout C-polysaccharide binding protein 1 (TCPBP). Primer sequences were chosen so that the product contained the 70-mer array oligonucleotide sequence to ensure validation of the microarray experiment, except for β-actin which was used only for normalization purposes. PCR was performed using a DNA Engine Cycler and Opticon 2 Detector (MJ Research, Waltham, MA). PCR was carried out for 35 cycles with denaturation at 94°C for 10 s, annealing at optimum temperature for primers (54-60°C) for 20 s and extension at 72°C for 12 s. DNA amplification was quantified (pg) from the C(T) value based on standard curves to ensure quantification was within a linear range. Standards were created from gel-purified PCR products (QIAX II, Qiagen, Valencia, CA) for each primer set after quantification with PicoGreen dsDNA Quantification Kit (Molecular Probes, Eugene, OR) and serial dilutions ranging from 0.25 to100 ng DNA. All signals were normalized against β-actin and ratios were calculated for

treated samples compared to sham-initiated control as for the microarray analysis. Expression of β-actin was not altered by treatment based on either microarray analysis or RT-PCR and so was found to be an appropriate housekeeping gene for normalization in this study.

Statistical analysis

Tumor incidence and incidence of multiple tumors in tumor-bearing fish were modeled by logistic regression (Genmod procedure in SAS v. 9.1). Variation between tanks was examined for consistency with the binomial assumption through examination of deviance residuals and comparison of the residual deviance to the degrees of freedom (Chi-square test). P-values for differences between pairs of treatments are Wald Chi-square tests.

RESULTS

Tumor incidence

Tumor incidence was significantly enhanced in trout fed 400 ppm DIM ($P = 0.0003$) and 5 ppm E2 ($P < 0.0001$) in the diet for 18 weeks post-initiation by AFB_1 (Fig. 4-1). No tumors were observed in sham-initiated animals. Multiplicity was not greatly enhanced by DIM and E2 treatments and the average number of tumors per tumor bearing animal was 1.00, 1.17, 1.20, 1.29 and 1.15 for OTD control, vehicle control, 120 ppm DIM, 400 ppm DIM and 5 ppm E2, respectively. Variation between tanks

was consistent with the binomial assumption based on examination of deviance residuals and a residual deviance lack of fit test (Chi-square p-value = 0.24). The spectrum of tumor types determined by histopathological examination was the same as previously observed (Bailey *et al.*, 1996) and included malignant or benign neoplasms

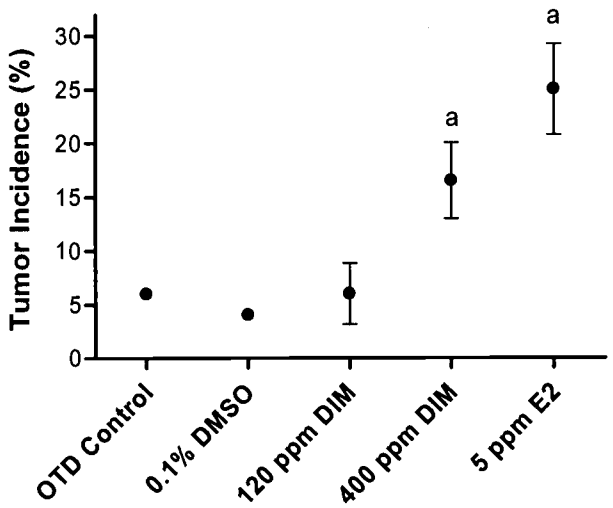

Figure 4-1. Liver tumor incidence (% of trout with tumors) in AFB_1-initiated trout fed 3,3'-diindolylmethane (DIM) and 17β-estradiol (E2). Each treatment consisted of duplicate tanks with between 70 and 100 animals. [a]Indicates significantly higher ($P < 0.001$) tumor incidence than vehicle control (0.1% DMSO) animals.

of hepatocellular, cholangiocellular or mixed hepatocellular/cholangiocellular origin (Table 4-1). While there was some variation in tumor types among treatments, the overall frequency of different tumor types in this study, including HCC, was consistent with historical observations in AFB_1-initiated trout (Nunez *et al.*, 1989; Oganesian *et al.*, 1999; Bailey *et al.*, 1996). Overall tumor occurrences were as follows: HCC (36.2%); mixed carcinoma (50.3%); hepatocellular adenoma (10.8%); and cholangiocellular carcinoma (2.7%). Only tumors histologically identified as

HCC were further evaluated for gene expression analysis. Histological examination of HCC tumors showed distinct structural differences between HCC and non-tumor tissues (representative images previously published in Tilton *et al.*, 2005a). Non-initiated control liver and non-cancerous liver surrounding HCC showed hepatocytes oriented in tubules with only two hepatocytes between adjacent sinusoids, while HCC samples showed both increased basophilia and cellularity between adjacent sinusoids. These structural differences provided distinct borders between the HCC tissue and surrounding liver.

TABLE 4-1

Histological Classification of Liver Tumors in AFB_1-Initiated Trout

	Percent of total tumors by tumor type[a]			
Treatment	HCC	MC	HCA	CCC
Control	44.4	44.4	11.1	0.0
0.1% DMSO	42.9	42.9	14.3	0.0
120 ppm DIM	45.5	54.5	0.0	0.0
400 ppm DIM	22.2	55.6	18.5	3.7
5 ppm E2	33.9	47.5	10.2	8.5
Overall average	37.8	49.0	10.8	2.4

[a]HCC, hepatocellular carcinoma; MC, mixed carcinoma; HCA, hepatocellular adenoma; CCC, cholangiocellular carcinoma.

Gene expression analysis

The OSUrbt v2.0 array was used to characterize transcriptional profiles in liver samples and in HCC tumors from animals fed promotional diets of E2 and DIM compared to control animals. Gene expression was analyzed in liver samples collected from sham and AFB_1-initiated trout treated with 0.1% DMSO vehicle, 5 ppm

E2 and 400 ppm DIM at the 3-week and 15-week timepoints during feeding of experimental diets. Each treatment is represented by biological replicates (n = 2) of RNA pooled from 3 individual liver samples. Array hybridizations were performed with a common reference sample using dye-swapping and final fold-change values are calculated as a ratio to appropriate control animals matched for timepoint and initiation-status. Pairwise analysis of all 1,672 features on the array indicated strong correlations in transcriptional patterns between E2 and 400 ppm DIM treatments in AFB_1-initiated animals at both the 3- and 15-week timepoints, R = 0.84 and 0.76 ($P < 0.001$), respectively (Fig. 4-2, panels A and B). Genes were considered differentially expressed if their mRNA levels were consistently changed ≥ or ≤ 1.8-fold compared to appropriate vehicle controls with $P < 0.05$ (Welch's t-test) among biological replicates. Genes that passed the stringency filter are listed in Table 4-2. Gene descriptions are provided based on sequence homology using the most significant ($E<10^{-6}$) BLASTX or BLASTN hit against the current GenBank databases. Genes were categorized by function based on putative trout homolog using the Gene Ontology and OMIM databases. Bidirectional hierarchical clustering of genes differentially regulated in at least one treatment group (Fig. 4-3) supported the pairwise analysis by Pearson correlation also indicating there was a high degree of similarity in gene expression patterns between E2 and DIM treatments. Clustering analysis further indicated distinct regulation patterns in all treatments between the two timepoints. Principal component analysis (PCA) is an exploratory multivariate statistical technique that reduces dimensionality by performing a covariance analysis between factors and was applied on conditions to explore correlations between

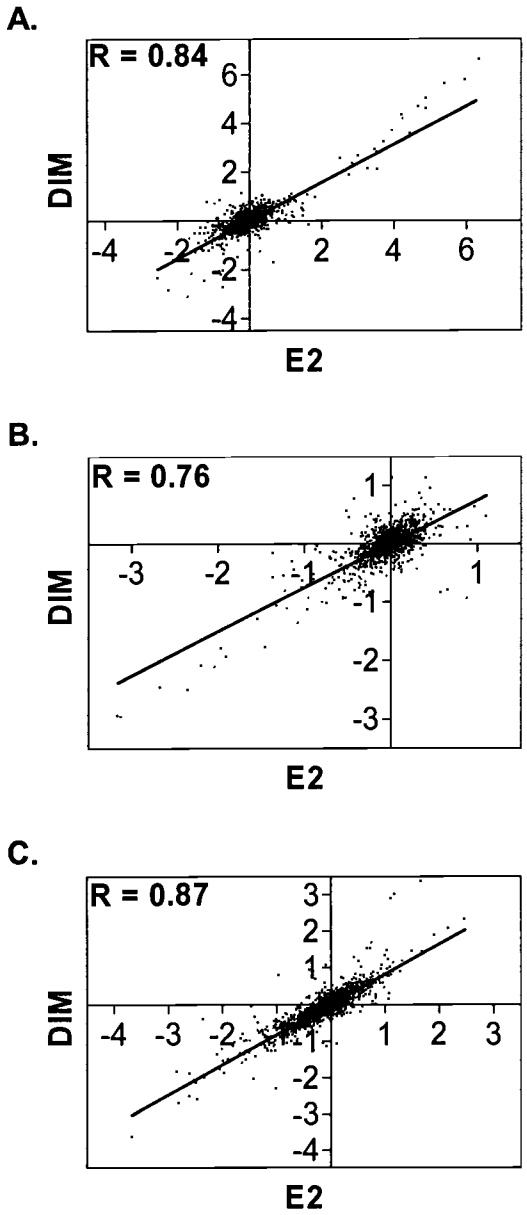

Figure 4-2. Pairwise correlations of gene profiles in (A) liver samples from AFB_1-initiated trout fed 5 ppm E2 and 400 ppm DIM for 3 weeks; (B) liver samples from AFB_1-initiated trout fed 5 ppm E2 and 400 ppm DIM for 15 weeks; (C) HCC tumors from trout fed 5 ppm E2 and 400 ppm DIM. Values are fold change (log_2) compared to appropriate vehicle-treated control samples and were plotted to generate correlation coefficients (R) among the treatments, $P < 0.001$.

TABLE 4-2

Select Genes Differentially Regulated in Trout Liver During Tumorigenesis on Promotional Diets

Array ID	TIGR ID[a]	Gene name (accession number, species)[b]	Average Fold Change (*P* value)[c]			
			Control AFB_1	DIM Sham	DIM AFB_1	E2 AFB_1
3-Week Timepoint:						
Liver specific proteins (vitellogenesis)						
OmyOSU222	TC47576	Vitellogenin precursor (X92804; *O. mykiss*)	0.68	**62.78** (0.001)	**99.23** (0.000)	**81.72** (0.000)
OmyOSU248	TC47577	Vitellogenin (X92804; *Oncorhynchus mykiss*)	0.84	**29.66** (0.000)	**49.49** (0.000)	**42.25** (0.000)
OmyOSU1542	TC85700	Zona radiata structural protein (AF407574; *O. mykiss*)	0.97	**26.64** (0.000)	**24.67** (0.000)	**29.57** (0.000)
OmyOSU203	TC47576	Vitellogenin precursor (X92804; *O. mykiss*)	0.95	**27.14** (0.000)	**25.56** (0.000)	**25.66** (0.000)
OmyOSU1540	TC65780	Vitelline envelope protein alpha (AF231706; *O. mykiss*)	1.19	**19.77** (0.000)	**18.14** (0.000)	**19.00** (0.000)
OmyOSU1552	TC55460	Vitelline envelope protein gamma (AF231708; *O. mykiss*)	0.85	**23.34** (0.000)	**20.31** (0.000)	**18.68** (0.000)
Cell proliferation (signal transduction, growth factors and apoptosis)						
OmyOSU212	TC70106	TATA-binding protein (AY168633; *D. rerio*)	0.84	**18.45** (0.000)	**12.89** (0.005)	**15.60** (0.001)
OmyOSU244	NP543968	Estrogen receptor beta (AJ289883; *O. mykiss*)	0.85	**4.62** (0.000)	**5.88** (0.000)	**5.73** (0.000)
OmyOSU151	TC88754	Estrogen receptor alpha (M31559; *O. mykiss*)	1.04	**3.01** (0.003)	1.73 (0.006)	**2.47** (0.000)
OmyOSU1615	TC81096	Transmembrane 4 superfamily member 5 (AF281357; *O. mykiss*)	0.80	1.83 (0.002)	**2.19** (0.007)	**2.78** (0.000)
OmyOSU511	TC86507	Ras-like GTPase (BC076026; *Danio rerio*)	1.26	**2.20** (0.000)	1.75 (0.003)	1.79 (0.003)
OmyOSU800	TC72880	Non-receptor tyrosine kinase 2 (TYK2) (AF173032; *M. musculus*)	1.03	**2.45** (0.014)	1.32	**2.82** (0.001)
OmyOSU915	TC78497	Cysteine-rich with EGF-like domains 1 (CR751234; *Danio rerio*)	1.07	**2.15** (0.003)	1.91 (0.005)	**2.29** (0.002)
OmyOSU313	TC76141	Bone morphogenic protein 7 (S77477; *Gallus gallus*)	1.04	**0.33** (0.005)	**0.33** (0.000)	**0.24** (0.000)
OmyOSU285	CA364711	Birc4 protein, XIAP (BC055246; *Danio rerio*)	1.10	**0.38** (0.015)	**0.41** (0.000)	**0.36** (0.000)
Protein stability and transport						
OmyOSU139	TC70102	Cathepsin D (U90321; *O. mykiss*)	0.86	1.99 (0.005)	**2.07** (0.007)	**3.05** (0.000)
OmyOSU853	TC81488	Heat shock protein hsp90 (BC075757; *Danio rerio*)	1.04	**2.55** (0.001)	1.97	**2.16** (0.004)

TABLE 4-2 (Contintued)

Array ID	TIGR ID[a]	Gene name (accession number, species)[b]	Average Fold Change (*P* value)[c]			
			Control AFB_1	DIM Sham	DIM AFB_1	E2 AFB_1
3-Week Timepoint:						
OmyOSU992	TC88878	MAL proteolipid protein 2 (BC078522; *Xenopus laevis*)	0.92	1.63 (0.001)	1.70 (0.002)	**2.08** (0.000)
Nucleic acid metabolism						
OmyOSU1518	TC80929	Uridine phosphorylase (D44464; *Mus musculus*)	0.95	**7.60** (0.000)	**7.07** (0.000)	**11.59** (0.000)
OmyOSU252	TC70900	Hypoxanthine-guanine phosphoribosyltransferase (AJ132697; *Gallus gallus*)	0.83	**5.71** (0.004)	**4.81** (0.009)	**7.37** (0.003)
Transcription and translation						
OmyOSU1667	TC78247	Poly A binding protein 1 (BC003870; *Mus musculus*)	1.06	**1.89** (0.000)	1.67 (0.007)	**1.90** (0.000)
OmyOSU217	TC86507	Ribosomal protein L13a (BC047855; *Danio rerio*)	1.03	**2.09** (0.000)	1.75 (0.005)	1.74 (0.000)
Immune function and acute phase response						
OmyOSU1106	TC77195	Recombination-activating protein 2 (U31670; *O. mykiss*)	0.87	1.89 (0.025)	**2.14** (0.029)	**2.26** (0.002)
OmyOSU1169	CA369420	Perforin 1 (XM_683237; *Danio rerio*)	1.08	**2.47** (0.000)	1.62	**2.80** (0.001)
OmyOSU539	TC87038	Precerebellin-like protein (AF192969; *O. mykiss*)	0.80	**0.44** (0.004)	0.70 (0.002)	**0.35** (0.000)
OmyOSU1563	TC78004	Immunoglobulin light chain F class (U25705; *I. punctatus*)	2.69	2.36 (0.010)	**0.12** (0.001)	**0.31** (0.005)
OmyOSU268	TC71098	Chemotaxin (AF271114; *Oncorhynchus mykiss*)	0.47	**0.16** (0.049)	**0.43** (0.006)	**0.41** (0.003)
Drug, lipid, retinol metabolism/homeostasis						
OmyOSU146	TC63282	Cytochrome P450 1A (AF059711; *Oncorhynchus mykiss*)	1.37	**2.42** (0.002)	1.42 (0.043)	0.95
OmyOSU352	TC72158	Cytochrome P450 2K1v2 (L11528; *Oncorhynchus mykiss*)	0.95	0.59 (0.017)	0.54 (0.019)	**0.38** (0.001)
OmyOSU354	TC72158	Cytochrome P450 2K3 (AF043551; *Oncorhynchus mykiss*)	0.97	0.66	0.61 (0.006)	**0.32** (0.001)
OmyOSU971	TC69719	Glutathione S-transferase (AB026119; *Oncorhynchus mykiss*)	0.74	0.58	0.52 (0.010)	**0.49** (0.009)
OmyOSU395	TC71381	Arachidonate 5-lipoxygenase (L42198; *Mus musculus*)	0.86	**0.52** (0.000)	**0.47** (0.019)	**0.49** (0.012)
OmyOSU343	TC69983	Biotinidase fragment 2 (AF281333; *Oncorhynchus mykiss*)	1.12	**0.48** (0.016)	**0.45** (0.000)	**0.40** (0.000)

TABLE 4-2 (Contintued)

Array ID	TIGR ID[a]	Gene name (accession number, species)[b]	Average Fold Change (*P* value)[c]			
			Control AFB_1	DIM Sham	DIM AFB_1	E2 AFB_1
15-Week Timepoint:						
Immune function and acute phase response						
OmyOSU232	TC91273	Differentially regulated trout protein (AF281355; *O. mykiss*)	2.88	0.58	**0.13** (0.00)	**0.11** (0.001)
OmyOSU148	TC91273	Differentially regulated trout protein (AF281355; *O. mykiss*)	2.75	0.66	**0.13** (0.001)	**0.11** (0.000)
OmyOSU268	TC71098	Chemotaxin (AF271114; *Oncorhynchus mykiss*)	1.09	**0.16** (0.049)	**0.18** (0.016)	**0.16** (0.005)
OmyOSU228	TC55313	Hepcidin (AF281354; *Oncorhynchus mykiss*)	1.81	0.72	**0.26** (0.001)	**0.27** (0.008)
OmyOSU878	CA367917	LECT2 neutrophil chemotactic factor (AF363272; *O. mykiss*)	0.92	**0.18** (0.025)	**0.29** (0.002)	**0.26** (0.015)
OmyOSU744	TC71412	Putative interlectin (AF281350; *O. mykiss*)	1.66	0.73	**0.29** (0.013)	**0.37** (0.042)
OmyOSU165	TC90142	Interferon Inducible Protein 2 (AJ313031; *O. mykiss*)	1.71 (0.026)	0.90	**0.39** (0.002)	**0.48** (0.003)
Drug, lipid, retinol metabolism/homeostasis						
OmyOSU1422	TC47183	Thioredoxin (AAH49031; *Danio rerio*)	1.00	0.38	**0.18** (0.009)	**0.20** (0.010)
OmyOSU115	TC78741	Glutathione S-transferase class-pi (L40381; *C. longicaudatus*)	2.76 (0.034)	0.54	**0.23** (0.010)	**0.22** (0.009)
OmyOSU153	TC89948	Liver fatty acid binding protein (AF281344; *O. mykiss*)	1.03	0.31	**0.23** (0.015)	**0.25** (0.012)

[a]TIGR ID number of the tentative consensus or singleton EST sequence corresponding to OSUrbt ver. 2 microarray feature.
[b]The most significant BLASTX is shown. If an EST has no significant (E-value < 10^{-6}) BLASTX hit, then the most significant BLASTN hit is shown. Genes have been categorized by function based on putative trout homolog using Gene Ontology and OMIM databases.
[c]Average fold change values represent background corrected, Lowess normalized signal ratios. Stringent criteria were used to filter for genes that were regulated at least 1.8-fold consistently in all features from biological replicates and had a p-value <0.05 by Welch's t-test. Fold change values for genes that passed stringency criteria are in bold. Animals were initiated with aflatoxin B_1 (AFB_1) or sham initiated (Sham) and then fed 3,3'-diindolylmethane (DIM) or 17β-estradiol (E2) in the diet for 18 weeks post-initiation.

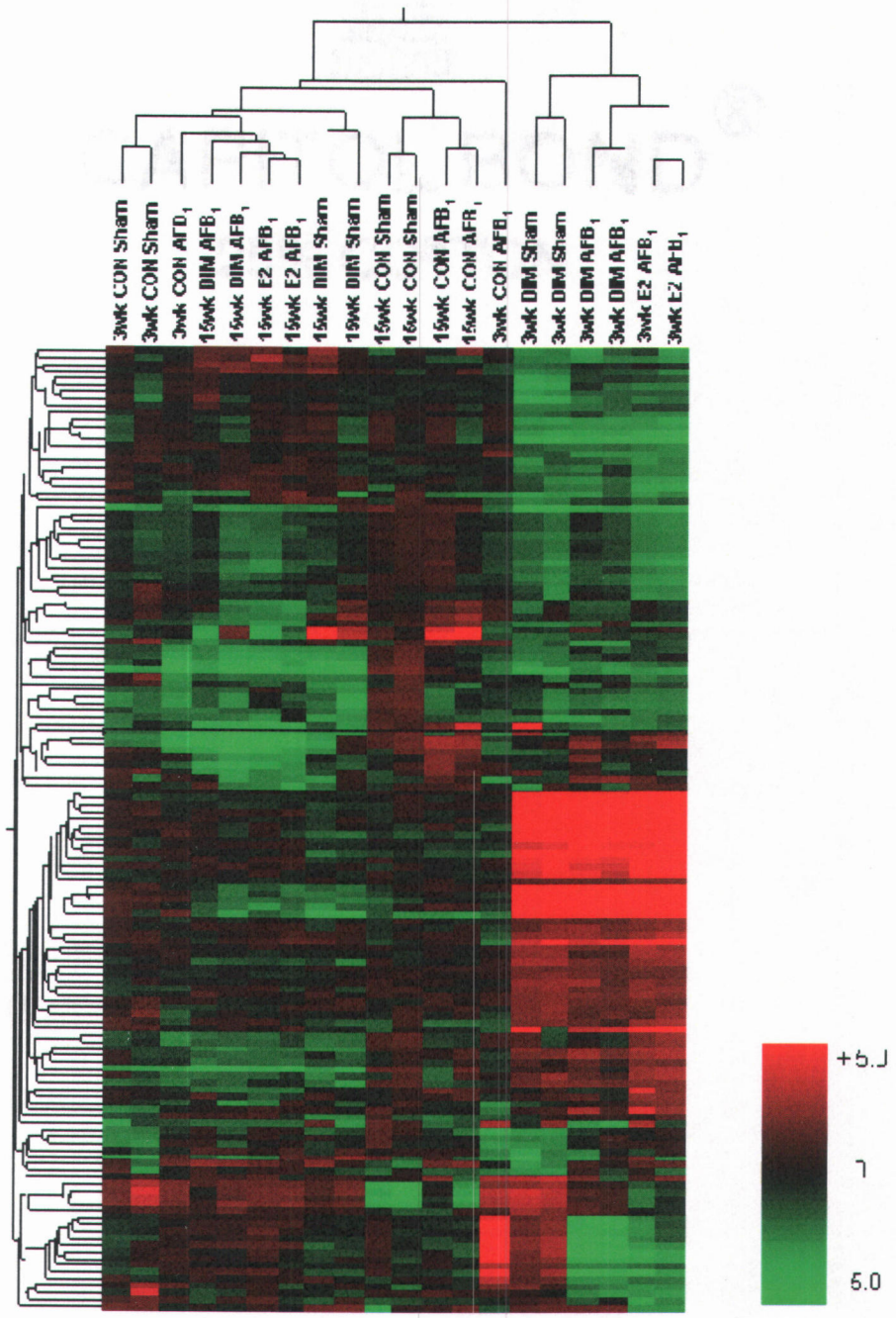

Figure 4-3. Clustering of gene expression in trout liver by Pearson correlation after dietary treatment with 0.1% DMSO vehicle control (CON), 5 ppm E2 and 400 ppm DIM for 3- and 15-week timepoints in sham and AFB1-initiated trout. Results are shown as fold change (n=2) compared to appropriate vehicle-treated control as follows: CON sham/sham, CON AFB1/sham, DIM sham/sham, DIM AFB1/AFB1, E2 AFB1/AFB1. *Red color*, upregulation; *green color*, downregulation; *black*, unchanged expression; *grey*, missing values. Heatmap reflects gene expression profiles for genes differentially regulated 1.8-fold up or down ($P < 0.05$) in at least

samples. PCA showed strong similarity between E2 and DIM treatments at both timepoints, however also indicated distinct transcriptional patterns between sham and AFB_1-initiated animals treated with DIM (Fig. 4-4). Transcripts encoding vitellogenic liver proteins were the most sensitive markers for the estrogenic response in trout at the 3-week timepoint, however a number of genes important for cell proliferation, protein transport, immune function and metabolism were also differentially regulated by DIM and E2 treatments. At the 15-week timepoint, fewer genes indicating an estrogenic response were regulated in liver and most genes were differentially downregulated, including those important for immune function and metabolism.

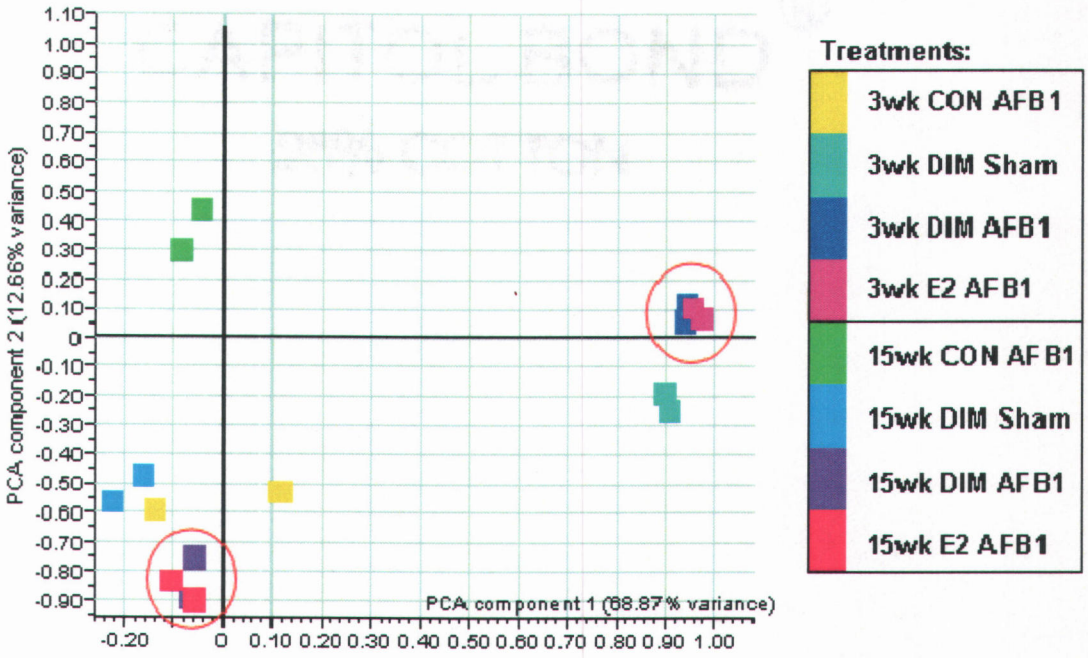

Figure 4-4. Principal component analysis on condition. Colored blocks represent biological replicates (n=2) for each dietary treatment of 0.1% DMSO vehicle control (CON), 5 ppm E2 or 400 ppm DIM after 3- and 15-week timepoints in liver samples from AFB_1-initiated or sham-initiated trout.

Gene expression was also analyzed in HCC tumors of trout from 5 ppm E2 and 400 ppm DIM treatments compared to HCC tumors in 0.1% DMSO vehicle control animals. Each treatment is represented by biological replicates (n = 3) of RNA isolated from individual HCCs. Pairwise analysis of all 1,672 features on the array indicated strong correlation of transcriptional patterns in HCC from E2 and DIM treated animals, R = 0.87 ($P < 0.001$; Fig. 4-2, panel C). Genes found to be differentially regulated (≥or ≤ 1.80-fold change, $P < 0.05$ by Welch's t-test) in HCCs from E2 or DIM treatments compared to control animals are listed by functional category in Table 4-3. Bidirectional hierarchical clustering of genes differentially regulated in at least one treatment group (Fig. 4-5) indicate there are distinct transcriptional patterns between tumors of animals on promotional diets and control tumors. Clustering also supported the pairwise analysis by Pearson correlation indicating there was a high degree of similarity in gene expression patterns in HCCs from E2 and DIM treated animals. Genes differentially regulated in HCC from animals treated with DIM and E2 included those important for the extracellular matrix, vascularization, immune function and redox regulation.

Microarray confirmation by qRT-PCR

The expression of select genes differentially increased or decreased in the microarray analysis, including UPAR, THX, COL2A, TCPBP VTG, HAMP and CTX, were confirmed by qRT-PCR using SYBR Green (Figs. 4-6, 4-7). The same RNA preparations were used for each technique and the mean expression ratios were compared for all replicates in a treatment. Values for duplicate spots and dye-

TABLE 4-3

Select Genes Differentially Regulated in HCC from DIM and E2-Treated Animals Compared to Controls

Array ID	TIGR ID[a]	Gene name (accession number, species)[b]	Average Fold Change (*P* value)[c]	
			DIM	E2
Extracellular matrix and vascularization factors				
OmyOSU1502	TC50691	Tissue factor, blood coagulation (AJ295167; *Oncorhynchus mykiss*)	**4.20** (0.006)	**4.50** (0.000)
OmyOSU759	TC79538	High-mobility-group (HMG) 1 (L32859; *O. mykiss*)	**0.42** (0.032)	**0.46** (0.041)
OmyOSU749	CA378743	Fibronectin 1a isoform 1 (XM_691570; *Danio rerio*)	**0.41** (0.012)	**0.47** (0.026)
OmyOSU562	TC62077	Collagen alpha 2(VIII) C1q (AF394686; *Salvelinus fontinalis*)	**0.47** (0.037)	**0.43** (0.008)
OmyOSU380	TC87593	CD87, Urokinase receptor (AF007789; *Rattus norvegicus*)	**0.40** (0.027)	**0.31** (0.012)
OmyOSU1263	TC62562	Plasminogen activator, urokinase receptor (AF007789; *R. norvegicus*)	**0.08** (0.012)	**0.08** (0.015)
OmyOSU33	TC87593	Plasminogen activator, urokinase receptor (NM_017350; *Rattus norvegicus*)	**0.17** (0.007)	**0.18** (0.017)
OmyOSU460	TC79578	Aldo-keto reductase family 1 member D1 (BC018333; *M. musculus*)	**2.26** (0.002)	**2.49** (0.000)
Redox regulation				
OmyOSU1422	TC47183	Thioredoxin (AAH49031; *Danio rerio*)	**0.24** (0.000)	**0.37** (0.000)
Immunoregulatory				
OmyOSU1236	CR375493	Apopolysialoglycoprotein precursor (J04051; *O. mykiss*)	**2.71** (0.016)	**3.22** (0.008)
OmyOSU1478	TC79233	Trout C-polysaccharide binding protein 1 (AF281345; *O. mykiss*)	**4.99** (0.009)	**5.53** (0.002)
OmyOSU1188	TC73422	Transport-associated protein, TAP2B (AF115538; *O. mykiss*)	**2.21** (0.023)	**2.24** (0.013)
OmyOSU1469	TC8260	Cathepsin S (AY950578; *Paralichthys olivaceus*)	**1.85** (0.024)	**2.45** (0.012)
OmyOSU1222	TC69315	ATPase H+ transporting lysosomal vacuolar proton pump (AY190685; *Pagrus major*)	**0.49** (0.019)	**0.48** (0.020)
OmyOSU882	TC78878	MHC class I heavy chain (AF318187; *O. mykiss*)	**0.35** (0.014)	**0.27** (0.006)
OmyOSU175	TC78877	MHC class I heavy chain (AF091785; *Oncorhynchus mykiss*)	**0.20** (0.003)	**0.15** (0.000)
OmyOSU790	TC86587	MHC class I heavy chain precursor (AF115523; *O. mykiss*)	**0.25** (0.003)	**0.20** (0.001)
OmyOSU401	NP543817	Complement component C5 (AF349001; *O. mykiss*)	0.57	**0.33** (0.004)

TABLE 4-3 (Continued)

Array ID	TIGR ID[a]	Gene name (accession number, species)[b]	Average Fold Change (*P* value)[c]	
			DIM	E2
OmyOSU981	TC78771	IgM heavy chain (S63348; *Oncorhynchus mykiss*)	**0.27** (0.026)	**0.26** (0.027)
OmyOSU373	TC81615	C1q-like adipose specific protein (AF394686; *Salvelinus fontinalis*)	**0.43** (0.008)	0.25

[a]TIGR ID number of the tentative consensus or singleton EST sequence corresponding to OSUrbt ver. 2 microarray feature.
[b]The most significant BLASTX is shown. If an EST has no significant (E-value < 10^{-6}) BLASTX hit, then the most significant BLASTN hit is shown. Genes have been categorized by function based on putative trout homolog using Gene Ontology and OMIM databases.
[c]Average fold change values represent background corrected, Lowess normalized signal ratios. Stringent criteria were used to filter for genes that were regulated at least 1.8-fold consistently in all features from biological replicates and had a p-value <0.05 by Welch's t-test. Fold change values for genes that passed stringency criteria are in bold.

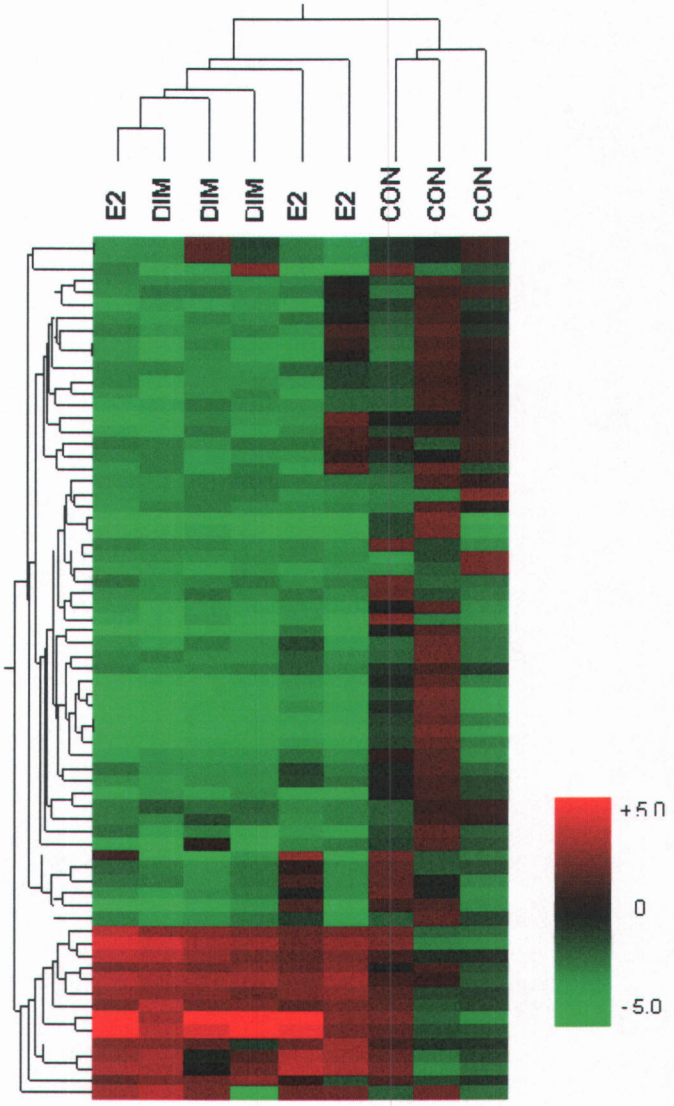

Figure 4-5. Clustering of gene expression in trout HCC tumors by Pearson correlation in AFB1-iniated trout treated with 0.1% DMSO vehicle control (CON), 5 ppm E2 and 400 ppm DIM. Results are shown as fold change (n=3) compared to HCC tumors from control trout. *Red color*, upregulation; *green color*, downregulation; *black*, unchanged expression; *grey*, missing values. Heatmap reflects gene expression profiles for genes differentially regulated 1.8-fold up or down ($P < 0.05$) in at least one treatment group.

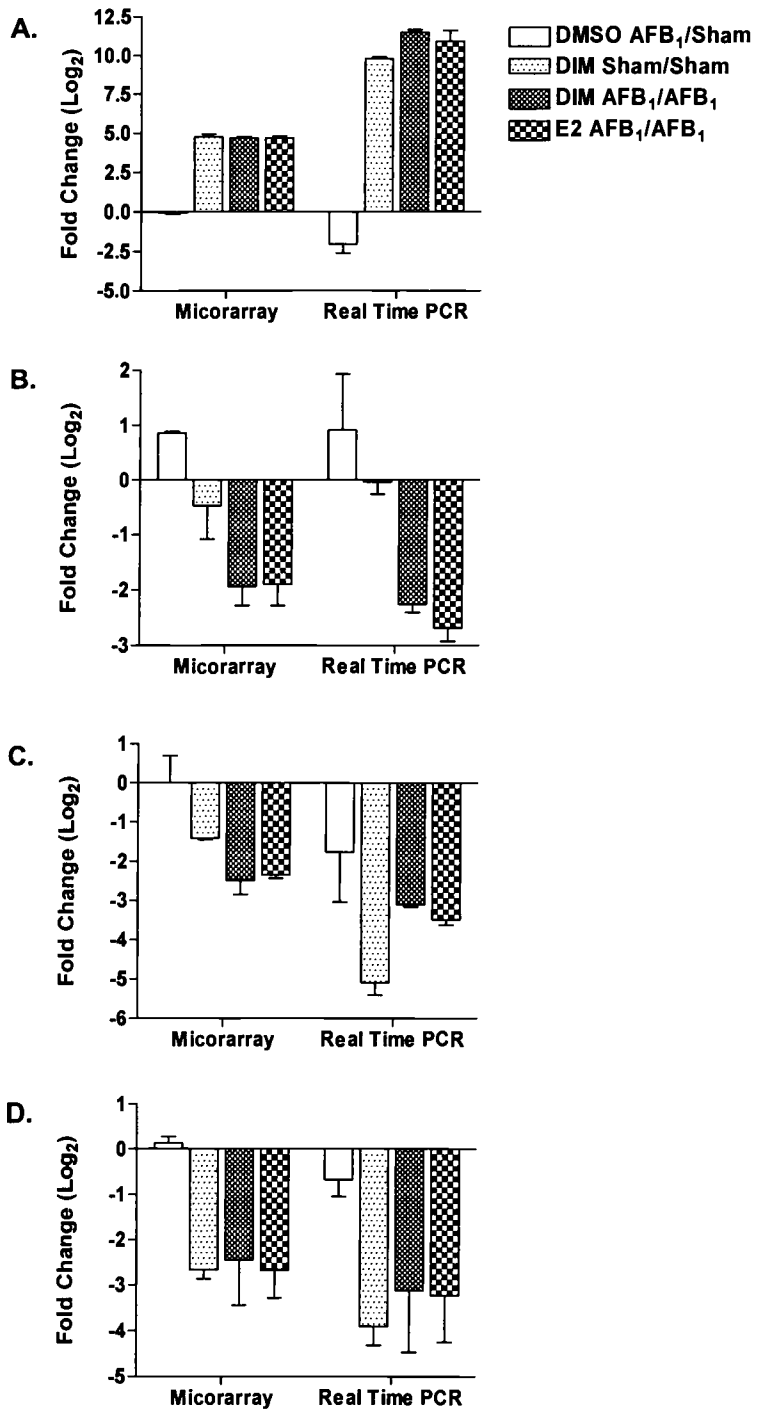

Figure 4-6. Hepatic gene expression in liver samples from trout treated with 5 ppm E2 and 400 ppm DIM for either 3- or 15-weeks measured by microarray and real time RT-PCR. Values are expressed as average fold change (log2) with standard deviation (n=2) compared to appropriate 0.1% DMSO vehicle-treated trout for select genes including (A) VTG at 3-weeks, (B) HAMP for 15-weeks, (C) THX for 15-weeks, (D) CTX for 15-weeks.

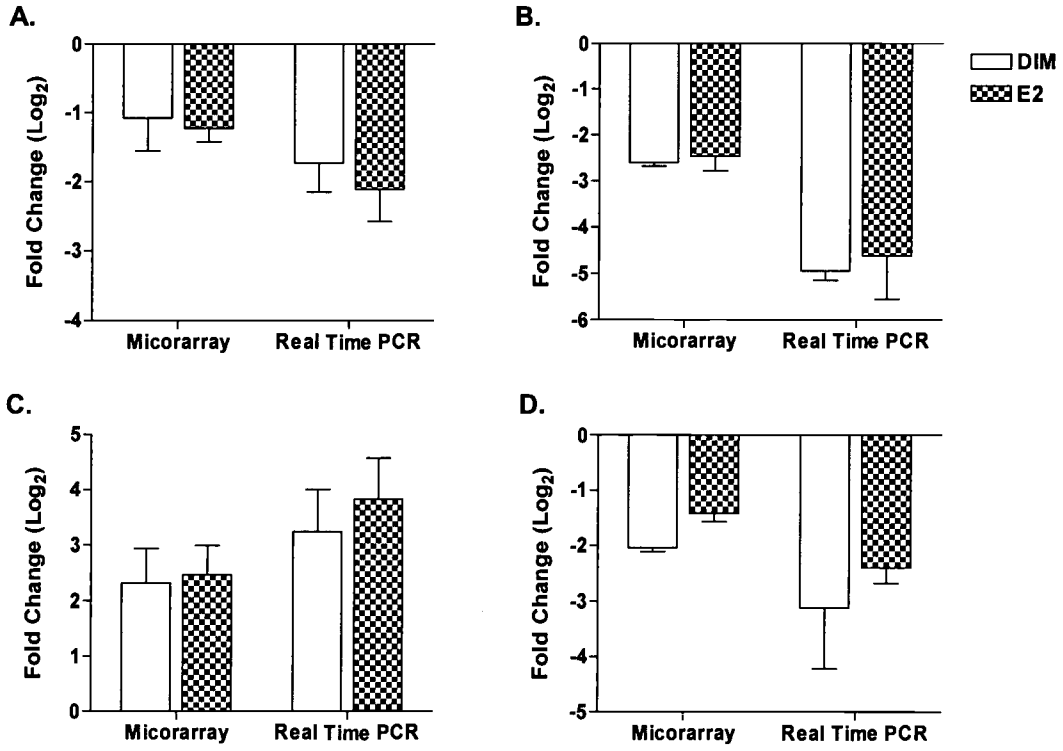

Figure 4-7. Hepatic gene expression in AFB_1-initiated HCC from trout treated with 5 ppm E2 and 400 ppm DIM measured by microarray and real time RT-PCR. Values are expressed as average fold change (log_2) with standard deviation (n=3) compared to HCC tumors from 0.1% DMSO vehicle-treated trout for select genes including (A) COL2A, (B) UPAR, (C) TCPBP, (D) THX.

swapped slides were averaged prior to analysis of biological replicates for microarray data. Overall, we were able to confirm gene expression profiles measured by oligonucleotides microarray analysis using qRT-PCR for both the liver samples and HCC tumors. These data indicate that our strict criteria for determining differential gene regulation by array, including 1.8-fold change in all biological replicates with $P < 0.05$, resulted in detection of meaningful changes that could be validated by other methods.

DISCUSSION

We previously reported that DIM has a transcriptional profile in trout liver similar to two known hepatic tumor promoters, I3C and E2, suggesting DIM may also enhance hepatocarcinogenesis by estrogenic mechanisms in the trout model (Tilton *et al.*, 2005b). Further, the data indicated that DIM may be an even more potent tumor promoter than I3C based on this mechanism. In the current study, 400 ppm DIM in the diet greatly enhanced hepatic tumor incidence similar to 5 ppm E2 in animals initiated with 50 ppb AFB_1, while no enhancement was observed at the lower concentration of 120 ppm DIM. Concentrations in the diet are equivalent to treatment with approximately 6 and 21 mg/kg/day DIM, 5 days per week for 18 weeks. These data are consistent with observations from previous studies in which I3C promoted AFB_1-induced hepatocarcinogenesis in trout and GST-P foci in Sprague-Dawley liver (Oganesian *et al.*, 1998; Stoner *et al.*, 2002). Comparison of the promotional potency of DIM reported here with previous studies using I3C indicate DIM is more potent as a tumor enhancer in the trout model. Promotional potency is a function of several factors including carcinogen dose, promotional dose and exposure duration (Dashwood *et al.*, 1991; Oganesian *et al.*, 1998). In the present study, 400 ppm DIM fed in the diet for 18 weeks post-initiation by 50 ppb AFB_1 resulted in 16.5% tumor incidence compared to 4% in control animals. In a previous study with I3C, a similar level of tumor incidence (18.9%) was achieved with 1000 ppm I3C fed in the diet for 11 months post-initiation by 50 ppb AFB_1 compared to 6.5% in control animals. The relative potency of DIM and I3C are further supported by the conservative nature of

the comparison using studies of markedly different exposure duration. Differences in potency may be explained by previous pharmacokinetic studies showing DIM is the primary *in vivo* component of I3C after oligomerization, absorption and disposition (Anderton *et al.*, 2004; Dashwood *et al.*, 1989; Stresser *et al.*, 1995a). DIM was found to comprise over 40% of the total hepatic radiolabel after oral gavage with radiolabeled I3C in trout (Dashwood *et al.*, 1989). Global hepatic gene profiles further indicate DIM is likely the biologically active I3C component in trout liver (Tilton *et al.*, 2005b) with signatures for both indoles showing a strong similarity to E2.

In this study, we determined DIM was also acting through estrogenic mechanisms during tumor enhancement using a toxicogenomic approach. Hepatic gene expression profiles were examined in liver samples from animals on promotional diets during the course of tumorigenesis and in hepatocellular carcinomas (HCCs) of initiated animals using a rainbow trout 70-mer oligonucleotide array. Strong transcriptional correlations were observed between DIM and E2 treatments at all timepoints examined. Gene expression in liver samples from DIM and E2 treatments at the 3-week timepoint was similar to that previously described for juvenile trout exposed to dietary I3C, DIM and E2 for two weeks (Tilton et al., 2005b). These included upregulation of transcripts for known estrogen-responsive proteins, such as vitellogenin, vitelline envelope, ER α/β and cathepsin D, and downregulation of genes important for acute phase response and drug, lipid and retinol metabolism. Interestingly, principal component analysis on condition indicated that transcriptional profiles were strongly similar between DIM and E2 treatments in AFB_1-initiated

animals, but distinct from DIM treatment in sham-initiated trout particularly at the 15-week timepoint. These data suggest that the effects of DIM on gene expression may be different in animals initiated with a chemical carcinogen compared to control animals. At the 15-week timepoint, genes associated with the typical 'estrogenic' gene signature were no longer differentially regulated and we observed downregulation of transcripts primarily involved in acute phase response and redox regulation. These transcriptional patterns indicate that the tumor enhancing effects of DIM are similar to E2 and are likely mediated through ER-dependent mitogenic signaling in trout liver. DIM was previously found to be estrogenic *in vitro* and stimulate cell proliferation at physiological concentrations through strong ligand-independent activation of ER in the presence of low levels of endogenous E2 (Riby *et al.*, 2000a; Leong *et al.*, 2004). Mitogenic signaling may provide initiated cells with a selective growth advantage an appropriate environment for proliferation and clonal expansion.

We also observed upregulation of genes at the 3-week timepoint involved in adaptive immunity, such as recombination-activating protein 2 (RAG2), perforin 1 and tumor-associated antigen TM4SF5, and involved in extracellular signaling cascades, including Ras-like GTPase and Janus kinase (similar to JAK1 or TYK2 based on sequence homology). RAG2 and perforin are both expressed in lymphocytes and are involved in lymphocyte-mediated tumor suppression through interferon gamma (IFNγ) signaling (Shankaran *et al.*, 2001). Perforin has also been found to mediate the potent anti-metastatic effects of natural killer (NK) cell cytotoxicity in mouse liver and lung metastatic models (Kodama *et al.*, 1999). Interferons are a group of immune

cytokines with antiviral and cytostatic functions mediated by Janus kinase activation of JAK/STAT signaling pathways. DIM was recently found to have immunomodulatory effects in rat *in vivo* and in breast tumor cells and Jurkat T cells *in vitro* (Exon and South, 2000; Xue *et al.*, 2005). In the latter studies, DIM stimulated IFNγ *in vitro* through an ER-independent mechanism that further induced expression of IFN-inducible genes and major histocompatability complex class-I (MHC-I) tumor-associated antigen presentation molecules (Riby *et al.*, 2005). We do not know if IFN expression is induced by DIM and/or E2 in trout liver, but transcriptional changes observed in this study in liver samples of animals treated with DIM and E2 indicate potentiation of adaptive immune function, including some increase in expression of MHC-I and MHC-II transcripts. Enhancement of immune function in cancer immunosurveillance and the ability of the body's immune system to identify and destroy tumors may be a primary defense against cancer. The immune activating properties of DIM previously observed in human cancer cells were associated with inhibition of cellular proliferation.

It is difficult to know what effect enhancement of adaptive immunity may have in trout chemoprotection since it was measured early in the course of tumorigenesis after treatment with concentrations of DIM and E2 that ultimately caused tumor promotion. However, while DIM and E2 increased tumor incidence in initiated animals, transcriptional profiles in HCC tumors from these animals indicated lower invasive and metastatic potential compared to HCCs from control animals. We have previously reported that gene expression in trout HCCs are indicative of tumors of an aggressive nature with high invasive potential (Tilton *et al.*, 2005a). Many of the

genes associated with cell migration, invasion or metastasis that were previously found to be differentially regulated in HCC were reversed in this study in HCCs from animals treated with DIM and E2. Transcriptional profiles showed strong downregulation of transcripts for fibronectin, collagen alpha 2, urokinase plasminogen activator receptor and high mobility group 1 (HMG1) and upregulation of tissue factor. Other factors associated with transport or loading of antigens to MHC-I/II molecules, including transport associated protein (TAP2B) and cathepsin S, were also upregulated even though transcripts for MHC-I antigen presentation molecules were downregulated in HCC tumors. It is unclear how DIM and E2 treatment may cause decreased HCC tumor invasion in trout, however early predictors of metaststic potential in liver samples at the 3-week timepoint include transcriptional upregulation of RAG2 and perforin and downregulation of bone morphogenic protein 7 (BMP7) and anti-apoptotic XIAP, all of which have been associated with tumors having decreased invasive potential or high prognosis for disease-free survival (Helms *et al.*, 2005; Kodama *et al.*, 1999; Rothhammer *et al.*, 2005; Shankaran *et al.*, 2001).

In summary, these data are the first to describe tumor enhancement by DIM. Promotion of AFB_1-initiated hepatocarcinogenesis by DIM was similar to E2 in the rainbow trout model. Toxicogenomic profiling of liver samples collected during the course of tumorigenesis showed strong transcriptional correlations between DIM and E2-treated animals suggesting that DIM promoted tumors through estrogenic mechanisms. However, HCC tumors from DIM and E2-treated animals had transcriptional signatures indicating decreased metastatic potential and may describe a novel chemoprotective effect of DIM in tumors *in vivo*. It is possible that DIM is

acting similar to E2 in trout liver and having a dual effect on tumorigenesis in which it may increase tumor incidence through ER-mediated mitogenic signaling and decrease potential for metastasis possibly through immune activation and potentiation, however these mechanisms need to be further explored. Overall, these data may help explain the dichotomy of chemoprotective and enhancing effects of dietary indoles on cancer development.

ACKNOWLEDGEMENTS

The authors wish to thank Eric Johnson and Greg Gonnerman for care and maintenance of fish and Sheila Cleveland for histological preparation. This work was supported by NIH grants ES07060, ES03850, ES00210, ES11267 and CA90890.

Chapter 5. Characterization of 3,3'-diindolylmethane estrogenicity in the rainbow trout model

Susan C. Tilton[1], Alexandre F. T. Yokochi[2], Christopher M. Lincoln[2], James D. White[2] and David E. Williams[1,3]

[1]Department of Environmental and Molecular Toxicology, Marine and Freshwater Biomedical Sciences Center and Linus Pauling Institute, [2]Department of Chemistry and [3]Environmental Health Sciences Center, Oregon State University, Corvallis, Oregon, 97331

ABSTRACT

3,3'-Diindolylmethane (DIM) is a major in vivo component of the glucobracissin, indole-3-carbinol (I3C) from cruciferous vegetables. We have previously reported DIM to have a strong estrogenic response in trout liver by induction of vitellogenin (VTG) protein markers and by global hepatic gene profiles. Further, we observed DIM to promote hepatocarcinogenesis in trout by estrogenic mechanisms based on comparison to 17β-estradiol (E2)-mediated tumor enhancement and transcriptional patterns. However, the mechanism by which DIM is acting as an estrogen in trout liver is currently unknown. In this study, we characterized the estrogenic response of DIM in rainbow trout liver by measuring its *in vitro* biological activity, its ability to directly bind to estrogen receptor (ER) and its potential for metabolism to estrogenic metabolites. We found DIM to have the highest estrogenic potency *in vitro* compared to other I3C oligomerization products with similar efficacy for VTG induction as E2 and 300-fold lower potency. However, DIM competitively bound to trout hepatic ER with a relative binding affinity 10,000-fold lower than E2 suggesting it is only a weak agonist for the trout ER. Differences between DIM receptor binding and biological activity may be explained in part by our observation in this study that VTG induction by DIM was inhibited by co-treatment with CYP450 inhibitors indicating that the active estrogen may be a DIM metabolite. DIM metabolism was measured in liver microsomes and identified by HPLC and LC/MS. We confirmed the production of a mono-hydroxylated metabolite of DIM that, as part of a metabolite mixture, was able to bind to trout ER and induce VTG *in vitro*. We

were also able to confirm the potential importance of non-genomic signaling cascades for estrogenic signaling by DIM with the use of inhibitors of kinases important in these pathways. These data support the role of DIM as a potent estrogen in trout liver that may require metabolism for ligand-dependent activation of ER or activation of extracellular signaling pathways for ligand-independent activation of ER. It is likely that multiple mechanisms are involved in the estrogenic activity of DIM, which may explain the cell/tissue and species-specific effects reported in the mechanisms of dietary indoles.

INTRODUCTION

3,3'-Diindolylmethane (DIM), is a major *in vivo* oligomerization product of the glucobracissin, indole-3-carbinol, from cruciferous vegetables (Grose and Bjeldanes, 1992). DIM and I3C are also available individually as dietary supplements. Both dietary indoles have well established chemoprotective effects in tumor cell lines and in several animal models *in vivo*, primarily by their ability to act as cytostatic agents or blocking agents, respectively (Dashwood *et al.*, 1994; Grubbs *et al.*, 1995; Kim and Milner, 2005; Kojima *et al.*, 1994; Leong *et al.*, 2001). However, I3C has been found to enhance carcinogenesis in a number of tumor models when provided in the diet long term post-initiation (Bailey *et al.*, 1987; Organesian *et al.*, 1999; Stoner *et al.*, 2002; Yoshida *et al.*, 2004). We recently reported tumor enhancement by DIM of trout aflatoxin B_1 (AFB_1)-initiated hepatocarcinogenesis. Toxicogenomic profiling

indicated that DIM is acting through estrogenic mechanisms in its ability to enhance tumors similar to 17β-estradiol (E2), a known hepatic tumor promoter in trout.

Identification of the individual characteristics of I3C acid condensation products has been an important part of understanding the mechanisms by which dietary indoles function. I3C is unstable in the acid environment of the stomach and forms several different oligomerization products (Bradfield and Bjeldanes, 1987). Two primary products formed are DIM and a linear trimer (LTR) 2-(indol-3-ylmethyl)-3.3-diindolylmethane. Other important oligomerization products produced in more minor amounts include a cyclic trimer (CTR) 5,6,11,12,17,18-hexahydrocyclonona[1,2-b:4,5-b':7,8-b"]triindole and indolo-[3,2-b]-carbazole (ICZ) among others. Pharmacokinetic studies indicate that DIM is also a primary *in vivo* component of I3C after absorption and disposition in rat, mouse and trout models (Anderton *et al.*, 2004; Dashwood *et al.*, 1989; Stresser *et al.*, 1995a). Toxicogenomic comparison of DIM and I3C effects in trout liver also suggest that DIM is the biologically active I3C component in this model through estrogenic mechanisms (Tilton *et al.*, 2005b).

However, the mechanism by which DIM causes estrogenic effects in trout liver is currently unknown. DIM has previously been found to have both antiestrogenic and estrogenic effects in human cancer cells *in vitro* that were not dependent on ligand binding to the estrogen receptor (ER), but rather through cross-talk of ER signaling with aryl hydrocarbon receptor (AhR) and extracellular kinase signaling cascades (Chen *et al.*, 1998; Leong *et al.*, 2004). DIM has also been found to be a weak agonist for the ER inhibiting E2-mediated signaling in breast cancer cells (Meng *et al.*, 2000).

Evidence in trout show the estrogenic effects of DIM are mediated through the ER and can be completely inhibited by the ER-antagonist, tamoxifen (Shilling *et al.*, 2001). Further, data suggested that co-treatment of DIM with a general CYP450 inhibitor in liver slices *in vitro* inhibited VTG induction suggesting the active estrogen may be a DIM metabolite. In this study, we characterized the estrogenic response of DIM in rainbow trout liver by measuring its *in vitro* biological activity, its ability to directly bind to ER and its potential for metabolism to estrogenic metabolites. We also evaluated the potential for ligand independent activation of ER by DIM in trout liver by co-treatment of liver slices with known receptor antagonists and kinase inhibitors.

.

MATERIALS AND METHODS

Materials. Analytical grade I3C, β-naphthoflavone (βNF) and E2 were purchased from Sigma Chemical (St. Louis, MO). DIM was obtained from BioResponse, Ltd. (Boulder, CO) and was subsequently analyzed by high resolution FAB mass spectrometry to determine purity (>99%). Radiolabeled [^{3}H]DIM was purchased from American Radiolabeled Chemicals, Inc. (St. Louis, MO) and purity (>98%) was confirmed by HPLC analysis. [^{3}H]DIM was diluted with unlabeled DIM carrier to an approximate specific activity of 125 mCi/mmol. Radiolabeled [^{3}H]E2, 95 Ci/mmol, was purchased from Sigma for receptor binding studies. ICI_{182780} (ICI) was purchased from Tocris Cookson Ltd. (Bristol, UK). CYP450 inhibitors, ketoconazole and SKF525A, were purchased from Sigma. Kinase inhibitors were purchased as

follows: PD98059 (Tocris), H-89 (Sigma), Gö6983 (Sigma), AG1478 (Calbiochem), JNK II inhibitor (Calbiochem, San Diego, CA), SB202190 (Calbiochem), LY294002 (Calbiochem). All other compounds were purchased from Sigma unless otherwise stated.

Isolation of I3C acid condensation products. A mixture of acid condensation products, processed to mimic the oligomerization of I3C in the stomach, was prepared using a modification of the method of Grose and Bjeldanes (1992). Briefly, I3C was dissolved in HPLC-grade ethanol, an aliquot was removed, and it was blown to dryness under nitrogen gas. Equal volumes of water and methanol were added to this to dissolve the powder. A 1 N hydrochloric acid solution was added and the mixture vortex was shaken for 1 min. The mixture was neutralized with 0.25 N ammonia and then HPLC-grade acetonitrile was added to produce the desired working concentration. The two major products of this procedure are DIM and the linear trimer (LTR) with the cyclic trimer (CTR) formed as a more minor product. Identification of LTR and CTR was confirmed by retention time of peaks previously identified by NMR (Stresser *et al.*, 1995a).

DIM structural modeling. X-ray crystallographic structure of DIM was determined on a Bruker P4 from a single crystal at room temperature. The crystalline sample used was obtained by recrystallization by slow evaporation of a chloroform solution of the bulk material provided. Determination of the crystallographic parameters, data collection and structure solution and refinement was done as

described elsewhere (Blakemore *et al.*, 2001) with the following details. From a mass of crystals, a needle shaped crystal of dimensions 0.4 x 0.1 x 0.1 mm^3 was selected and mounted on the tip of a thin glass fiber using epoxy glue. The structure was solved using direct methods as programmed in SHELXS-90, which revealed the positions of all atoms in the unique indolyl moiety. Computer molecular modeling was performed using PCSpartan Pro, v. 1.0.6 (Wavefunction, Inc., Irvine, CA), to compare structure of DIM to E2.

DIM metabolism. DIM metabolism was determined *in vitro* with male rainbow trout, Sprague Dawley rat and CD-1 mouse liver microsomes (BD Gentest, Woburn, MA). Trout microsomes were made as previously described (Donohoe and Curtis, 1996). [^{3}H]-DIM (20 or 250 μM final concentration) was incubated in 100 mM potassium phosphate, pH 7.4, with 5 mM $MgCl_2$, 10 mM glucose-6-phosphate, 1 U/ml glucose-6-phosphate dehydrogenase, 1 mM NADPH and 1 mg/ml microsomes in 500 μl final volume at 30°C for 60 min for trout and 37°C for 45 min for rat and mouse. Reactions were terminated with 1 volume ice-cold acetonitrile, extracted with three times with 1 volume ethyl acetate, dried under N_2, resuspended in acetonitrile and analyzed by HPLC and LC/MS. HPLC analysis was performed with a Waters 2690 pump equipped with a 996 diode array detector, Packard Radiomatic flow scintillation analyzer 500TR Series and a Beckman Ultrasphere C18 column (5 μm, 4.6 mm × 250 mm). Flow rates were 1.0 ml/min and column temperature was 30°C. Samples were analyzed with a gradient system of 80% water and 20% acetonitrile from 0 to 30 min, 15% water and 85% acetonitrile from 30 to 45 min, and 100%

acetonitrile from 45 to 55 min. Absorption was measured at 280 nm. A number of peaks more polar than the DIM parent were formed after NADPH microsomal incubation. The identity of select peaks was verified by LC/MS analysis using a Shimadzu HPLC with LC-10 pumps connected to a Perkin-Elmer Sciex API III mass spectrometer run in positive ion mode with an orifice voltage of +60 V, source temperature of 60°C and scanning from *m/z* 150 to 400. Samples were introduced via the heated nebulizer interface set at 450°C. For determination of estrogenic metabolites, larger scale reactions (5 ml final volume) were performed with DIM similar to those described above.

Liver slicing. High precision cut rainbow trout liver slices were utilized to determine the effects of DIM and other I3C acid condensation products and metabolites on VTG and CYP1A protein *in vitro* in the presence or absence of different inibitors. All glassware and tools were sterilized at 105°C for 30 min prior to use. The slicing and incubations are based on the method previously optimized in our lab (Shilling *et al.*, 2001). Briefly, livers were excised from juvenile Mt. Shasta strain male rainbow trout (<18 mos) after euthanasia by deep anesthesia with tricaine methanesulfonate. Mt. Shasta rainbow trout were hatched and reared at the Oregon State University Sinnhuber Aquatic Research Laboratory in 14°C carbon-filtered flowing well water on a 12:12 h light:dark cycle. All animal protocols were performed in accordance with Oregon State University Institutional Animal Care and Use Committee guidelines. Livers were kept in ice-cold Hanks' modified salts buffer containing 10 mM Hepes and 8 mM sodium bicarbonate, pH 7.2, and filter sterilized

through a 0.22-mM filter and cut into 8 mm cylindrical cores. Precision cut liver slices, 250 μm thick, were made using a Krumdieck tissue slicer (Alabama Research and Development Corp, Munford, AL). Slices were incubated with test compound (0.2% DMSO) in Hank's media supplemented with 1% BSA, 0.1% gentamicin and 25% fetal bovine serum on an orbital shaker at 12°C saturated with 95% O_2 / 5% CO_2 for 96 hours. Cell viability in slices was determined by histology and by ATP activity (Sigma; method of Adams, 1963). Two liver slices were pooled, homogenized in ice-cold buffer [10 mM potassium phosphate, 150 mM KCl, 1 mM EDTA and 0.1 mM PMSF, pH 7.5] and stored at -80C for immunoassay analysis. Protein concentrations were determined by BioRad protein assay (Hercules, CA).

CYP1A Western blotting. CYP1A was detected in whole homogenates of liver slices by Western blotting. Each sample (10 μg protein) was separated on NuPAGE 3-8% Tris-acetate polyacrylamide gels (Invitrogen) by electrophoresis and transferred to PVDF membranes. Membranes were incubated in BSA block buffer [2% BSA in PBS, pH 7.4] for 1 h at room temperature. Blots were probed with CYP1A mouse anti-trout monoclonal clone C10-7 (1:500 dilution; Biosense, Bergen, Norway) for 1 h at room temperature. Membranes were washed four times for 5 min in Tween buffer [0.05% Tween-20 in PBS, pH 7.4]. Membranes were incubated in antimouse secondary horseradish peroxidase-conjugated antibody (1:500; BioRad) for 1 h at room temperature and washed again in Tween buffer. Peroxidase activity was detected using Western Lighting Chemiluminescence Reagent (PerkinElmer) according to the manufacturer's instructions. Bands were visualized using an Alpha

Image 1220 Documentation and Analysis System (Alpha Innotech, San Leandro, CA) and quantified as percent above control with Scion Image software (Frederick, MD).

Quantification of VTG by ELISA. VTG was detected in whole homogenates of liver slices by ELISA previously described (Donohoe and Curtis, 1996; Shilling and Williams, 2001). Briefly, cytosol samples were incubated in 96-well plates at 4°C for 24 h with rabbit anti-chum salmon VTG (1:1500), which was graciously provided by A. Hara at Hokkaido University. Samples were transferred to plates coated with 25 ng/well purified rainbow trout VTG (pre-blocked with 1% BSA) and incubated for 24 h at 4°C. Plates were then incubated with biotin-linked donkey anti-rabbit IgG and streptavidin horseradish peroxidase conjugate (Amersham, Buckinghamshire, England) for 2 h at 37°C and developed with 0.01% 3,3'5,5'-tetramethylbenzidine and 0.01% hydrogen peroxide in 0.5 M sodium acetate, pH 6.0. Colorimetric reactions were stopped after 10 min with 2 M sulfuric acid and optical density was measured on a SpectraMax 190 plate reader with SoftMax Pro 4.0 software (Molecular Devices, Sunnyvale, CA). VTG concentrations were determined based on comparison to a trout VTG standard curve with a detection limit for this assay of 6.25 ng/ml. VTG was normalized to protein concentration for each sample and ratios were calculated for treated samples compared to vehicle control similar to microarray analysis.

Estrogen receptor (ER) binding assay. ER competitive binding studies were performed using methods adapted from Lazier *et al.*, 1985. Briefly, hepatic cytosol was prepared from 2-year old female trout by homogenization in ice-cold buffer with

initial centrifugation at 10,000×g for 15 min at 4°C. The supernatant was mixed 2:1 with TEMS buffer [10 mM Tris-HCl, 1 mM EDTA, 12 mM monothioglycerol, 20 mM sodium molybdate, 10% glycerol, pH 7.4] containg 5% (v/v) activated charcoal and 0.5% dextran. The mixture was vortexed and incubated on ice for 15 min prior to final centrifugation of E2-stripped supernatant at 100,000×g for 1 hour at 4°C. The supernatant was assayed for protein concentration following manufacturer's protocol (BioRad) and stored at-80°C for binding studies. Saturation binding was performed by incubating cytosolic ER with 0.04-25 nM [^{3}H]-E2 in the absence or presence of 100-fold excess unlabeled diethylstilbestrol for 24 hours at 12°C. Free estrogen was removed with charcoal-dextran [TEMS containing 2.5% charcoal and 0.5% dextran] and the supernatent counted by liquid scintillation. Competitive binding studies were performed with 3 nM [^{3}H]-E2 in the presence of increasing concentrations of inhibitor; $1x10^{-4}$ to $3.16x10^{-9}$ M DIM or metabolites, $1x10^{-5}$ to $3.16x10^{-10}$ M E2 or ICI. Non-specific binding was calculated using $1x10^{-4}$ M E2 and $1x10^{-3}$ M DIM. Similar binding assays were performed with sheep uterine cytosolic ER for comparison as described previously (van Lipzig *et al.*, 2005).

RESULTS

Characterization of DIM estrogenicity in vitro

The ability of DIM and other I3C acid condensation products, CTR and LTR, to induce VTG and CYP1A was determined in vitro using precision cut liver slices

(Fig. 5-1). Induction of VTG and CYP1A are commonly used as markers for ER- and AhR-mediated activation, respectively. DIM induced VTG with similar efficacy as E2, which was used as a positive control for comparison, but with lower potency. The EC_{50} values for VTG induction by E2 and DIM were 14.2 nM and 4.3 μM, respectively, indicating approximately 300-fold difference in potency. DIM was able to maximally induce VTG at concentrations as low as 10 μM. CTR and LTR were both weak inducers of VTG at all concentrations measured. In contrast, LTR and CTR induced CYP1A with similar efficacy as βNF, which was used as a positive control for comparison, but with lower potency of approximately 50-fold and 140-fold, respectively. DIM was only a weak CYP1A inducer at most concentrations measured.

The ability of DIM and I3C to bind to trout hepatic ER was determined by competitive binding with [^{3}H]-E2. Receptor binding assays were highly reproducible and Fig. 5-2 shows a typical [^{3}H]-E2 saturation binding curve and Scatchard plot for trout liver cytosol preparation incubated with varying concentrations of [^{3}H]-E2 in the presence or absence of 100× excess of DES for 24 hr at 12°C. The mean equilibrium dissociation constant (Kd) for E2 binding was 2.9 nM, which is similar to that previously reported in salmon and trout (Lazier *et al.*, 1985; Miller *et al.*, 1999). The effects of adding increasing concentrations of DIM, I3C and ICI, a known ER antagonist, to the [^{3}H]-E2 binding assay were determined using a fixed concentration of 3 nM [^{3}H]-E2. Competitive binding curves (Fig. 5-3) indicate the EC_{50} for inhibition by E2, ICI, DIM and I3C were $1.2x10^{-8}$, $5.6x10^{-8}$, $1.1x10^{-4}$, $1.0x10^{-3}$ M, respectively. These values translate to E2 relative binding affinities for ICI, DIM and

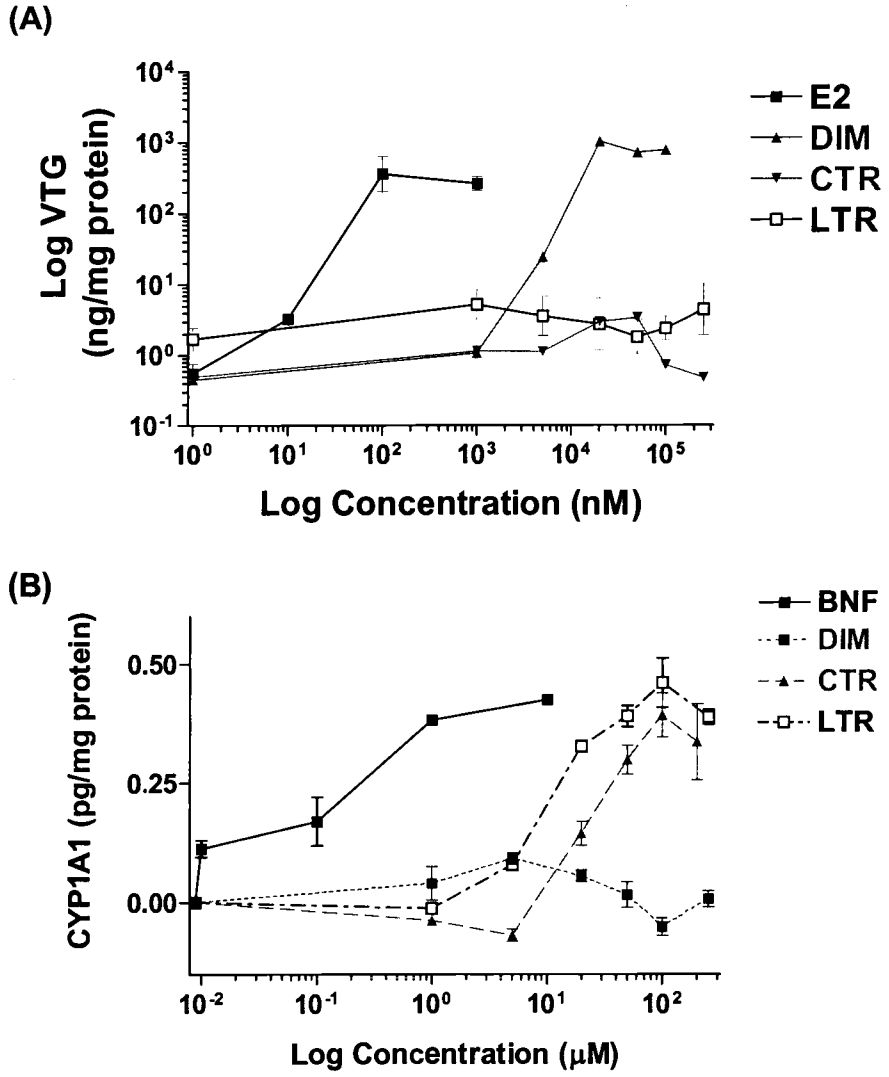

Figure 5-1. (A) VTG induction and (B) CYP1A induction in trout liver slices after exposure to I3C acid condensation products, DIM, LTR and CTR for 96 hours. E2 and βNF were included as positive controls. Values are means with standard deviations (n=6).

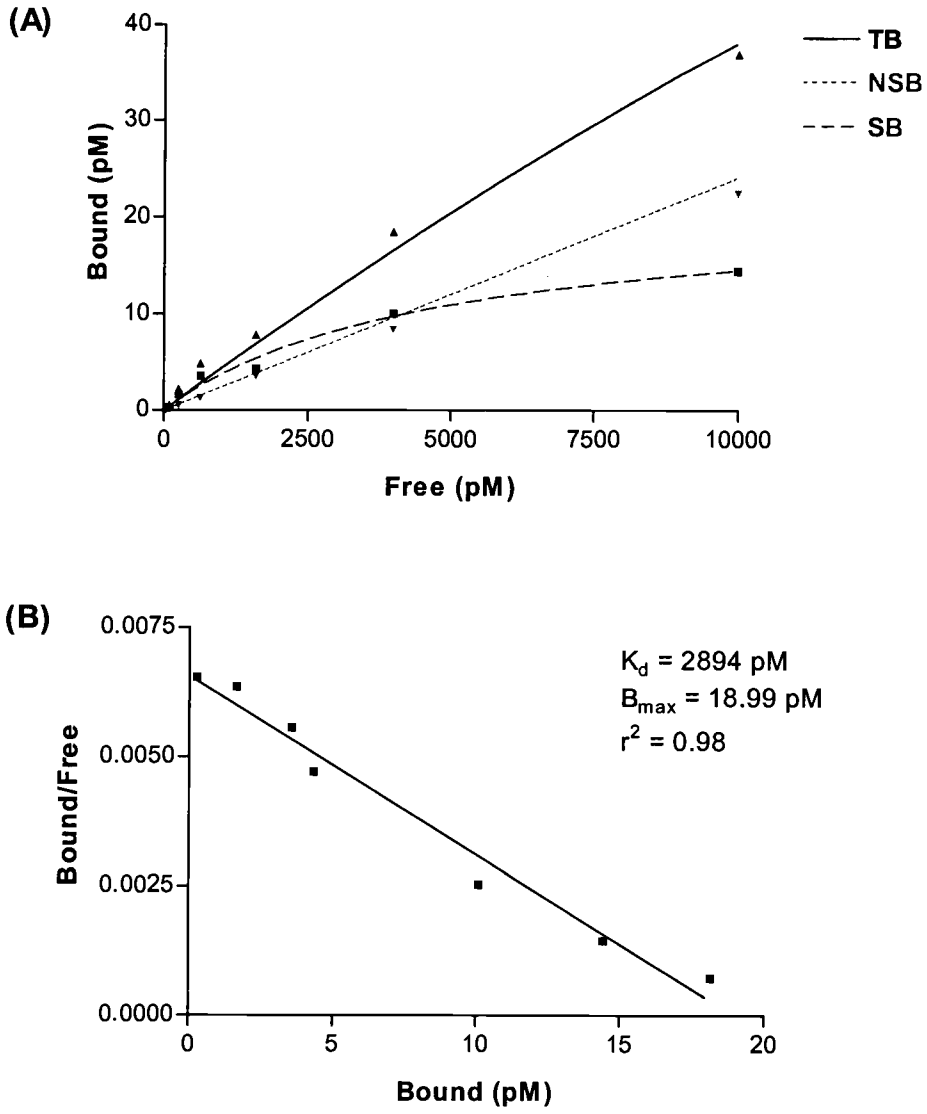

Figure 5-2. (A) Saturation binding of [^{3}H]-E2 by rainbow trout cytosolic estrogen receptor. (B) Scatchard plot of specific binding, Kd = 2.9 nM.

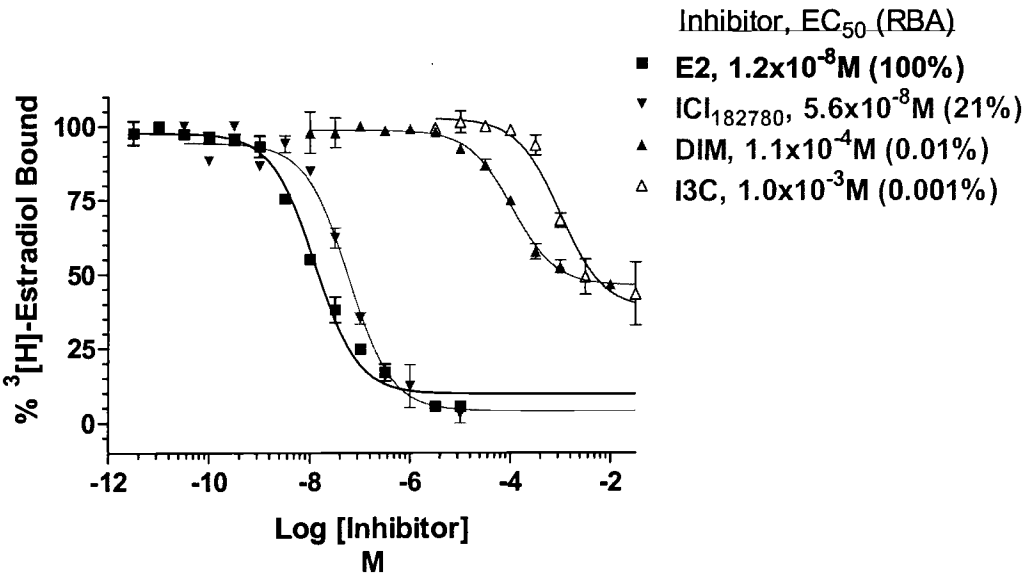

Figure 5-3. Competitive inhibition of [^{3}H]-E2 in trout liver cytosol by E2, ICI_{182780}, DIM and I3C. Results are expressed as percent of [^{3}H]-E2 bound.

I3C of 21%, 0.1%, and 0.01%, respectively, or as 5-fold, 10,000-fold, and 100,000-fold lower binding, respectively. Neither DIM nor I3C were able to completely inhibit E2 from binding to the ER at the concentrations tested, although, for DIM, this may be due to the fact we were approaching maximum solubility. I3C itself showed some binding affinity for the ER, however the incubation cytosol was not examined for the possible conversion of I3C to other acid condensation products.

DIM metabolism

The x-ray crystal structure of DIM was determined in order to model DIM compared to E2 for possible binding to the estrogen receptor (Fig. 5-4). The X-ray structure shows the dihedral between two planes defined by the indole rings. The

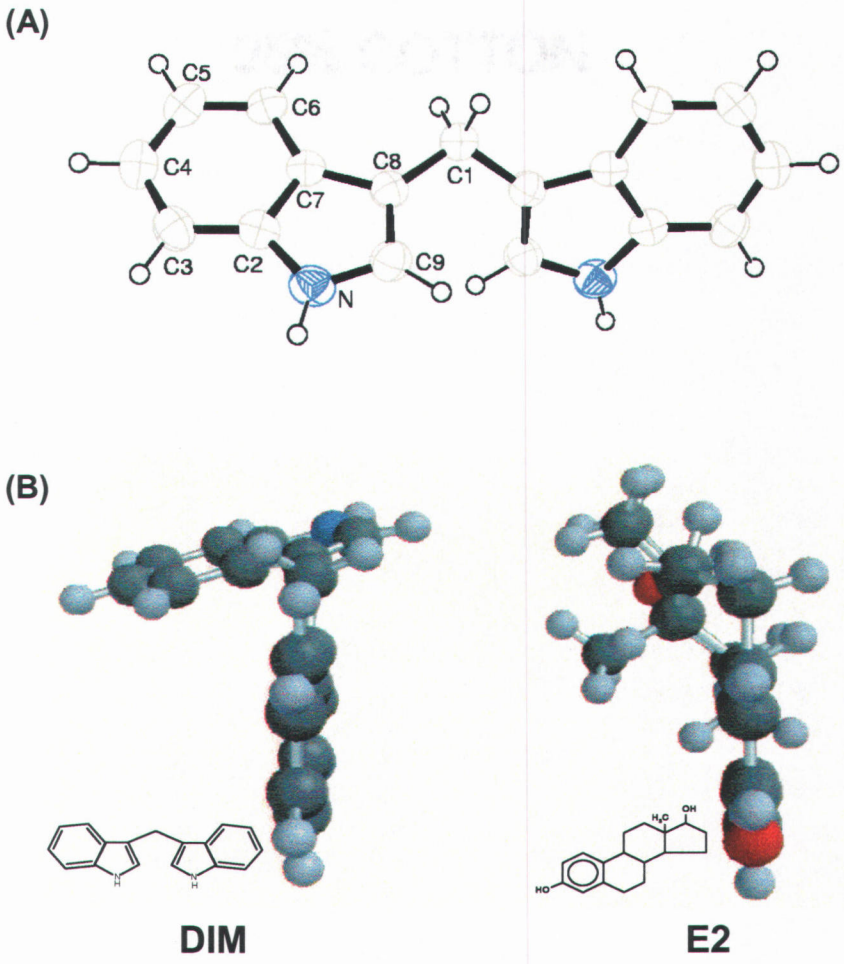

Figure 5-4. (A) X-ray crystal structure of DIM and (B) Computer model of DIM compared to E2.

dihedral angle is about 60 and the two indole nitrogens are on the same (syn) rather than opposite side of the vertical plane through the CH_2. The crystal structure was used to computer model DIM compared to E2 as a possible agonist for the ER. ER agonists are comprised by a group of structurally diverse compounds, however typical structural elements that indicate possible ER binding include existence of a ring structure, heteroatom such as nitrogen and existence and placement of hydroxyl

groups (Fang *et al.*, 2001). Based on this information, we determined the possibility for formation of hydroxylated DIM metabolites in liver microsomes. Previous evidence in trout liver slices found VTG induction by DIM was inhibited by a non-specific CYP450 inhibitor, SKF525A, suggesting the active estrogen may be a DIM metabolite (Shilling *et al.*, 2001). In the present study, trout liver slices were coexposed to E2 or DIM with two different non-specific CYP450 inhibitors in trout, SKF525A and ketoconazole. VTG induction was significantly inhibited in slices exposed to DIM, but not in slices exposed to E2 suggesting the CYP450 inhibitors are not general ER antagonists (Fig. 5-5).

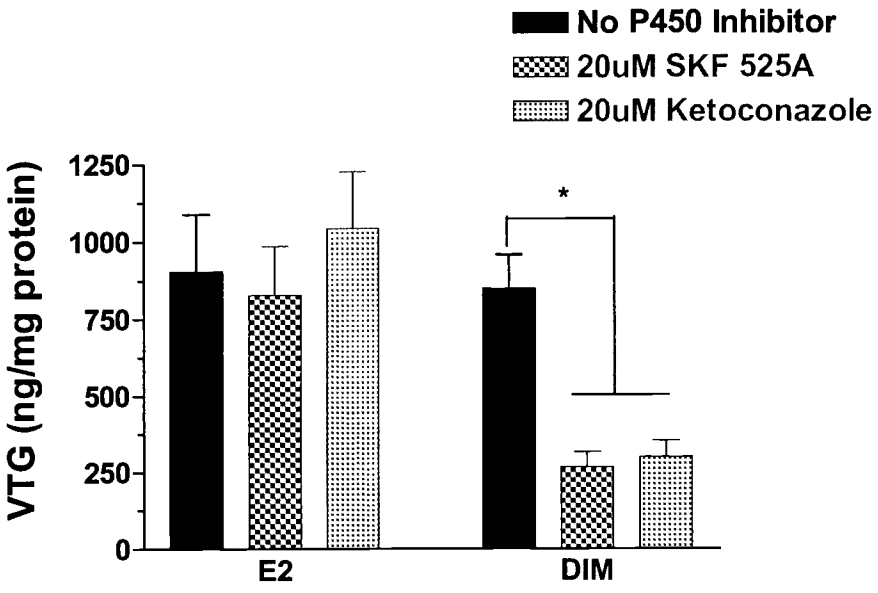

Figure 5-5. VTG induction in trout liver slices after 96 hour exposure to 100 nM E2 and 20 μM DIM in the presence or absence of 20 μM CYP450 inhibitors. Values are means with standard deviations (n=6). *Indicates significant difference from control values ($P < 0.05$).

To determine the extent of DIM metabolism in liver, [^{3}H]-DIM was incubated with liver microsomes from male trout, rat and mouse in the presence of a NADPH regenerating system. A primary polar metabolite was detected at t = 19 min in all incubations and is shown in a representative image (Fig. 5-6) from rat microsomes. Analysis of the metabolite by LC/MS indicated the peak had a molecular weight of 261.1 compared to parent DIM, mw 245.2, suggesting the metabolite was mono-hydroxylated (OH-DIM; Fig. 5-7). Species differences were observed in metabolite production such that rat > mouse > trout. The percent of [^{3}H]-DIM (20 μM incubation) metabolized by each species was 95%, 56% and 5%, respectively. Interestingly, no difference in metabolite production was observed with microsomes from aroclor or 3-methylcholanthrene treated rats, which would be expected to induce CYP1A.

DIM metabolite(s) were examined for estrogenicity in ER binding assays and by VTG induction. However, since the primary metabolite was produced in amounts too low to effectively isolate by HPLC, entire NADPH incubations were extracted with ethyl acetate and concentrated for use in estrogen assays. DIM metabolite mixture from rat and trout microsomal incubations were used in ER binding assays with sheep uterine cytosol and trout liver cytosol, respectively. Rat DIM metabolite mixture had approximately 31-fold higher relative binding affinity compared to DIM while trout metabolite mixture showed no difference in binding affinity compared to DIM (Fig. 5-8). These differences may be due to species differences observed in the extent of DIM metabolism. Therefore, all metabolites from DIM hydroxylation reactions with trout, rat and mouse microsomes were isolated as a mixture in order to

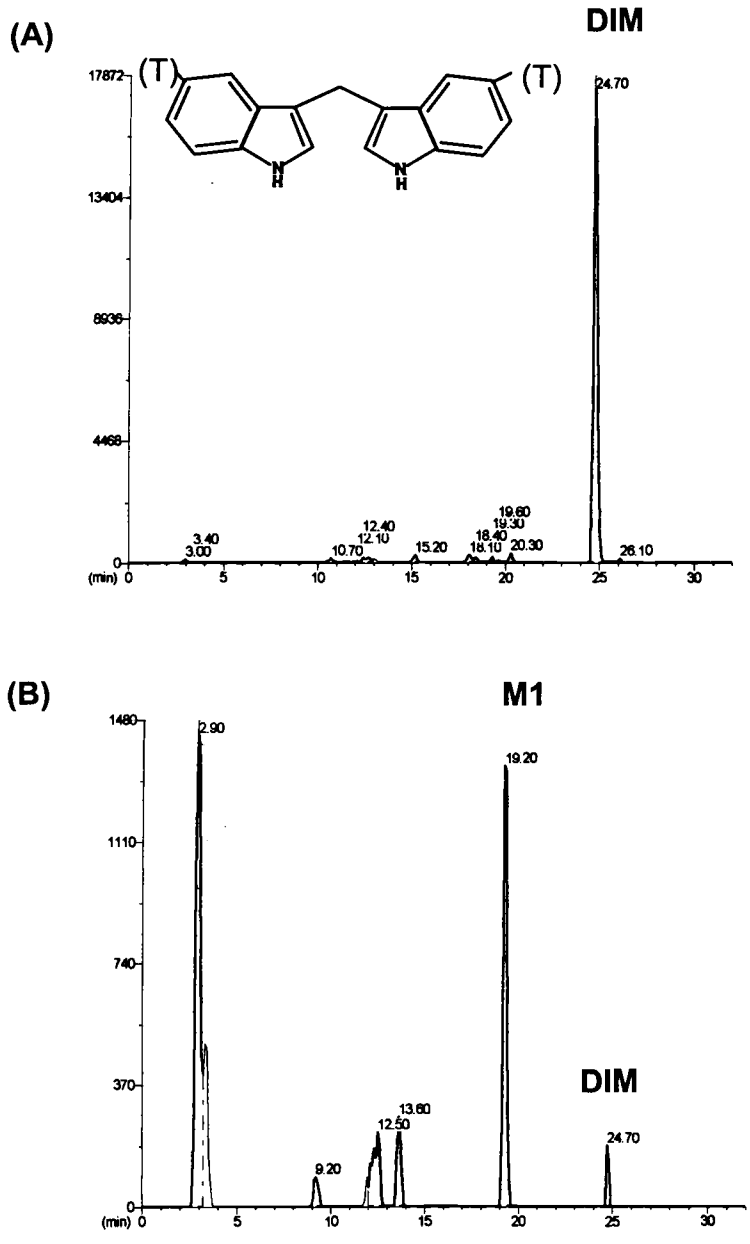

Figure 5-6. Representative HPLC chromatogram of 1 μM [^{3}H]-DIM incubated with (A) heat inactivated Sprague-Dawley liver microsomes and (B) SD liver microsomes in the presence of a NADPH regenerating system at 37°C for 45 minutes. M1 is a primary metabolite eluting at t = 19 minutes.

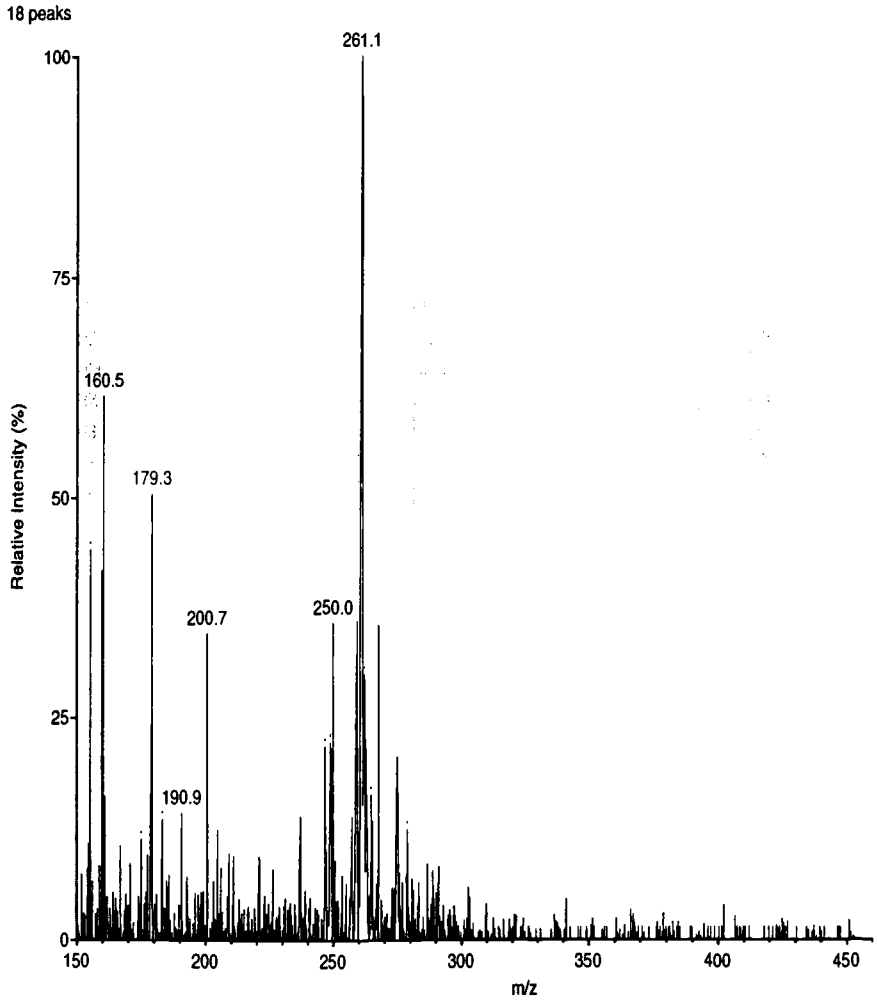

Figure 5-7. Mass fragmentation spectra for the primary DIM metabolite (t = 19 min) from liver microsomes, m/z = 261.1.

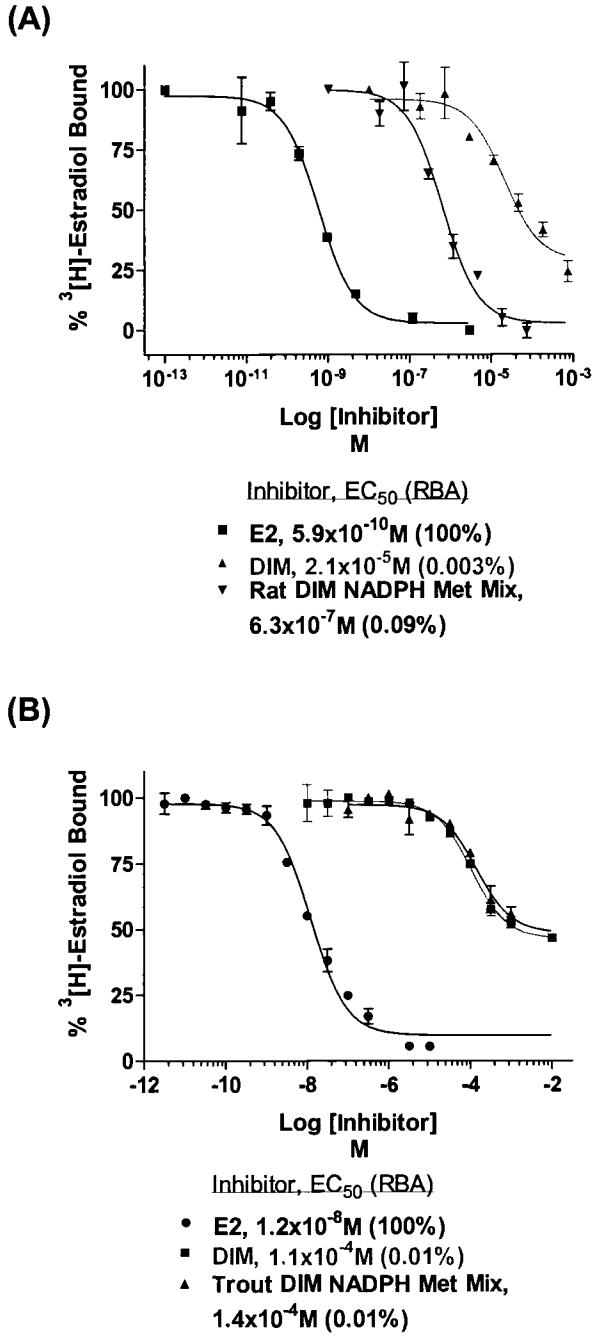

Figure 5-8. Competitive inhibition of [^{3}H]-E2 in by E2, DIM and DIM NADPH metabolite mixture from incubation with (A) Sprague-Dawley rat liver microsomes and (B) trout liver microsomes.

remove parent DIM. Concentrated extracts of equivalent concentrations using extinction coefficient for DIM were used in binding studies and in VTG assays (Fig. 5-9). Interestingly, we observed similar binding affinities for the metabolite mixtures from all species, although they only approximately 2-fold greater binding affinity than DIM for trout ER. These metabolite mixtures did show biological estrogenic activity in liver slices *in vitro* measured by induction of VTG, however we were unable to determine relative estrogenicity of any particular metabolite compared to DIM.

Kinase inhibition studies

The ability of E2 and DIM to induce VTG in liver slices *in vitro* was evaluated in the presence or absence of different receptor antagonists or kinase inhibitors to better understand potential signaling mechanisms involved. In the first study, VTG induction was measured in liver slices as a marker for ER-mediated signaling after 96 hr exposure to 20 μM cAMP, 100 nM E2 and 20 μM DIM in the presence or absence of 5 – 100 μM H89, a PKA inhibitor, or PD98059, a MAPK inhibitor (Fig. 5-10). Concentrations of E2 and DIM were chosen based on their ability to maximally induce VTG in liver slices. All E2 and DIM treatments significantly induced VTG greater than controls, while cAMP did not. Co-incubation of both DIM and E2 with PD98059 significantly inhibited induction of VTG, $P < 0.01$. However, PKA exposure did not cause a change in VTG induction by either DIM or E2. In the second study, VTG induction was measured in liver slices after 96 hr exposure to 50 nM E2 or 5 μM DIM in the presence or absence of 1 μM ICI, an ER antagonist, 50 μM PD98059, 20 μM U0126, a MAPK inhibitor, 10 μM SB202190, a p38 inhibitor, 20 μM AG1478, an

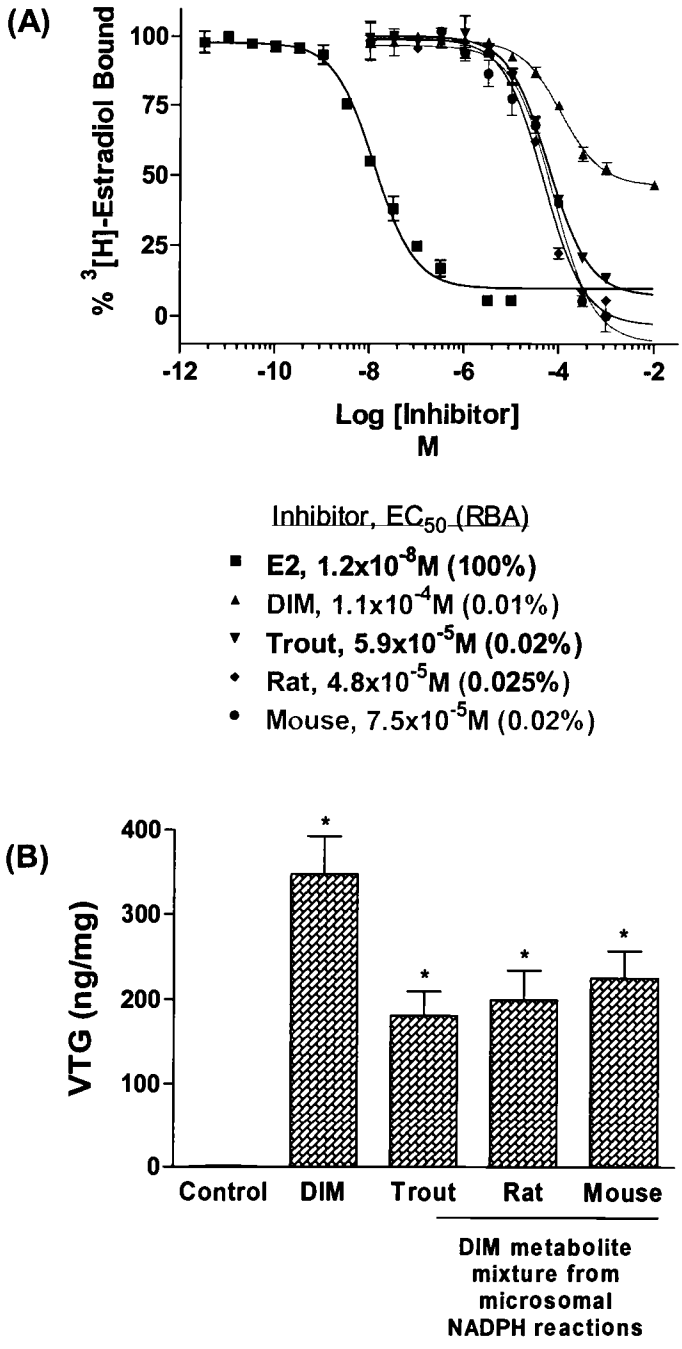

Figure 5-9. (A) Competitive inhibition of [^{3}H]-E2 in by E2, DIM and DIM metabolite mixture isolated separately from DIM parent. (B) VTG induction in liver slices after 96 hr exposure to 20 μM DIM and 20 uM 'DIM-equivalent' concentrations of metabolite mixture from trout, rat and mouse liver microsomes. *Indicates significant difference from control values ($P < 0.05$).

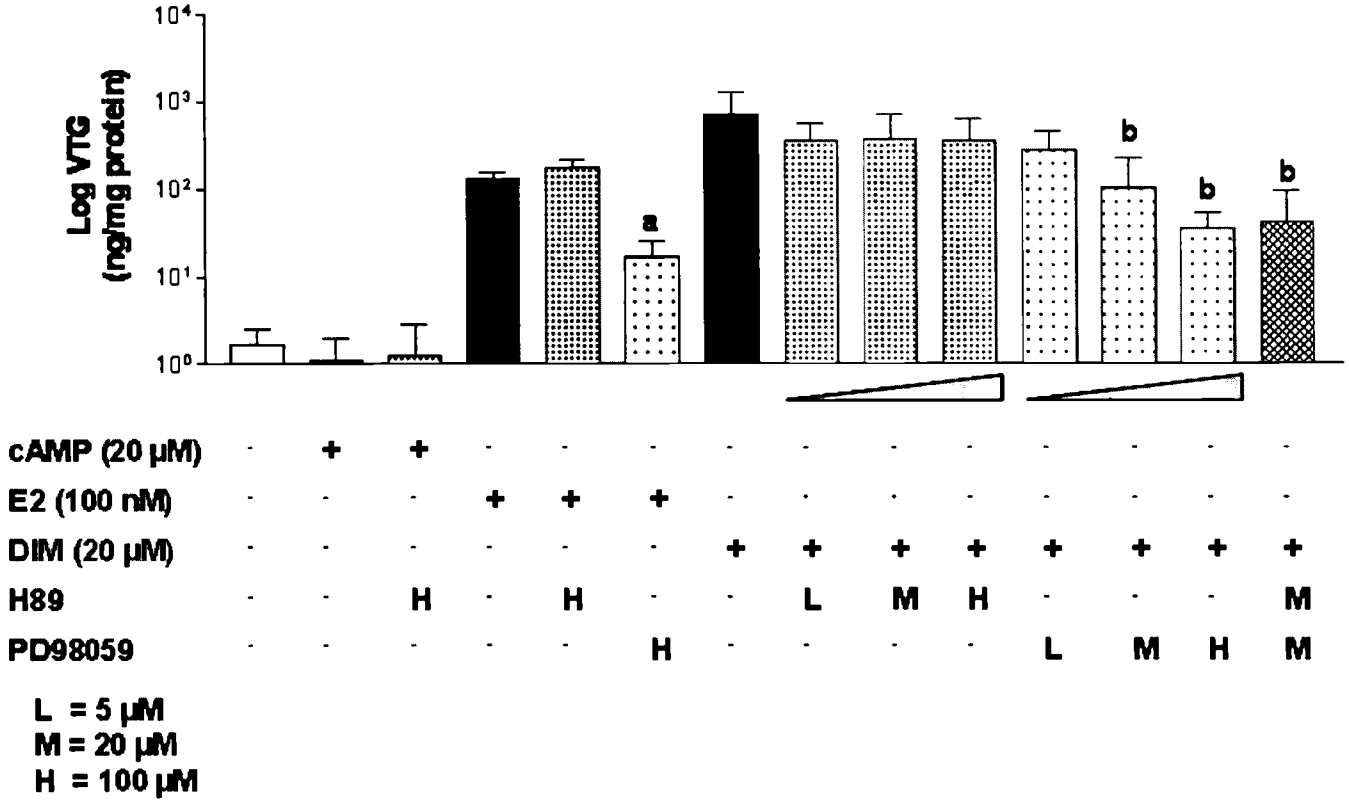

Figure 5-10. VTG induction from liver slices after 96 hr exposure to 20 µM cAMP, 100 nM E2 and 20 µM DIM in the presence or absence of 5 – 100 µM H89, a PKA inhibitor, or PD98059, a MAPK inhibitor. All E2 and DIM treatments were significantly greater than controls. [a]Indicates significant difference from E2 treatment. [b]Indicates significant difference from DIM treatment, $P < 0.01$.

EGFR inhibitor, 5 μM Gö6983, a PKC inhibitor, 20 μM LY294002, a PI3K inhibitor, 25 μM JNK II, a JNK inhibitor (Fig. 5-11). The concentrations of DIM and E2 used were EC50 values for VTG induction in liver slices. Concentrations of all receptor antagonists and kinase inhibitors used in both studies were chosen based on previously reported effectiveness *in vitro*. The DIM and E2 positive controls significantly induced VTG above vehicle controls and ICI and PD98059 inhibited VTG induction in both treatments, $P < 0.01$. Interestingly, another MAPK inhibitor, U0126, only inhibited VTG induction by DIM and not E2. Similarly, other kinase inhibitors, Gö6983, LY294002 and JNK II also significantly inhibited VTG induction by DIM and not E2, $P < 0.01$. Values for many E2 treatments showed large variability and so should be repeated with increasing concentrations of each inhibitor. However, these data indicate that other signaling pathways may be involved in ER-mediated activation of transcription in trout liver, particularly by DIM.

DISCUSSION

We have previously reported DIM to have a strong estrogenic response in trout liver by induction of VTG protein markers and by global hepatic gene profiles (Shilling *et al.*, 2001; Tilton *et al.*, 2005b). Further, we observed DIM to promote hepatocarcinogenesis in trout by estrogenic mechanisms based on comparison to E2-mediated tumor enhancement and gene transcriptional patterns. However, the mechanism by which DIM is acting as an estrogen in trout liver is currently unknown.

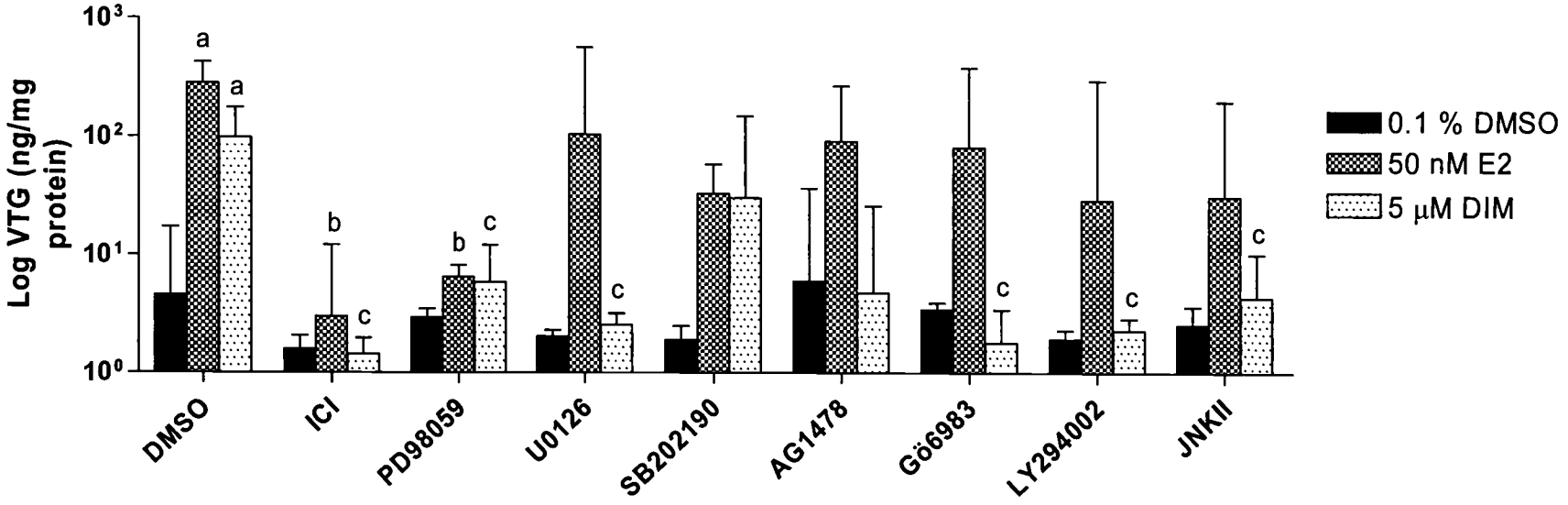

Figure 5-11. VTG induction from liver slices after 96 hr exposure to 50 nM E2 or 5 μM DIM in the presence or absence of 1 μM ICI, an ER antagonist, 50 μM PD98059, a MAPK inhibitor, 20 μM U0126, a MAPK inhibitor, 10 μM SB202190, a p38 inhibitor, 20 μM AG1478, an EGFR inhibitor, 5 μM Gö6983, a PKC inhibitor, 20 μM LY294002, a PI3K inhibitor, 25 μM JNK II, a JNK inhibitor. [a]Indicates signficant change from DMSO control. [b]Indicates significant difference from E2 treatment. [c]Indicates significant difference from DIM treatment, $P < 0.01$.

In this study, we characterized the estrogenic response of DIM in rainbow trout liver by measuring its *in vitro* biological activity, its ability to directly bind to ER and its potential for metabolism to estrogenic metabolites.

In the acid environment of the stomach, I3C forms several acid condensation products, including DIM, LTR, CTR and ICZ. DIM was found to be the most prominent derivative present in liver extracts after oral administration of ^{3}H-I3C comprising 40% of total label in trout and 1.1% in rat, suggesting species differences in metabolism, I3C ACP formation, DIM intestinal absorption or liver uptake (Dashwood *et al.*, 1989; Stresser *et al.*, 1995a). The ability of DIM to cause such a potent estrogenic response in trout liver compared to I3C suggests it is also the primary biologically active component of I3C in trout liver. We have confirmed this by examining VTG and CYP1A induction in liver slices *in vitro* by DIM compared to CTR and LTR. VTG and CYP1A are markers for activation of ER and AhR-mediated responses, respectively. DIM was the only I3C oligomerization product to induce VTG with similar efficacy as E2, although with approximately 300-fold lower potency. LTR and CTR both only had weak ability to induce VTG in liver slices. In contrast, DIM was a weak inducer of CYP1A while LTR and CTR were both able to induce CYP1A with similar efficacy as βNF. There may be species differences in the ability of different I3C acid condensation products to cause an estrogenic response. CTR was previously found to be a potent estrogen in MCF-7 cells causing enhanced cell growth and proliferation through ER-dependent mechanisms (Riby *et al.*, 2000b). In the trout model, DIM is the most potent estrogen of the I3C acid condensation products and is likely responsible for the estrogenic effects of I3C in trout *in vivo*.

Despite the ability of DIM to cause a relatively potent estrogenic biological response, it was only found to be a weak agonist for the ER receptor in trout liver cytosol having a relative binding affinity 10,000-fold lower than E2. DIM was an even less potent competitive inhibitor of [^{3}H]-E2 in sheep uterine cytosol having a relative binding affinity 35,000-fold lower than E2. DIM was also previously reported to be a weak agonist to human ERα (Riby *et al.*, 2000a). One possible explanation for differences in biological activity compared to receptor binding in trout is potential metabolism of DIM to an active estrogenic metabolite. As suggested above, species differences in DIM metabolism may also explain species differences measured in hepatic concentrations of DIM after I3C disposition *in vivo*. Previous data indicated that a non-specific CYP450 inhibitor, SKF525A, in trout could reduce VTG induction by DIM *in vitro* (Shilling *et al.*, 2001). We confirmed that CYP450-mediated inhibition of VTG was specific for DIM and did not occur with E2. Interestingly, when DIM metabolism was examined in liver microsomes, a similar primary metabolite, at t = 19 min, was found to be produced by all species examined, including trout, mouse and rat, although there were species differences in the extent of DIM metabolism; rat > mouse > trout. Greater metabolism of DIM in rat liver compared to trout would support the differences in hepatic DIM concentrations previously reported in pharmacokinetic studies (Dashwood *et al.*, 1989; Stresser *et al.*, 1995a). Mass fragmentation spectra indicated that the metabolite was a mono-hydroxylated form of DIM. Computer modeling of DIM compared to E2 suggested that mono- or di-hydroxylation of DIM would structurally enhance its potential as an ER-agonist. Our data indicate that the mixture of polar metabolites formed were able

to bind to ER with a higher relative binding affinity than DIM and also have some biological activity in VTG induction assays. Future research is required to identify specific DIM metabolites and their estrogenic and/or anti-estrogenic effects. However, our data indicate that DIM is metabolized to more polar metabolites that bind to ER and show biological estrogenic activity and that there is marked species difference in DIM metabolism among trout, mouse and rat.

Recent data indicate that the estrogenic actions of DIM in breast and endometrial cancer cells *in vitro* are distinct from E2 in that they were mediated through ligand-independent activation of ER by MAPK and PKA signaling pathways (Leong *et al.*, 2004). Further DIM has been found to stimulate interferon gamma (IFNγ) through p38 and JNK signaling pathways (Xue *et al.*, 2005). These data show that DIM can mediate biological effects, including estrogenic effects, through extracellular signaling pathways. We investigated whether these pathways may be relevant for DIM estrogenicity in trout liver. We observed inhibition of DIM and E2-mediated VTG induction by co-treatment with the MAPK (MEK1) inhibitor, PD98059, indicating that ligand-independent activation of ER in trout may not only be important for DIM, but also for endogenous E2. Further, we also observed inhibition of VTG by DIM with inhibitors of MEK1 phosphorylation, PI3K, JNK and PKC suggesting tyrosine kinase signaling and intracellular calcium are involved in the estrogenic response of DIM. Unfortunately, variability was too high in the E2 exposures to determine if these effects were specific to DIM or are general for estrogenic signaling in trout. The role of extracellular signaling cascades in trout E2-dependent and independent mechanisms have not been well described. However,

estrogenic responses in trout liver were previously reported to involve both genomic and non-genomic signaling cascades, the latter of which required activation of MAPK (Kullman *et al.*, 2003). Further, oxidative stress by metals in trout hepatoma cells was mediated through ligand-independent tyrosine kinase signaling requiring activation of p38, JNK and STAT (Burlando et al., 2003).

We have previously observed DIM and E2-mediated transcriptional upregulation of Janus kinase similar to non-receptor tyrosine kinase (TYK2) or JAK1 based on sequence homology and factors that are important in G-protein activation of cell surface receptors (Tilton *et al.*, 2005b). TYK2 is known to mediate JAK/STAT signaling, which is important for cell proliferation, differentiation and cytokine signaling. The significance of these findings is supported by the present observations that inhibition of kinases within these pathways also inhibits ER-mediated VTG induction by DIM and/or E2. A recent publication reported that a known inducer of oxidative stress, procymidone, was able to induce VTG in hepatocytes through a mechanism that induced MAPK and was blocked by co-treatment with the anti-oxidant α-tocopherol (Radice *et al.*, 2004). It is possible that oxidative mechanisms may also be involved in the non-genomic signaling by E2/DIM observed in this study. Cross-talk between estrogen and growth factor signaling and between estrogen and cytokine signaling has been reported in other models as mechanisms important for endocrine homeostasis and signaling (Hayashi *et al.*, 2003; Sekine *et al.*, 2004). More research is required to further evaluate the mechanism and significance of non-genomic signaling by DIM and E2 in trout liver and the importance of oxidative stress. However, these data support a potential role for ligand-independent activation of ER

by DIM, which may provide another possible explanation for the differences in potency observed between ER-binding and biological activity of DIM *in vitro*.

ACKNOWLEDGEMENTS

The authors wish to thank Eric Johnson and Greg Gonnerman for care and maintenance of fish and Sheila Cleveland for histological preparation of liver slices. We would also like to acknowledge M. M. van Lipzig, N. P. Vermeulen and T. J. Meerman for their assistance of metabolism studies with sheep uterine ER binding assays. This work was supported by NIH grants ES07060, ES03850, ES00210, ES11267 and CA90890.

Chapter 6. Conclusion

In these studies, we applied a toxicogenomic approach to determine the mechanism for tumor enhancement by dietary indole phytochemicals, indole-3-carbinol (I3C) and 3,3'-diindolylmethane (DIM), in rainbow trout hepatocarcinogenesis. I3C was previously found to promote hepatocarcinogenesis in rainbow trout (*Oncorhynchus mykiss*) at concentrations that differentially activated estrogen receptor (ER) or aryl hydrocarbon receptor (AhR)-mediated responses based on individual protein biomarkers. The relative importance of these pathways was evaluated on a global scale as potential mechanisms for I3C using a salmonid cDNA microarray. Hepatic gene expression profiles were examined after dietary exposure to I3C and DIM compared to 17β-estradiol (E2), an ER agonist, and β-naphthoflavone, an AhR agonist. We demonstrate that I3C and DIM acted similar to E2 at the transcriptional level based on correlation analysis of expression profiles and on clustering of gene responses. Of all the genes 2-fold differentially regulated by E2, approximately 87 – 92% were also similarly regulated by DIM and 71% by I3C. The correlations are likely conservative based on the stringent criteria used to determine differential regulation by array analysis and the lower sensitivity of microarray results observed in comparison to qRT-PCR. These data highlight the strong overlap in transcriptional signatures of dietary indoles with endogenous E2 and suggests that the promotional ability of I3C in trout is through estrogenic mechanisms.

The transcriptional profiles in this study for E2, DIM and I3C provide insight into the estrogenic mechanisms that may be important for promotion in trout liver

including cell proliferation, signaling pathways and protein stability. Transcriptional upregulation of both ER chaperone proteins and downstream targets indicate the responses to E2 and dietary indoles are ER-mediated. We observed consistent downregulation of genes involved in redox regulation and lipid, glucose and retinol homeostasis and metabolism by estrogenic treatments. Also, an unexpected and consistent downregulation of genes important for angiogenesis, formation of the extracellular matrix, and immune response were measured after estrogenic treatment. These data indicate evolutionary conservation of a dual role for estrogens in which they can simultaneously stimulate tumor growth, but may also have some protective effects against tumor invasion and motility. This data also suggests that DIM may be an even more potent promoter of hepatocarcinogenesis in trout by estrogenic mechanisms.

In a following study, DIM was found to promote aflatoxin B_1 (AFB_1)-induced hepatocarcinogenesis in trout similar to E2. Trout embryos were initiated with 50 ppb AFB_1 and then juvenile fish were fed diets containing 120 and 400 ppm DIM or 5 ppm E2 for 18 weeks. Tumor incidence was elevated in AFB_1-initiated trout fed 400 ppm DIM and 5 ppm E2. To evaluate the mechanism of tumor promotion, hepatic gene expression profiles were examined in animals on promotional diets during the course of tumorigenesis and in hepatocellular carcinomas (HCCs) of initiated animals using a rainbow trout 70-mer oligonucleotide array. Strong transcriptional correlations were observed between DIM and E2 treatments at all timepoints examined. A strong transcriptional estrogenic signature was measured in liver samples after 3-weeks of DIM and E2 treatment, which included upregulation of transcripts for known

estrogen-responsive proteins, such as vitellogenin, vitelline envelope, ER α/β and cathepsin D, and downregulation of genes important for acute phase response and drug, lipid and retinol metabolism. These transcriptional patterns indicate that the tumor enhancing effects of DIM are similar to E2 and are likely mediated through ER-dependent mitogenic signaling in trout liver.

We also observed upregulation of genes at the 3-week timepoint involved in adaptive immunity and in cytokine-related extracellular signaling cascades indicating possible potentiation of immune function by DIM and E2. Enhancement of immune function in cancer immunosurveillance may be a primary defense against cancer. It is difficult to know what effect enhancement of adaptive immunity may have in trout chemoprotection. However, while DIM and E2 increased tumor incidence in initiated animals, transcriptional profiles in HCC tumors from these animals indicated lower invasive and metastatic potential compared to HCCs from control animals. It is possible that DIM is acting similar to E2 in trout liver and, as described above, may have a dual effect on tumorigenesis in which it may increase tumor incidence through ER-mediated mitogenic signaling and decrease potential for metastasis possibly through immune activation and potentiation, however these mechanisms need to be further explored. These data may help explain the dichotomy of chemoprotective and enhancing effects of dietary indoles on cancer development.

Transcriptional profiles were also examined in histologically confirmed HCCs compared to non-cancerous adjacent tissue for individual tumors. Hepatocellular carcinoma is one of the most common malignant tumors worldwide and its occurrence is associated with a number of environmental factors including ingestion of the dietary

contaminant aflatoxin B_1 (AFB_1). Research over the last 40 years has revealed rainbow trout (*Oncorhynchus mykiss*) to be an excellent research model for study of AFB_1-induced hepatocarcinogenesis, however little is currently known about changes at the molecular level in trout tumors. We have developed a rainbow trout oligonucleotide array containing 1,672 elements representing over 1,400 genes for use in studies relevant for toxicology, comparative immunology, carcinogenesis, endocrinology and stress physiology. We observed distinct gene regulation patterns in HCC compared to non-cancerous tissue including upregulation of genes important for cell cycle control, transcription, cytoskeletal formation and the acute phase response and down regulation of genes involved in drug metabolism, lipid metabolism and retinol metabolism. Overall, transcriptional profiles indicate that AFB_1-induced HCC in trout is of an invasive and aggressive nature and may also be indicative of changes observed during chronic inflammatory liver diseases, which further enhances the merits of the trout as a model for human HCC. Interestingly, expression profiles observed in trout HCC are similar to transcriptional changes reported in studies of human and rodent HCC. The fact that these studies utilized HCC of different etiologies (many viral) supports the likelihood that some processes of HCC pathogenesis have been conserved during long periods of evolutionary time.

The estrogenic response of DIM was further characterized in rainbow trout liver by measuring its *in vitro* biological activity, its ability to directly bind to ER and its potential for metabolism to estrogenic metabolites. We found DIM to have the highest estrogenic potency *in vitro* compared to other I3C oligomerization products with similar efficacy for VTG induction as E2 and 300-fold lower potency. However,

DIM competitively bound to trout hepatic ER with a relative binding affinity 10,000-fold lower than E2 suggesting it is only a weak agonist for the trout ER. Differences between DIM receptor binding and biological activity may be explained in part by our observation in this study that VTG induction by DIM was inhibited by co-treatment with CYP450 inhibitors indicating that the active estrogen may be a DIM metabolite. DIM metabolism was measured in liver microsomes and identified by HPLC and LC/MS. We confirmed the production of a mono-hydroxylated metabolite of DIM that, as part of a metabolite mixture, was able to bind to trout ER and induce VTG *in vitro*. We were also able to confirm the potential importance of non-genomic signaling cascades for estrogenic signaling by DIM with the use of inhibitors of kinases important in these mechanisms. These data support the role of DIM as a potent estrogen in trout liver that may require metabolism for ligand-dependent activation of ER or activation of extracellular signaling pathways for ligand-independent activation of ER.

Overall, these studies show that I3C and DIM are tumor enhancers in trout liver through estrogenic mechanisms similar to E2. However, novel chemoprotective effects of both DIM and E2 have been determined transcriptionally in liver and in tumors from treated animals. Of particular interest, is the potential for decreased angiogenesis and metastasis, which may be mediated through the immunomodulatory effects of DIM and E2. Current evidence suggests that DIM and E2 are acting through similar mechanisms in trout, however there may be some differences in their ability to activate ER through extracellular signaling pathways. More research is required to further evaluate the mechanism and significance of non-genomic signaling by DIM

and E2 in trout liver. It is likely that multiple mechanisms are involved in the estrogenic activity of DIM, which may explain the cell/tissue and species-specific effects reported in the mechanisms of dietary indoles.

Bibliography

Akiba, J., Yano, H., Ogasawara, S., Higaki, K., and Kojiro, M. (2001). Expression and function of interleukin-8 in human hepatocellular carcinoma. *Intl. J. Oncol.* **18**, 257-264.

Anderton, M. J., Manson, M. M., Vershoyle R. D., Gescher A., Lamb, J. H., Farmer, P. B., Steward, W. P., and Williams, M. L. (2004). Pharmacokinetcs and tissue disposition of indole-3-carbinol and its acid condensation products after oral administration to mice. *Clin. Cancer Res.* **10**, 5233-5241.

Ashley, L. M. and Halver, J. E. (1961). Hepatomagenesis in rainbow trout. *Fed Proc* **20**:290.

Bailey,G.S., Selivonchick,D. and Hendricks,J.D. (1987) Initiation, promotion and inhibition of carcinogenesis in rainbow trout. *Environ. Health Persp.* **71**, 147-153.

Bailey, G. S., Goeger, D. E., and Hendricks, J. D. (1989). Factors influencing experimental carcinogenesis in laboratory fish models. In *Metabolism of Polynuclear Hydrocarbons in the Aquatic Environment* (U. Varanasi, Ed.), pp. 253-268. CRC Press, Boca Raton, FL.

Bailey, G. S., Dashwood, R. H., Fong, A. T., Williams, D. E., Scanlan, R. A., and Hendricks, J. D. (1991). Modulation of mycotoxin and nitrosamine carcinogensis by indole-3-carbinol: Quantitative analysis of inhibition versus promotion. In *Relevance to Human Cancer of N-Nitroso Compounds*. (I. K.

O'Neill, J. Chen, and H. Bartsch, Eds.), pp. 275-280. IARC Press, Lyon, France.

Bailey, G. S., Williams, D. E., and Hendricks, J. D. (1996). Fish models for environmental carcinogenesis: The rainbow trout. *Environ. Health Perspect.* **104**(Suppl), 5-19.

Bei, H., Zhong-Bi, W., and You-Bing, R. (1998). Expression of nm23 gene expression in hepatocellular carcinoma tissue and its relation with metastasis. *World J. Gastroenterol.* **4**, 266-267.

Bjeldanes,L.F., Kim,J.Y., Grose,K.R., Bartholomew,J.C. and Bradfield,C.A. (1991) Aromatic hydrocarbon responsiveness-receptor agonists generated from indole-3-carbinol in vitro and in vivo: comparisons with 2,3,7,8-tetrachlorodibenzo-p-dioxin. *PNAS.* **88**, 9543-9547.

Bjorge, L., Hakulinen, J., Vintermyr, O. K., Jarva, H., Jensen, T. S., Iversen, O. E., and Meri, S. (2005). Ascitic complement system in ovarian cancer. *Br. J. Cancer.* **14**, 895-905.

Blakemore, P. R., Kim, S. K., Schulze, V. K., White, J. D. and Yokochi, A. F. T. (2001). Asymmetric synthesis of (+)-Ioline, a pyrrolizidine alkaloid from rye grass and tall fescue. *J. Chem. Soc., Per. Trans. 1.* **15**, 1831-1847.

Borlak, J., Meier, T., Halter, R., Spanel, R., and Spanel-Borowski, K. (2005). Epidermal growth factor-induced hepatocellular carcinoma: gene expression profiles in precursor lesions, early stage and solitary tumours. *Oncogene.* **10**, 1809-1819.

Bowman, C. J., Kroll, K. J., Gross, T. G., and Denslow N. D. (2002). Estradiol-induced gene expression in largemouth bass (*Micropterus salmoides*). *Mol. Cell. Endocrinol.* **196**, 67-77.

Bradfield,C.A. and Bjeldanes,L.F. (1984) Effect of dietary indole-3-carbinol on intestinal and hepatic monooxygenase, glutathione S-transferase and epoxide hydrolase activities in the rat. *Fd. Chem. Toxicol.* **22**, 977-982.

Bradfield, C. A. and Bjeldanes, J. F. (1987). Structure-activity relationships of dietary indoles: a proposed mechanism of action as modifiers of xenobiotic metabolism. *J. Toxicol. Environ. Health.* **21**, 311-322.

Breinholt, V., Hendricks, J. D., Pereira, C. B., Arbogast, D., and Bailey, G. S. (1995). Dietary chlorophyllin is a potent inhibitor of aflatoxin B_1 hepatocarcinogenesis in rainbow trout. *Cancer Res.* **55**, 57-62.

Breitkreutz, B. J., Jorgensen, P., Breitkreutz, A., and Tyers, M. (2001). AFM 4.0: a toolbox for DNA microarray analysis. *Genome Biol.* **2**, software0001.1-0001.3.

Burlando, B., Magnelli, V., Panfoli, I., Berti, E. and Viarengo, A. (2003). Ligand-independent tyrosine kinase signaling in RTH 149 trout hepatoma cells: comparison among heavy metals and pro-oxidants. *Cell Physiol. Biochem.* **13**, 147-154.

Carrello, A., Allan, R. K., Morgan, S. L., Owen, B. A., Mok, D., Ward, B. K., Minchin, R. F., Toft, D. O., and Ratajczak, T. (2004). Interaction of the Hsp90 cochaperone cyclophylin 40 with Hsc70. *Cell Stress Chaperones.* **9**, 167-181.

Carruba, G., Cocciadiferro, L., Bellavia, V., Rizzo, S., Tsatsanis, C., Spandidos, D., Muti, P., Smith, C., Mehta, P., and Castagnetta. (2004). Intercellular

communication and human hepatocellular carcinoma. *Ann. NY Acad. Sci.* **1028**, 202-212.

Cavailles, V., Augereau, P., and Rochefort, H. (1991). Cathepsin D gene of human MCF7 cells contains estrogen-responsive sequences in its 5' proximal flanking region. *Biochem. Biophys. Res. Comm.* **174**, 816-824.

Chen, C. J., Wang, L. Y., Lu, S. N., Wu, M. H., Lou, S. L., Zhang, Y. J., Wang, L. W., and Santella, R. M. (1996). Elevated aflatoxin exposure and increased risk of hepatocellular carcinoma. *Hepatol.* **24**, 38-42.

Chen,I., McDougal,A., Wang,F. and Safe,S. (1998) Aryl hydrocarbon receptor-mediated antiestrogenic and antitumorigenic activity of diindolylmethane. Carcinogenesis. **19**, 1631-1639.

Chen, W., Cai, M. Y., Wei, D. P., and Wang, X. (2005). Pivotal molecules of MHC I pathway in human primary hepatocellular carcinoma. *World J. Gastroenterol.* **11**, 3297-3299.

Choi, J. K., Choi, J. Y., Kim, D. G., Choi, D. W., Kim, B. Y., Lee, K. H., Yeom Y. I., Yoo, H. S., Yoo, O. J., and Kim, S. (2004). Integrative analysis of multiple gene expression profiles applied to liver cancer study. *FEBS Lett.* **565**, 93-100.

Dashwood, R. H., Uyetake, L., Fong, A. T., Hendricks, J. D., and Bailey, G. S. (1989). In vivo disposition of the natural anti-carcinogen indole-3-carbinol after po administration to rainbow trout. *Fd. Chem. Toxic.* **27**, 385-392.

Dashwood,R.H., Fong,A.T., Williams,D.E., Hendricks,J.D. and Bailey,G.S. (1991) Promotion of aflatoxin B1 carcinogenesis by the natural tumor modulator

indole-3-carbinol: influence of dose, duration, and intermittent exposure on indole-3-carbinol promotional potency. *Cancer Res.* **51**, 2362-2365.

Dashwood, R. H., Fong, A. T., Arbogast, D. N., Bjeldanes, L. F., Hendricks, J. D., and Bailey, G. S. (1994). Anticarcinogenic activity of indole-3-carbinol acid products: Ultrasensitive bioassay by trout embryo microinjection. *Cancer Res.* **54**, 3617-3619.

Ding, S., Gong, B. D., Yu, J., Gu, J., Zhang, H. Y., Shang, Z. B., Fei, Q., Wang, P., and Zhu, J. D. (2004). Methylation profile of the promoter CpG islands of 14 "drug-resistance" genes in hepatocellular carcinoma. *World J. Gastroenterol.* **10**, 3433-3440.

Donohoe, R. M. and Curtis, L.R. (1996). Estrogenic activity of chlordecone, *o,p'*-DDT and *o,p'*-DDE in juvenile rainbow trout: Induction of vitellogenesis and interaction with hepatic estrogen binding sites. *Aquat. Toxicol.* **36**, 31-52.

Egner, P., Wang, J., Zhu, Y., Zhang, B., Wu, Y., Zhang, Q., Qian, G. S., Kuang, Y. S., Gange, S. J., Jacobson, L. P., Helzlsouer, K. J., Bailey, G. S., Groopman, J. D., and Kensler, T. W. (2001). Chlorophyllin intervention reduces aflatoxin-DNA adducts in individuals at high risk for liver cancer. *Proc. Natl. Acad. Sci.* **98**, 14601-14606.

El-Serag, H. B. and Mason, A. C. (1999). Rising incidence of hepatocellular carcinoma in the United States. *N. Engl. J. Med.* **340**, 745-750.

Exon,J.H. and South,E.H. (2000) Dietary indole-3-carbinol alters immune functions in rats. *J. Toxicol. Environ. Health A.* **59**, 271-279.

Fang, H., Tong, W., Shi, L. M., Blair, R., Perkins, R., Branham, W., Hass, B. S., Xie, Q., Dial, S. L., Moland, C. L. and Sheehan, D. M. (2000). Structure-activity relationships for a large diverse set of natural, synthetic and environmental estrogens. *Chem. Res. Toxicol.* **14**, 280-294.

Ficazzola, M. A., Fraiman, M., Gitlin, J., Woo, K., Melamed, J., Rubin, M. A., and Walden, P. D. (2001). Antiproliferative B cell translocation gene 2 protein is down-regulated post-transcriptionally as an early event in prostate carcinogenesis. *Carcinogenesis*. **22**, 1271-1279.

Graveel, C. R., Jatkoe, T., Madore, S. J., Holt, A. L., and Farnham, P. J. (2001). Expression profiling of novel genes in hepatocellular carcinomas. *Oncogene*. **20**, 2704-2712.

Groopman, J. D., Scholl, P., and Wang, J. S. (1996). Epidemiology of human aflatoxin exposures and their relationship to human liver cancer. *Can. J. Physiol. Pharmacol.* **74**, 203-209.

Grose, K. R. and Bjeldanes, L. F. (1992). Oligomerization of indole-3-carbinol in aqueous acid. *Chem. Res. in Toxicol.* **5**, 188-193.

Grubbs, C. J., Steele, V. E., Casebolt, T., Juliana, M. M., Eto, I., Whitaker, L. M., Dragnev, K. H., Kelloff, G. J., and Lubert, R. L. (1995). Chemoprevention of chemically-induced mammary carcinogenesis by indole-3-carbinol. *Anticancer Res.* **15**, 709-716.

Hayashi, S. I., Sakamoto, T., Inoue, A., Yoshida, N., Omoto, Y. and Yamaguchi, Y. (2003). Estrogen and growth factor signaling pathway: basic approaches for clinical application. *J. Steroid. Biochem. Mol. Biol.* **86**, 433-442.

Helms,M.W., Packeisen,J., August,C., Schittek,B., Boecker,W., Brandt,B.H. and Buerger,H. (2005) First evidence supporting a potential role for the BMP/SMAD pathway in the progression of oestrogen receptor-positive breast cancer. *J. Pathol.* **206**, 366-376.

Hendricks, J. D., Meyers, T. R., and Shelton, D. W. (1984). Histological progression of hepatic neoplasia in rainbow trout (*Salmo gairdneri*). *Monogr. Natl. Cancer Inst.* **65**, 321-336.

Jazaeri, A. A., Yee, C. J., Sotiriou, C., Brantley, K. R., Boyd, J., and Liu, E. T. (2002). Gene expression profiles of BRCA1-linked, BRCA2-linked, and sporadic ovarian cancers. *J. Natl. Cancer Inst.* **94**, 990-1000.

Kakhlon, O., Gruenbaum, Y., and Cabantchik, Z. I. (2001). Repression of ferritin expression increases the labile iron pool, oxidative stress, and short-term growth of human erythroleukemia cells. *Blood.* **97**, 2863-2871.

Kanetaka, K., Sakamoto, M., Yamamotot, Y., Yamasaki, S., Lanza, F., Kanematsu, T., and Hirohashi, S. (2001). Overexpression of tetraspanin CO-029 in hepatocellular carcinoma. *J. Hepatol.* **35**, 637-642.

Kim,D.J., Han,B.S., Ahn,B., Hasegawa,R., Shirai,T., Ito,N. and Tsuda,H. (1997) Enhancement by indole-3-carbinol of liver and thyroid gland neoplastic development in rat medium-term multiorgan carcinogenesis model. *Carcinogenesis.* **18**, 377-381.

Kim, Y. S., and Milner, J. A. (2005). Targets for indole-3-carbinol in cancer prevention. *J. Nutr. Biochem.* **16**, 65-73.

Kodama,T., Takeda,K., Shimozato,O., Hayakawa,Y., Atsuta,M., Kobayashi,K., Ito,M., Yagita,H. and Okumura,K. (1999) Perforin-dependent NK cell cytotoxicity is sufficient for anti-metastatic effect of IL-2. *Eur. J. Immunol.* **29**:1390-1396.

Koh, K. K. (2002). Effects of estrogen on the vascular well: vasomotor function and inflammation. *Cardiovascular Res.* **55**, 714-726.

Kojima, T., Tanaka, T., and Mori, H. (1994). Chemoprevention of spontaneous endometrial cancer in female Donryu rats by dietary indole-3-carbinol. *Cancer Res.* **54**, 1446-1449.

Krasnov, A., Koskinen, H., Pehkonen, P., Rexroad III, C. E., Afanasyev, S., and Molsa, H. (2005). Gene expression in the brain and kidney of rainbow trout in response to handling stress. *BMC Genomics.* **6**, 3.

Krasnov, A., Koskinen, H., Rexroad, C., Afanasyev, S., Molsa, H., and Oikari, A. (2005). Transcriptome responses to carbon tetrachloride and pyrene in the kidney and liver of juvenile rainbow trout (*Oncorhynchus mykiss*). *Aquatic Toxicol.* **74**, 70-81.

Kullman, S. W., Matsamura, F., and Hinton, D. E. (2003). Estrogen signaling in trout liver: Estrogen receptor mitogenic mediated cellular responses. *Environ. Sci.* **10**, 223-237.

Kulomaa, M. S., Weigel, N. L., Kleinsek, D. A., Beattie, W. G., Conneely, O. M., March, C., Zarucki-Schulz, T., Schrader, W. T., and O'Malley, B. W. (1986). Amino acid sequence of a chicken heat shock protein derived from the complementary DNA nucleotide sequence. *Biochem.* **25**, 6244-6251.

Kwon, J. Y., Prat, F., Randall, C., and Tyler, C. R. (2001). Molecular characterization of putative yolk processing enzymes and their expression during oogenesis and embyogenesis in rainbow trout (*Oncorhynchus mykiss*). *Biol. Reprod.* **65**, 1701-1709.

Larkin, P., Sabo-Attwood, T., Kelso, J., and Denslow, N. D. (2002). Gene expression analysis of largemouth bass exposed to estradiol, nonylphenol, and p,p'-DDE. *Comp. Biochem. Physiol.* B. **133**, 543-557.

Larkin, P., Folmar, L. C., Hemmer, M. J., Poston, A. J., and Denslow N. D. (2003). Expression profiling of estrogenic compounds using sheepshead minnow cDNA macroarray. *Environ. Health Perspect.* **111**, 839-846.

Lazier, C. B., Lonergan, K. and Mommsen, T. P. (1985). Hepatic estrogen receptors and plasma estrogen-binding activity in the Atlantic salmon. *Gen. Comp. Endocrinol.* **57**, 234-245.

Lee, B. C., Hendricks, J. D., and Bailey, G. S. (1989). Iron resistance of hepatic lesions and nephroblastoma in rainbow trout (*Salmo gairdneri*) exposed to MNNG. *Toxicol. Pathol.* **17**, 474-482.

Lee B. C., Hendricks J. D., Bailey G. S. (1991). Toxicity of microtoxins in the feed of fish. In *Mycotoxins and Animal Feedstuff: Natural Occurrence, Toxicity and Control* (J. E. Smith, Ed.), pp. 607-626. CRC Press, Boca Raton, FL.

Leong, H., Firestone, G. L. and Bjeldanes, L. F. (2001). Cytostatic effects of 3,3'-diindolylmethane in human endometrial cancer cells result from an estrogen receptor-mediated increase in transforming growth factor-α expression. *Carcinogenesis.* **22**, 1809-1817.

Leong, W. I. and Lonnerdal, B. (2004). Hepcidin, the recently identified peptide that appears to regulate iron absorption. *J. Nutr.* **134**, 1-4.

Leong, H., Riby, J. E., Firestone, G. L., and Bjeldanes, L. F. (2004). Potent ligand-independent estrogen receptor activation by 3,3,'-diindolylmethane is mediated by cross-talk between protein kinase A and mitogen-activated protein kinase signaling pathways. *Mol. Endocrinol.* **18**, 291-302.

Li, F. and Stormo, G. D. (2001). Selection of optimal DNA oligos for gene expression arrays. *Bioinformatics*. **17**, 1067-1076.

Lindsley, J. E., and Rutter, J. (2004). Nutrient sensing and metabolic decisions. *Comp. Biochem. Physiol. B*. **139**, 543-559.

Lodygin, D., Epanchintsev, A., Menssen, A., Diebold, J., and Hermeking, H. (2005). Functional epigenomics identifies genes frequently silenced in prostate cancer. *Cancer Res*. **65**, 4218-4227.

Lord, R. S., Bongiovanni, B., and Bralley, J. A. (2002). Estrogen metabolism and the diet-cancer connection: Rationale for assessing the ratio of urinary hydroxylated estrogen metabolites. *Altern. Med. Rev.* **7**, 112-129.

Lu, Z. L., Luo, D. Z., and Wen J. M. (2005). Expression and significance of tumor-related genes in HCC. *World J. Gastroenterol.* **11**, 3850-3854.

Manson, M. M., Hudson, E. A., Ball, H. W. L., Barrett, M. C., Clark, H. L., Judah, D. J. Verschoyle, R. D., and Neal, G. E. (1998). Chemoprevention of aflatoxin B1-induced carcinogenesis by indole-3-carbinol in rat liver- predicting the outcome using early biomarkers. *Carcinogenesis*. **19**, 1829-1836.

McDanell, R., McLean, A. E., Hanley, A. B., Heaney, R. K., and Fenwick, G. R. (1988). Chemical and biological properties of indole glucosinolates (glucobrassicin): A review. *Fd. Chem. Toxicol.* **26**, 59-70.

Meng, Q., Yuan, F., Goldberg, I. D., Rosen, E. M., Auborn, K., and Fan, S. (2000). Indole-3-carbinol is a negative regulator of estrogen receptor-α signaling in human tumor cells. *J. Nutr.* **130**, 2927-2931.

Meyer, K., Lee, J. S., Dyck, P. A., Cao, W. Q., Rao, M. S., Thorgeirsson, S. S., and Reddy, J. K. (2003). Molecular profiling of hepatocellular carcinomas developing spontaneously in acyl-CoA oxidase deficient mice: Comparison with liver tumors induced in wild-type mice by a peroxisome proliferator and a genotoxic carcinogen. *Carcinogenesis*. **24**, 975-984.

Miller, M. R., Wentz, E. and Ong, S. (1999). Acetaminophen alters estrogenic responses in vitro: inhibition of estrogen-dependent vitellogenin production in trout liver cells. *Toxicol. Sci.* **48**, 30-37.

Moriwaki, H., Tajika, M., Miwa, Y., Kato, M., Yasuda, I., Shiratori, Y., Okuno, M., Kato, T., Ohnishi, H., and Muto, Y. (2000). Nutritional pharmacotherapy of chronic liver disease: from support of liver failure to prevention of liver cancer. J. Gastroenterol. **35**(Suppl 12), 13-17.

Morse,M.A., LaGreca,S.D., Amin,S.G. and Chung,F.L. (1990) Effects of indole-3-carbinol on lung tumorigenesis and DNA methylation induced by 4-(methylnitrosamino)-1-(3-pyridyl)-1-butanone (NNK) and on the metabolism and disposition of NNK in A/J mice. *Cancer Res.* **50**, 2613-2617.

Neo, S. Y., Leow, C. K., Vega, V. B., Long, P. M., Islam, A. F. M., Lai, P. B. S., Liu, E. T., and Ren, E. C. (2004). Identification of discriminators of hepatoma by gene expression profiling using a minimal dataset approach. *Hepatology*. **39**, 944-953.

Nunez, O., Hendricks, J. D., Arbogast, D. N., Fong, A. T., Lee, B. C., and Bailey, G. S. (1989). Promotion of aflatoxin B1 hepatocarcinogenesis in rainbow trout by 17β-estradiol. *Aquat. Toxicol.* **15**, 289-302.

Oganesian, A., Hendricks, J. D. and Williams, D. E. (1997). Long term dietary indole-3-carbinol inhibits diethylnitrosamine-initiated hepatocarcinogenesis in the infant mouse model. *Cancer Lett.* **118**, 87-94.

Oganesian, A., Hendricks, J. D., Pereira, C. B., Orner, G. A., Bailey, G. S., and Williams, D. E. (1999). Potency of dietary indole-3-carbinol as a promoter of aflatoxin B_1-induced hepatocarcinogenesis: Results from a 9000 animal tumor study. *Carcinogenesis*. **20**, 453-458.

Oka, R., Sasagawa, T., Ninomiya, I., Miwa, K., Tanii, H., and Saijoh, K. (2001). Reduction in the local expression of complement component 6 (C6) and 7 (C7) mRNAs in oesophageal carcinoma. *Eur. J. Cancer*. **37**, 1158-1165.

Okabe, H., Satoh, S., Kato, T., Kitahara, O., Yanagawa, R., Yamaoka, Y., Tsunoda, T., Furukawa, Y., and Nakamura, Y. (2001). Genome-wide analysis of gene expression in human hepatocellular carcinomas using cDNA microarray: Identification of genes involved in viral carcinogenesis and tumor progression. *Cancer Res*. **61**, 2129-2137.

Okihiro, M. S., and Hinton, D. E. (1999). Progression of hepatic neoplasia in medaka (Oryzias latipes) exposed to diethylnitrosamine. *Carcinogenesis*. **20**, 933-940.

Otero, A. S. (2000). NM23/Nucleoside diphosphate kinase and signal transduction. *J. Bioenerget. Biomembranes*. **32**, 269-275.

Ouyang, G. L., Li, Q. F., Peng, X. X., Liu, Q. R., and Hong S. G. (2002). Effects of tachyplesin on proliferation and differentiation of human hepatocellular carcinoma SMMC-7721 cells. *World J. Gastroenterol*. **8**, 1053-1058.

Ovejero, C., Cavard, C., Perianin, A., Hakvoort, T., Vermeulen, J., Godard, C., Fabre, M., Chafey, P., Suzuki, K., Romagnolo, B., Yamagoe, S., and Perret, C. (2004). Identification of the leukocyte cell-derived chemotaxin 2 as a direct target gene of β-catenin in the liver. *Hepatol*. **40**, 167-176.

Pence,B.B., Budingh,F. and Yang,S.P. (1986) Multiple dietary factors in the enhancement of dimethylhydrazine carcinogenesis: main effect of indole-3-carbinol. *J. Natl. Cancer Inst*. **77**, 269-276.

Pitot, H.C., Dragan, Y.P., Teeguarden, J., Hsia, S., and Campbell, H. (1996). Quantitation of multistage carcinogenesis in rat liver. *Toxicol. Pathol*. **24**, 119-128.

Poole, T. M. and Drinkwater, N. R. (1996). Strain dependent effects of sex hormones on hepatocarcinogenesis in mice. *Carcinogenesis*. **17**, 191-196.

Poon, R. T. P., Lau, C. P. Y., Ho, J. W. Y., Yu, W. C., Fan, S. T., and Wong, J. (2003). Tissue factor expression correlates with tumor angiogenesis and invasiveness in human hepatocellular carcinoma. *Clin. Cancer Res*. **9**, 5339-5345.

Platet, N., Cathiard, A. M., Gleizes, M., and Garcia, M. (2004). Estrogens and their receptors in breast cancer progression: a dual role in cancer proliferation and invasion. *Crit. Rev. Oncol. Hematol.* **51**, 55-67.

Radice, S., Fumagalli, R., Chiesara, E., Ferraris, M., Frigerio, S. and Marabini, L. (2004). Estrogenic activity of procymidone in rainbow trout (*Oncorhynchus mykiss*) hepatocytes: a possible mechanism of action. *Chem. Biol. Interact.* **147**, 185-193.

Rees, C. B., and Li, G. (2004). Development and application of a real-time quantitative PCR assay for determining CYP1A transcripts in three genera of salmonids. *Aquat. Toxicol.* **66**, 357-368.

Riby, J. E., Chang, G. H. F., Firestone, G. L., and Bjeldanes, L. F. (2000a). Ligand-independent activation of estrogen receptor function by 3,3,'-diindolylmethane in human breast cancer cells. *Biochem. Pharmacol.* **60**, 167-177.

Riby, J. E., Feng, C., Chang, Y. C., Schaldach, C. M., Firestone, G. L. and Bjeldanes, L. F. (2000b). The major cyclic trimeric product of indole-3-carbinol is a strong agonist of the estrogen receptor signaling pathway. *Biochemistry.* **39**, 910-918.

Riby,J.E., Xue,L., Chatterj,U., Bjeldanes,E.L., Firestone,G.L. and Bjeldanes,L.F. (2005) Activation and potentiation of interferon-γ signaling by 3,3'-diindolylmethane in MCF-7 breast cancer cells. *Mol. Pharmaol.* Nov. 2, doi:10.1124/mol.105.017053.

Rise, M. L., Jones, S. R. M., Brown, G. D., von Schalburg, K. R., Davidson, W. S., and Koop, B. F. (2004a). Microarray analyses identify molecular biomarkers

of Atlantic salmon macrophage and hematopoietic kidney response to *Piscirickettsia salmonis* infection. *Physiol. Genomics.* **20**, 21-35.

Rise, M. L., von Schalburg, K. R., Brown, G. D., Mawer, M. A., Devlin, R. H., Kuipers, N., Busby, M., Beetz-Sargent, M., Alberto, R., Gibbs, A. R., Hunt, P., Shukin, R., Zeznik, J. A., Nelson, C., Jones, S. R. M., Smailus, D. E., Jones, S. J. M., Schein, J. E., Marra, M. A., Butterfield Y. S. N., Stott, J. M., Ng, S. H. S., Davidson, W. S., and Koop, B. F. (2004b). Development and application of a salmonid EST database and cDNA microarray: Data mining and interspecific hybridization characteristics. *Gen. Res.* **14**, 478-490.

Rothhammer,T., Poser,I., Soncin,F., Bataille,F., Moser,M. and Bosserhoff,A.K. (2005) Bone morphogenic proteins are overexpressed in malignant melanoma and promote cell invasion and migration. *Cancer Res.* **65**, 448-456.

Rutter, J., Michnoff, C. H., Harper, S. M., Gardner, K. H., and McKnight, S. L. (2001). PAS kinase: An evolutionarily conserved PAS domain-regulated serine/threonine kinase. *Proc. Natl. Acad. Sci.* **98**, 8991-8996.

Saal, H. L., Troein, C., Vallon-Christersson, J., Gruverger, S., Borg, A., and Peterson, C.. (2002). BioArray Software Environment: A platform for comprehensive management and analysis of microarray data. *Genome Biol.* **3**, software0003.1-0003.6.

Safe, S., Wang, F., Porter, W., Duan, R., and McDougal, A. (1998). Ah receptor agonists are endocrine disruptors: antiestrogenic activity and mechanisms. *Toxicol. Lett.* **102-103**, 343-347.

Sauer, G., Windisch, J., Kurzeder, C., Heilmann, V., Kreienberg, R., and Deissler, H. (2003). Progression of cervical carcinomas is associated with down-regulation of CD9 but strong local re-expression at sites of transendothelial invasion. *Clin Cancer Res.* **9**, 6426-6431.

Schmitt-Graff, A., Ertelt, V., Allgaier, H. P., Koelbe, K., Olschewski, M., Nitschke, R., Bochaton-Piallat, M. L., Gabbiani, G., and Blum, H. E. (2003). Cellular retinol-binding protein-1 in hepatocellular carcinoma correlates with beta-catenin, Ki-67 index, and patient survival. *Hepatology.* **38**, 470-480.

Segal, E., Friedman, N., Kaminski, N., Regev, A., and Koller, D. (2005). From signatures to models: understanding cancer using microarrays. *Nat. Genet.* **37**, 538-545.

Sekine, Y., Yamamoto, T., Yumioka, T., Imoto, S., Kojima, H. and Matsuda, T. (2004). Cross-talk between endocrine-disrupting chemicals and cytokine signaling through estrogen receptors. *Biochem. Biophys. Res. Comm.* **315**, 692-698.

Shah, Y. M., Basrur, V., and Rowan, B. G. (2004). Selective estrogen receptor modulator regulated proteins in endometrial cancer cells. *Mol. Cell. Endocrinol.* **219**, 127-139.

Shankaran,V., Ikeda,H., Bruce,A.T., White,J.M., Swanson,P.E., Old,L.J. and Schreiber,R.D. (2001) IFNγ and lymphocytes prevent primary tumour development and shape tumour immunogenicity. *Nature.* **410**, 1107-1111.

Shilling, A. D., and Williams, D. E. (2001). 3,3'-Diindolylmethane, a major condensation product of indole-3-carbinol, is a potent estrogen in rainbow trout. *Toxicol. Appl. Pharmacol.* **170**, 191-200.

Sinnhuber, R. O., Wales, J. H., Ayres, J. L., Engebrecht, R. H., and Amend, D. L. (1968). Dietary factors and hepatoma in rainbow trout (*Salmo gairdneri*). 1. Aflatoxins in vegetable protein feedstuffs. *J. Natl. Cancer Inst.* **41**, 711-718.

Stahlberg, N., Merino, R., Hernandez, L. H., Fernandez-Perez, L., Sandelin, A., Engstrom, P., Tollet-Egnell, P., Lenhard, B., and Flores-Morales, A. (2005). Exploring hepatic hormone actions using a compilation of gene expression profiles. *BMC Physiol.* **5**, [E. publication].

Stoner, G., Casto, B., Ralston, S., Roebuck, B., Pereira, C., and Bailey, G. (2002). Development of a multi-organ rat model for evaluating chemopreventive agents: Efficacy of indole-3-carbinol. *Carcinogenesis.* **23**, 265-272.

Stresser, D. M., Williams, D. E., Griffin, D. A., and Bailey, G. S. (1995a). Mechanisms of tumor modulation by indole-3-carbinol: Disposition and excretion in male Fischer 344 rats. *Drug Metab. Dispos.* **23**, 965-975.

Stresser, D.M., Bjeldanes, L.F., Bailey, G.S. and Williams, D.E. (1995b). The anticarcinogen 3,3-diindolylmethane is an inhibitor of cytochrome P-450. *J. Biochem. Toxicol.* **10**, 191-201.

Su, B., Guan, M., Xia, J., and Lu, Y. (2003). Stimulation of lipocalin-type prostaglandin D synthase by retinoic acid coincides with inhibition of prolieration in human 3AO ovarian cancer cells. *Cell Biol. Intl.* **27**, 587-592.

Suzui,M., Inamine,M., Kaneshiro,T., Morioka,T., Yoshimi,N., Suzuki,R., Kohno,H. and Tanaka,T. (2005) Indole-3-carbinol inhibits the growth of human colon carcinoma cells enhances the tumor multiplicity and volume of azoxymethane-induced rat colon carcinogenesis. *Int. J. Oncology.* **27**, 1391-1399.

Tanaka,T., Mori,Y., Morishita,Y., Hara,A., Ohno,T., Kojima,T. and Mori,H. (1990) Inhibitory effect of sinigrin and indole-3-carbinol on diethylnitrosamine-induced hepatocarcinogenesis in male ACI/N rats. *Carcinogenesis.* **11**, 1403-1406.

Thirunavukkarasu, C., Singh, J. P. V., Selvendiran, K., and Sakthisekaran. (2001). Chemoprotective efficacy of selenium against N-nitrosodiethylamine-induced hepatoma in albino rats. *Cell Biochem. Funct.* **19**, 265-271.

Tilton,S.C., Gerwick,L.G., Hendricks,J.D., Rosato,C., Corley-Smith,G., Givan,S.A., Bailey,G.S., Bayne,C.J. and Williams,D.E. (2005a) Use of a rainbow trout oligonucleotide microarray to examine transcriptional patterns in aflatoxin B_1-induced hepatocellular carcinoma compared to adjacent liver. *Toxicol. Sci.* **88**, 319-330.

Tilton,S.C., Givan,S.A., Pereira,C., Bailey,G.S. and Williams,D.E. (2005b) Toxicogenomic profiling of the hepatic tumor promoters indole-3-carbinol, 17β-estradiol and β-naphthoflavone in rainbow trout. *Toxicol. Sci.* Sept. 28. 10.1093/toxsci/kfi341

Tumminello, F. M., Leto, G., Pizzolanti, G., Candiloro, V., Crescimanno, M., Crosta, L., Flandina, C., Montalto, G., Soresi, M., Carroccio, A., Bascone, F., Ruggeri, I., Ippolito, S., and Gebbia, N. (1996). Cathepsin D, B and L

circulating levels as prognostic markers of malignant progression. *Anticancer Res.* **16**, 2315-2319.

Van Lipzig, M. M. H., Commandeur, J. N., de Kanter, F. J. J., Damsten, M. C., Vermeulen, N. P. E., Maat, E., Groot, E. J., Brouwer, A., Kester, M. H. A., Visser, T. J. and Meerman, J. H. N. (2005). Bioactivation of dibromated biphenyls by cytochrome P450 activity to metabolites with estrogenic activity and estrogen sulfotransferase inhibition capacity. *Chem. Res. Toxicol.* **18**, 1691-1700.

Wattenberg,L.W. and Loub,W.D. (1978) Inhibition of polycyclic aromatic hydrocarbon-induced neoplasia by naturally occurring indoles. *Cancer Res.* 38, 1410-1413.

Wei, S. J., Trempus, C. S., Ali, R. C., Hansen, L. A., and Tennant, R. W. (2004). 12-O-Tetradecanoylphorbol-13-acetate and UV radiation-induced nucleoside diphosphate kinase protein kinase B mediates neoplastic transformation of epidermal cells. *J. Biol. Chem.* **279**, 5993-6004.

Weinstein, D. A., Roy, C. N., Fleming, M. D., Loda, M. F., Wolfsdorf, J. I., and Andrews, N. C. (2002). Inappropriate expression of hepcidin is associated with iron refractory anemia: implications for anemia of chronic disease. *Blood.* **100**, 3776-3781.

Xu,M., Bailey,G.S., Hernaez,J.F., Taoka,C.R., Schut,H.A. and Dashwood,R.H. (1996) Protection by green tea, black tea, and indole-3-carbinol against 2-amino-3-methylimidazo[4,5-*f*]quinoline-induced DNA adducts and colonic aberrant crypts in the F344 rat. *Carcinogenesis.* **17**, 1429-1434.

Xue,L., Firestone,G.L. and Bjeldanes,L.F. (2005) DIM stimulates IFNγ gene expression in human breast cancer cells via the specific activation of JNK and p38 pathways. *Oncogene.* **24**, 2343-2353.

Yager, J. D., and Liehr, J. G. (1996). Molecular mechanisms of estrogen carcinogenesis. *Annu. Rev. Pharmacol. Toxicol.* **36**, 203-232.

Yoshida, M., Katashima, S., Ando, J., Tanaka, T., Uematsu, F., Nakae, D., and Maekawa, A. (2004). Dietary indole-3-carbinol promotes endometrial adenocarcinoma development in rats initiated with *N*-ethyl-*N'*-nitro-*N*-nitrosoguanidine, with induction of cytochrome P450s in the liver and consequent modulation of estrogen metabolism. *Carcinogenesis.* **25**, 2257-2264.

Yoshikawa, S., Kamada, M., Maegawa, M., Yamamoto, S., Irahara, M., Yamano, S., Aono, T., Kido, H., Koide, S. S. (2000). Hormonal control of mRNA expression of immunoglobulin binding factor in uterine cervix. *Biochem. Biophys. Res. Comm.* **279**, 898-903.

Zheng, Q., Tang, Z. Y., Xue, Q., Shi, D. R., Song, H. Y., and Tang, H. B. (2000). Invasion and metastasis of hepatocellular carcinoma in relation to urokinase-type plasminogen activator, its receptor and inhibitor. *J Cancer Res. Clin. Oncol.* **126**, 641-646.